Supplementary information

Caesium Carbonate Promoted Regioselective *O*-Functionalization of 4,6-Diphenylpyrimidin-2(1*H*)-ones Under Mild Conditions and Mechanistic Insight

Vijay Kumar[1], Praval Pratap Singh[2], Ashish Ranjan Dwivedi[1,3], Naveen Kumar[1], Rakesh kumar[1], Sudip Chakraborty[2] and Vinod Kumar[1*]

[1]*Laboratory of Organic and Medicinal Chemistry, Department of Chemistry, Central University of Punjab, Bathinda*

[2]*Department of Computational Sciences, School of Basic Sciences, Central University of Punjab, 151401, India*

[3]*Gitam School of Pharmacy, Hyderabad, Telangana, 502329, India*

Contents

Experimental procedure and analytical data of 2a to2o and 3a

To a 25 ml round bottom flask (RBF), 4,6-diphenylpyrimidin-2(1H)-one (0.16 mmol), caesium carbonate (0.16 mmol) was added and solubilized in DMF as solvent. The reaction mixture was then heated at 60 ℃ for 10 minutes. After 10 minutes the RBF was kept inside an ice bath and addition of organic halide (0.19 mmol) was carefully done at 0 ℃. The reaction mixture was kept for stirring at room temperature for 8 hours. The progress of reaction was monitored by TLC and GC-MS. To the reaction mixture (15 ml) water was added and aqueous phase was extracted with ethyl acetate (20 ml × 3), washed with brine, dried over sodium sulphate and the organic solvent was evaporated under vacuum using rotary evaporator to obtain 2a-2r and 3a.

4,6-bis(4-methoxyphenyl)-2-(prop-2-yn-1-yloxy)pyrimidine (2a)

Yield = 89%; Crystalline white powder; Melting point 190-193 °C; **^{1}H NMR** (400 MHz, $CDCl_3$) δ 8.17 (d, *J* = 8.8 Hz, 4H), 7.72 (s, 1H), 7.04 (d, *J* = 8.8 Hz, 4H), 5.19 (d, *J* = 2.0 Hz, 2H), 3.91 (s, 6H), 2.51 (s, 1H); **^{13}C NMR** (100 MHz, $CDCl_3$) δ 166.32, 164.60, 162.05, 129.26, 128.88, 114.16, 105.29, 78.99, 74.33, 55.45, 54.76; HRMS: m/z $[M+Na]^+$ for $C_{21}H_{18}N_2NaO_3^+$ calculated 369.1210; observed: 369.1173.

4-(4-bromophenyl)-6-(4-methoxyphenyl)-2-(prop-2-yn-1-yloxy)pyrimidine (2b)

Yield = 89%; Crystalline white powder; Melting point 179-181 °C; **^{1}H NMR** (400 MHz, $CDCl_3$) δ 8.16 (d, *J* = 9.2 Hz, 2H), 8.04 (d, *J* = 8.4 Hz, 2H), 7.73 (s, 1H), 7.65 (d, *J* = 8.8 Hz, 2H), 7.02 (d, *J* = 9.2 Hz, 2H), 5.17 (d, *J* = 2.4 Hz, 2H), 3.89 (s, 3H), 2.49 (t, *J* = 2.4 Hz, 1H); **^{13}C NMR** (100 MHz, $CDCl_3$) δ 166.95, 165.67, 164.70, 162.30, 135.75, 132.07, 128.99, 128.89, 128.82, 125.63, 114.25, 105.89, 78.75, 74.50, 55.47, 54.92; HRMS: m/z $[M+H]^+$ for $C_{20}H_{16}BrN_2O_2^+$, calculated 395.0395; observed: 395.0403.

4-(2,4-dichlorophenyl)-6-phenyl-2-(prop-2-yn-1-yloxy)pyrimidine (2c)

Yield = 84%; Crystalline white powder; Melting point 180-182 °C; ^{1}H NMR (400 MHz, $CDCl_3$) δ 8.15 (t, *J* = 2.0 Hz, 2H), 7.84 (s, 1H), 7.75 (d, *J* = 6.8 Hz, 1H), 7.54 (d, *J* = 1.2 Hz, 1H), 7.52 (d, *J* = 4.4 Hz, 3H), 7.40 (dd, *J* = 5.2 Hz, 1.6 Hz, 1H), 5.16 (d, *J* = 2.0 Hz, 2H), 2.50 (s, 1H); **^{13}C NMR** (100 MHz, $CDCl_3$) δ 166.66, 165.69, 164.62, 136.36, 136.30, 135.23, 133.09, 132.56, 131.39, 130.32, 128.97, 127.65, 127.49, 111.83, 78.62, 74.65, 55.11: HRMS: m/z $[M+H]^+$ for $C_{19}H_{13}Cl_2N_2O^+$, calculated 355.0405; observed: 355.0446.

4-(4-chlorophenyl)-6-(4-methoxyphenyl)-2-(prop-2-yn-1-yloxy)pyrimidine (2d)

Yield = 87%; Crystalline white powder; Melting point 151-153 °C; **^{1}H NMR** (400 MHz, $CDCl_3$) δ 8.18 (d, *J* = 8.8 Hz, 2H), 8.14 (d, *J* = 8.6 Hz, 2H), 7.76 (s, 1H), 7.51 (d, *J* = 8.5 Hz, 2H), 7.05 (d, *J* = 8.8 Hz, 2H), 5.19 (d, *J* = 2.4 Hz, 2H), 3.92 (s, 3H), 2.52 (t, *J* = 2.4 Hz, 1H); **^{13}C NMR** (100 MHz, $CDCl_3$) δ 166.93, 165.61, 164.70, 162.30, 137.19, 135.30, 129.12, 129.00, 128.91, 128.62, 114.27, 105.94, 78.55, 74.51, 55.49, 54.93; HRMS: m/z $[M+H]^+$ for $C_{20}H_{16}ClN_2O_2^+$, calculated 351.0900; observed: 351.0929.

4-(3-bromophenyl)-6-phenyl-2-(prop-2-yn-1-yloxy)pyrimidine (2e)

Yield = 81%; Crystalline white powder; Melting point 171-173 °C; **^{1}H NMR** (600 MHz, $CDCl_3$) δ 8.32 (t, *J* = 1.8 Hz, 1H), 8.17 (m, 2H), 8.09 (dt, *J* = 4.8 Hz, 1.8 Hz, 1H), 7.78 (s, 1H), , 7.64 (dq, *J* = 5.4 Hz, 1.2 Hz, 1H), 7.53 (dd, *J* = 3.6 Hz, 1.8 Hz, 3H)7.39 (t, *J* = 7.8 Hz, 1H), 5.18 (d, *J* = 2.4 Hz, 2H), 2.50 (t, *J* = 2.4 Hz, 1H); **^{13}C NMR** (150 MHz, $CDCl_3$) δ 167.56, 165.67, 164.78, 138.76, 136.43, 133.97, 131.33, 130.41, 130.39, 128.94, 127.40, 125.90, 123.18, 107.09, 78.62, 74.65, 55.10; HRMS: m/z $[M+Na]^+$ for $C_{19}H_{13}BrN_2NaO^+$, calculated 387.0104; observed: 387.0075.

4-(3-bromophenyl)-6-(3,4-dimethoxyphenyl)-2-(prop-2-yn-1-yloxy)pyrimidine (2f)

Yield = 84%; Crystalline white powder; Melting point 191-193 °C; **^{1}H NMR** (400 MHz, $CDCl_3$) δ 8.31 (t, *J* = 1.2 Hz, 1H), 8.08 (d, *J* = 6.4 Hz, 1H), 7.83 (d, *J* = 1.6 Hz, 1H), 7.74 (dd, *J* = 5.2 Hz, 1.6 Hz, 2H), 7.64 (d, *J* = 6.4 Hz, 1H), 7.39 (t, *J* = 6.4 Hz, 1H), 6.98 (d, *J* = 6.8 Hz, 1H), 5.17 (d, *J* = 2.0 Hz, 2H), 4.01 (s, 3H) 3.97 (s, 3H), 2.50 (t, *J* = 2.0 Hz, 1H); **^{13}C NMR** (100 MHz, $CDCl_3$) δ 167.29, 165.36, 164.81, 152.12, 149.54, 139.07, 133.98, 130.50, 129.33, 126.01, 123.27, 120.77, 111.07, 110.34, 106.55, 78.89, 74.68, 56.28, 56.21, 55.18; HRMS: m/z $[M+H]^+$ for $C_{21}H_{18}BrN_2O_3^+$, calculated 425.0500; observed: 425.528.

4-(4-methoxyphenyl)-6-phenyl-2-(prop-2-yn-1-yloxy)pyrimidine (2g)

Yield = 87%; Crystalline white powder; Melting point 153-156 °C; **^{1}H NMR** (400 MHz, $CDCl_3$) δ 8.16 (d, *J* = 8.4 Hz, 4H), 7.76 (s, 1H), 7.52 (d, *J* = 2.4 Hz, 3H), 7.02 (d, *J* = 8.8 Hz, 2H), 5.17 (d, *J* = 2.0 Hz, 2H), 3.89 (s, 1H), 2.49 (s, 1H); **^{13}C NMR** (100 MHz, $CDCl_3$) δ 166.80, 166.66, 164.66, 162.15, 136.84, 130.96, 129.06, 128.93, 128.83, 127.29, 114.19,106.17, 78.88, 74.40, 55.44, 54.84; HRMS: m/z $[M+Na]^+$ for $C_{20}H_{16}N_2NaO_2^+$, calculated 339.1109; observed: 339.1085.

4-(4-chlorophenyl)-6-phenyl-2-(prop-2-yn-1-yloxy)pyrimidine (2h)

Yield = 91%; Crystalline white powder; Melting point 182-185 °C; **^{1}H NMR** (400 MHz, $CDCl_3$) δ 8.17 (d, *J* = 3.6 Hz, 2H), 8.12 (d, *J* = 6.4 Hz, 2H), 7.79 (s, 1H), 7.53 (s, 3H), 7.49 (d, *J* = 6.4 Hz, 2H) 5.18 (d, *J* = 2H), 2.50 (s, 1H); **^{13}C NMR** (100 MHz, $CDCl_3$) δ, 167.59, 166.11, 164.91, 137.49, 136.66, 135.25, 131.40, 129.29, 129.06, 128.78, 127.50, 106.95, 78.81, 74.72, 55.16; HRMS: m/z $[M+Na]^+$ for $C_{19}H_{13}ClN_2NaO^+$, calculated 343.0614; observed: 343.0617.

4-(3-nitrophenyl)-6-phenyl-2-(prop-2-yn-1-yloxy)pyrimidine (2i)

Yield = 89%; Crystalline white powder; Melting point 146-149 °C; **^{1}H NMR** (400 MHz, $CDCl_3$) δ9.00 (t, *J* = 2.0 Hz, 1H), 8.56 (dt, *J* = 4.8 Hz, 1.2 Hz, 1H), 8.39 (dq, *J* = 4.8 Hz, 1.2 Hz, 1H), 7.90 (s, 1H), 8.21 (dd, *J* = 3.2 Hz, 2.0 Hz, 2H), 7.73 (t, *J* = 8.0 Hz, 1H), 7.56 (dd, *J* = 3.2 Hz, 2.0 Hz, 3H), 5.21 (d, *J* = 2.4 Hz, 2H) 2.53 (t, *J* = 2.4 Hz, 1H); **^{13}C NMR** (100 MHz, $CDCl_3$) δ 168.26, 165.03, 164.76, 148.91, 138.63, 136.28, 133.33, 131.75, 130.18, 129.18, 127.61, 125.70, 122.40, 107.31, 78.57, 74.97, 55.41; HRMS: m/z $[M+H]^+$ for $C_{19}H_{14}N_3O_3^+$, calculated 332.1035; observed: 332.1030.

4-(4-methoxyphenyl)-2-(prop-2-yn-1-yloxy)-6-(p-tolyl)pyrimidine (2j)

Yield = 84%; Crystalline white powder; Melting point 174-177 °C; **^{1}H NMR** (400 MHz, $CDCl_3$) δ 8.15 (d, *J* = 9.2 Hz, 2H), 8.06 (d, *J* = 8.0 Hz, 2H), 7.73 (s, 1H), 7.31 (d, *J* = 8.0 Hz, 2H), 7.01 (d, *J* = 8.8 Hz, 2H), 5.16 (d, *J* = 2.4 Hz, 2H), 3.88 (s, 3H), 2.48 (t, *J* = 2.4 Hz, 1H), 2.43 (s, 3H**); ^{13}C NMR** (100 MHz, $CDCl_3$) δ 166.88, 166.59, 164.76, 162.21, 141.53,134.14, 129.69, 129.30, 129.03, 127.34, 114.29, 105.92, 79.07, 74.48, 55.56, 54.91, 21.61; HRMS: m/z $[M+H]^+$ for $C_{21}H_{19}N_2O_2$+, calculated 331.1447; observed: 331.1440.

4-(3-bromophenyl)-2-(prop-2-yn-1-yloxy)-6-(p-tolyl)pyrimidine (2k)

Yield = 87%; Crystalline white powder; Melting point 182-185 °C; **^{1}H NMR** (400 MHz, $CDCl_3$) 8.31 (t, *J* = 1.6 Hz, 1H), 8.08 (d, *J* = 8.0 Hz, 3H), 7.76 (s, 1H), 7.64 (dq, *J* = 5.2 Hz, 0.8 Hz, 1H), 7.38 (d, *J* = 8.4 Hz, 1H), 7.32 (d, *J* = 8.0 Hz, 2H), 5.17 (d, *J* = 2.4 Hz, 2H), 2.50 (t, *J* = 2.4 Hz, 1H), δ 2.44 (s, 3H),; ^{13}C NMR (100 MHz, $CDCl_3$) δ 167.60, 165.57, 164.83, 138.95, 142.00, 134.00, 133.70, 130.50, 130.49, 129.80, 127.44, 126.00, 123.26, 106.85, 78.79, 74.74, 55.17, 21.65; HRMS: m/z $[M+H]^+$ for $C_{20}H_{16}BrN_2O^+$, calculated 379.0446; observed: 379.0439

2-(allyloxy)-4,6-bis(4-methoxyphenyl)pyrimidine (2l)

Yield = 88%; Crystalline white powder; Melting point 161-164 °C; **^{1}H NMR** (400 MHz, $CDCl_3$) δ 8.12 (d, *J* = 8.7 Hz, 4H), 7.64 (s, 1H), 7.00 (d, *J* = 8.7 Hz, 4H), 6.20 (dq, *J* = 10.9, 5.8 Hz, 1H), 5.47 (d, *J* = 17.2 Hz, 1H), 5.28 (d, *J* = 10.4 Hz, 1H), 5.05 (d, *J* = 5.7 Hz, 2H), 3.87 (s, 6H); **^{13}C NMR** (100 MHz, $CDCl_3$) δ 166.30, 165.44, 162.01, 133.47, 129.55, 128.89, 118.13, 114.19, 104.95, 77.44, 77.12, 76.81, 68.25, 55.52; EI-MS: m/z $[M]^+$ for $C_{21}H_{20}N_2O_3^+$ calculated: 348.15; observed: 347.18.

4,6-bis(4-methoxyphenyl)-2-propoxypyrimidine (2m)

Yield = 81%; Crystalline white powder; Melting point 165-168 °C; **^{1}H NMR** (400 MHz, $CDCl_3$) δ 8.12 (d, *J* = 8.7 Hz, 4H), 7.63 (s, 1H), 6.99 (d, *J* = 8.7 Hz, 4H), 4.47 (t, *J* = 6.8 Hz, 2H), 3.87 (s, 6H), 1.92 (dd, *J* = 14.3, 7.3 Hz, 2H), 1.08 (t, *J* = 7.4 Hz, 3H); **^{13}C NMR** (100 MHz, $CDCl_3$) δ 166.24, 165.93, 161.95, 129.68, 128.88, 114.16, 104.79, 77.44, 77.12, 76.81, 69.15, 55.51, 22.43, 10.76; EI-MS: m/z $[M]^+$ for $C_{21}H_{22}N_2O_3^+$ calculated: 350.16; observed: 350.35.

2-(benzyloxy)-4,6-bis(4-methoxyphenyl)pyrimidine (2n)

Yield = 90%; Crystalline white powder; Melting point 195-197 °C; **^{1}H NMR** (400 MHz, $CDCl_3$) δ 8.12 (d, *J* = 8.8 Hz, 4H), 7.65 (s, 1H), 7.56 (d, *J* = 7.4 Hz, 2H), 7.36 (t, *J* = 7.4 Hz, 2H), 7.31 (d, *J* = 7.3 Hz, 1H), 7.00 (d, *J* = 8.9 Hz, 4H), 5.59 (s, 2H), 3.87 (s, 6H); **^{13}C NMR** (100 MHz, $CDCl_3$) δ 166.36, 165.58, 162.01, 137.22, 129.58, 128.92, 128.46, 127.96, 114.20, 105.13, 69.07, 55.52; EI-MS: m/z $[M]^+$ for $C_{25}H_{22}N_2O_3$ calculated: 398.16; observed: 398.30.

2-isopropoxy-4,6-bis(4-methoxyphenyl)pyrimidine (2o)

Yield = 84%; White solid; Melting point 185-189 °C; **^{1}H NMR** (600 MHz, $CDCl_3$) δ 8.13 (d, J = 8.8 Hz, 4H), 7.62 (s, 1H), 7.01 (d, J = 8.8 Hz, 4H), 5.52 (hept, J = 6.2 Hz, 1H), 3.88 (s, 6H), 1.49 (d, J = 6.2 Hz, 6H); **^{13}C NMR** (150 MHz, $CDCl_3$) δ 166.33, 165.47, 162.01, 129.83, 129.00, 128.84, 114.32, 114.10, 104.58, 69.95, 55.54, 22.23, 22.11; EI-MS: m/z $[M]^+$ for $C_{21}H_{22}N_2O_3^+$ calculated: 350.16; observed: 350.20.

2-butoxy-4,6-bis(4-methoxyphenyl)pyrimidine (2p)

Yield = 87%; Crystalline white powder; Melting point 172-175 °C;Yield = 90%; **^{1}H NMR** (600 MHz, $CDCl_3$) δ 8.13 (d, J = 8.7 Hz, 4H), 7.63 (s, 1H), 7.01 (d, J = 8.8 Hz, 4H), 4.53 (t, J = 6.7 Hz, 2H), 3.88 (s, 6H), 1.92 – 1.86 (m, 2H), 1.56 (dt, J = 14.8, 7.5 Hz, 2H), 1.01 (t, J = 7.4 Hz, 3H); **^{13}C NMR** (150 MHz, $CDCl_3$) δ 166.28, 165.98, 161.99, 129.75, 128.94, 128.85,

114.26, 114.11, 104.82, 67.32, 55.50, 31.20, 19.41, 14.02; EI-MS: m/z $[M]^+$ for $C_{22}H_{24}N_2O_3^+$ calculated: 364.45; observed: 364.20.

4,6-bis(4-methoxyphenyl)-2-(pentyloxy)pyrimidine (2q)

Yield = 82%; White powder; Melting point 165-168 °C; **^{1}H NMR** (600 MHz, $CDCl_3$) δ 8.13 (d, J = 9.0 Hz, 4H), 7.64 (s, 1H), 7.01 (d, J = 8.8 Hz, 4H), 4.52 (t, J = 6.8 Hz, 2H), 3.88 (s, 6H), 1.94 – 1.88 (m, 2H), 1.52 (dt, J = 15.2, 7.3 Hz, 2H), 1.42 (h, J = 7.4 Hz, 2H), 0.95 (t, J = 7.3 Hz, 3H); **^{13}C NMR** (150 MHz, $CDCl_3$) δ 166.28, 165.98, 161.99, 129.75, 128.98, 128.90, 128.81, 114.29, 114.07, 104.79, 67.63, 55.50, 28.83, 28.36, 22.62, 14.14; EI-MS: m/z $[M]^+$ for $C_{23}H_{26}N_2O_3^+$ calculated: 348.47; observed: 378.25.

4,6-bis(4-methoxyphenyl)-2-(octyloxy)pyrimidine (2r)

Yield = 81%; Crystalline white powder; Melting point 155-157 °C; **^{1}H NMR** (600 MHz, $CDCl_3$) δ 8.13 (d, J = 8.9 Hz, 4H), 7.64 (s, 1H), 7.01 (d, J = 9.0 Hz, 4H), 4.52 (t, J = 6.8 Hz, 2H), 3.88 (s, 6H), 1.90 (p, J = 7.7, 7.1 Hz, 2H), 1.55 – 1.49 (m, 2H), 1.42 – 1.36 (m, 2H), 1.34 – 1.22 (m, 6H), 0.89 (t, J = 6.9 Hz, 3H); **^{13}C NMR** (150 MHz, $CDCl_3$) δ 166.21, 165.91, 161.91, 129.69, 128.82, 114.15, 114.11, 114.06, 104.72, 67.57, 55.46, 55.43, 55.39, 31.86, 29.45, 29.29, 29.08, 26.14, 22.68, 14.12; EI-MS: m/z $[M]^+$ for $C_{26}H_{32}N_2O_3^+$ calculated: 420.55; observed: 420.15.

4,6-bis(4-methoxyphenyl)-1-(prop-2-yn-1-yl)pyrimidin-2(1*H*)-one (3a)

Yield = 11%; white powder; Melting point 178-180 °C; **^{1}H NMR** (400 MHz, $CDCl_3$) δ 8.17 – 8.08 (m, 2H), 7.60 – 7.51 (m, 2H), 7.10 – 7.02 (m, 2H), 7.01 – 6.93 (m, 2H), 6.69 (s, 1H), 4.64 (d, *J* = 2.4 Hz, 2H), 3.89 (d, *J* = 11.5 Hz, 6H), 2.38 – 2.31 (m, 1H). **^{13}C NMR** (100 MHz, $CDCl_3$) δ 202.88, 165.13, 163.78, 132.62, 114.74, 108.18, 102.64, 97.12, 83.11, 77.44, 77.33, 77.12, 76.80, 74.79, 26.46; EI-MS: m/z $[M]^+$ for $C_{21}H_{18}N_2O_3^+$ calculated: 346; observed: 346.

Experimental procedure and analytical data of 5a to 5c and 6a to 6c

To a 25 ml round bottom flask (RBF), 2-phenylquinazolin-4(3H)-one (0.16 mmol), caesium carbonate (0.16 mmol) was added and solubilized in DMF as solvent. The reaction mixture was then heated at 60 ℃ for 10 minutes. After 10 minutes the RBF was kept inside an ice bath and addition of organic halide (0.19 mmol) was carefully done at 0 ℃. The reaction mixture was kept for stirring at room temperature for 8 hours. The progress of reaction was monitored by TLC and GC-MS. To the reaction mixture (15 ml) water was added and aqueous phase was extracted with ethyl acetate (20 ml × 3), washed with brine, dried over sodium sulphate and the

organic solvent was evaporated under vacuum using rotary evaporator to obtain 5a-5c and 6a-6c.

4-(2-(2-ethoxy-4-(4-(prop-2-yn-1-yloxy)quinazolin-2-yl)phenoxy)ethyl)morpholine (5a)

Yield = 71%; Off white powder; Melting point 169-171 °C; **^{1}H NMR** (600 MHz, $CDCl_3$) δ 8.17 (dq, J = 5.7, 2.1 Hz, 3H), 7.96 (dt, J = 8.4, 0.9 Hz, 1H), 7.81 (ddd, J = 8.4, 7.0, 1.5 Hz, 1H), 7.50 (ddd, J = 8.1, 6.9, 1.1 Hz, 1H), 7.00 (d, J = 8.9 Hz, 1H), 5.32 (d, J = 2.4 Hz, 2H), 4.25 (d, J = 6.9 Hz, 4H), 3.76 (t, J = 4.7 Hz, 4H), 2.89 (t, J = 5.8 Hz, 2H), 2.66 (t, J = 4.7 Hz, 4H), 2.56 (t, J = 2.4 Hz, 1H), 1.50 (d, J = 7.0 Hz, 3H); **^{13}C NMR** (150 MHz, $CDCl_3$) δ 165.32, 159.39, 152.14, 150.92, 148.82, 133.71, 131.28, 127.79, 126.27, 123.46, 121.95, 114.71, 113.31, 113.17, 78.33, 75.04, 75.02, 67.07, 66.97, 64.54, 57.50, 54.17, 14.93; EI-MS: m/z $[M]^+$ for $C_{25}H_{27}N_3O_4^+$ calculated: 433.20; observed: 433.15.

4-(2-(4-(4-(prop-2-yn-1-yloxy)quinazolin-2-yl)phenoxy)ethyl)morpholine (5b)

Yield = 73%; Off white powder; Melting point 152-154 °C; **^{1}H NMR** (600 MHz, $CDCl_3$) δ 8.53 (d, *J* = 8.8 Hz, 2H), 8.17 (dd, *J* = 8.2, 1.5 Hz, 1H), 7.95 (dd, *J* = 8.4, 1.0 Hz, 1H), 7.81 (ddt, *J* = 8.4, 6.9, 1.3 Hz, 1H), 7.49 (ddd, *J* = 8.1, 7.0, 1.2 Hz, 1H), 7.02 (d, *J* = 8.8 Hz, 2H), 5.33 (dd, *J* = 2.5, 1.0 Hz, 2H), 4.21 (t, *J* = 5.7 Hz, 2H), 3.76 (t, *J* = 4.7 Hz, 4H), 2.85 (t, *J* = 5.7 Hz, 2H), 2.62 (t, *J* = 4.5 Hz, 4H); **^{13}C NMR** (150 MHz, $CDCl_3$) δ 165.38, 160.93, 159.44, 152.17, 133.72, 130.77, 130.16, 127.76, 126.22, 123.47, 114.70, 114.42, 78.31, 75.08, 66.91, 65.87, 57.62, 54.16, 54.14; EI-MS: m/z $[M]^+$ for $C_{23}H_{23}N_3O_3^+$ calculated: 389.17; observed: 389.10.

4-(2-(3-(4-(prop-2-yn-1-yloxy)quinazolin-2-yl)phenoxy)ethyl)morpholine (5c)

Yield = 68%; Off white powder; Melting point 156-158 °C; **^{1}H NMR** (600 MHz, $CDCl_3$) δ 8.24 – 8.19 (m, 2H) 8.18-8.16 (m, 1H), 7.83 (ddd, J = 8.4, 6.9, 1.5 Hz, 1H), 7.53 (ddd, J = 8.1, 6.9, 1.1 Hz, 1H), 7.41 (t, J = 7.9 Hz, 1H), 7.05 (ddd, J = 8.1, 2.7, 1.0 Hz, 1H), 5.34 (d, J = 2.4 Hz, 2H), 4.26 (t, J = 5.7 Hz, 2H), 3.78 – 3.74 (m, 4H), 2.87 (t, J = 5.7 Hz, 2H), 2.68 – 2.59 (m, 4H), 2.57 (d, J = 4.8 Hz, 1H); **^{13}C NMR** (150 MHz, $CDCl_3$) δ 165.50, 159.41, 159.01, 152.02, 139.37, 133.79, 129.46, 128.02, 126.72, 123.48, 121.31, 117.44, 115.01, 114.09, 78.24, 75.18, 66.98, 65.88, 57.76, 54.30, 54.14; EI-MS: m/z $[M]^+$ for $C_{23}H_{23}N_3O_3^+$ calculated: 389.17; observed: 389.10.

2-(3-ethoxy-4-(2-morpholinoethoxy)phenyl)-3-(prop-2-yn-1-yl)quinazolin-4(3H)-one (6a)

Yield = 29%; Off white powder; Melting point 165-167 °C; **^{1}H NMR** (600 MHz, $CDCl_3$) δ 8.35 (dd, *J* = 8.0, 1.5 Hz, 1H), 7.80 – 7.71 (m, 2H), 7.51 (ddd, *J* = 8.1, 6.9, 1.4 Hz, 1H), 7.32 – 7.28 (m, 2H), 7.02 (d, *J* = 8.7 Hz, 1H), 4.70 (d, *J* = 2.5 Hz, 2H), 4.23 (t, *J* = 5.8 Hz, 2H), 4.15 (q, *J* = 7.0 Hz, 2H), 3.76 – 3.74 (m, 4H), 2.88 (t, *J* = 5.7 Hz, 2H), 2.65 (dd, *J* = 5.8, 3.7 Hz, 4H), 2.37 (t, *J* = 2.4 Hz, 1H), 1.46 (t, *J* = 7.0 Hz, 3H); **^{13}C NMR** (150 MHz, $CDCl_3$) δ 161.85, 155.29, 150.27, 148.97, 147.22, 134.68, 127.59, 126.92, 121.29, 120.54, 113.74, 113.05, 78.93, 72.62, 67.40, 67.00, 64.60, 57.42, 54.19, 36.68, 14.85; EI-MS: m/z $[M]^+$ for $C_{25}H_{27}N_3O_4^+$ calculated: 433.20; observed: 433.15.

2-(4-(2-morpholinoethoxy)phenyl)-3-(prop-2-yn-1-yl)quinazolin-4(3H)-one (6b)

Yield = 27%; Light yellow powder; Melting point 169-171 °C; **^{1}H NMR** (600 MHz, $CDCl_3$) δ 8.35 (dd, *J* = 8.0, 1.5 Hz, 1H), 7.77 (td, *J* = 7.6, 6.9, 1.5 Hz, 1H), 7.75 – 7.69 (m, 3H), 7.51 (ddd, *J* = 8.2, 6.9, 1.4 Hz, 1H), 7.05 (d, *J* = 8.7 Hz, 2H), 4.70 (d, *J* = 2.4 Hz, 2H), 4.22 (t, *J* = 5.6 Hz, 2H), 3.77 (t, *J* = 4.7 Hz, 4H), 2.88 (t, *J* = 5.7 Hz, 2H), 2.64 (t, *J* = 4.8 Hz, 4H), 2.36 (d, *J* = 4.9 Hz, 1H); **^{13}C NMR** (150 MHz, $CDCl_3$) δ 161.87, 160.26, 155.30, 147.25, 134.66, 129.89, 127.58, 127.41, 127.11, 126.93, 120.52, 114.88, 78.62, 72.67, 66.80, 65.98, 57.48, 54.09, 36.51; EI-MS: m/z $[M]^+$ for $C_{23}H_{23}N_3O_3^+$ calculated: 389.17; observed: 389.10.

2-(3-(2-morpholinoethoxy)phenyl)-3-(prop-2-yn-1-yl)quinazolin-4(3H)-one (6c)

Yield = 32%; Off white powder; Melting point 170-173 °C; **^{1}H NMR** (600 MHz, $CDCl_3$) δ 8.36 (dd, *J* = 8.0, 1.5 Hz, 1H), 7.82 – 7.73 (m, 2H), 7.53 (t, *J* = 7.5 Hz, 1H), 7.45 (t, *J* = 7.9 Hz, 1H), 7.31 (d, *J* = 7.5 Hz, 1H), 7.27 (d, *J* = 4.1 Hz, 1H), 7.10 (dd, *J* = 8.4, 2.6 Hz, 1H), 4.68 (d, *J* = 2.5 Hz, 2H), 4.19 (t, *J* = 5.6 Hz, 2H), 3.74 (t, *J* = 4.6 Hz, 4H), 2.84 (t, *J* = 5.6 Hz, 2H), 2.65 – 2.50 (m, 4H), 2.35 (d, *J* = 2.5 Hz, 1H); **^{13}C NMR** (150 MHz, $CDCl_3$) δ 161.62, 158.91, 155.15, 147.10, 135.79, 134.74, 130.17, 127.65, 127.34, 126.95, 120.67, 120.48, 117.22, 113.95, 78.57, 72.64, 66.91, 66.09, 57.54, 54.07, 36.38; EI-MS: m/z $[M]^+$ for $C_{23}H_{23}N_3O_3^+$ calculated: 389.17; observed: 389.10.

Computational details

All calculations were performed using DFT method in the Gaussian 16 suite.[1] The intermediates and the transition states were optimized in the gas phase without any symmetry constraints using B3LYP exchange-correlation functional for all structures[2] with grimme empirical dispersion correction D3[3] in conjunction with Karlsruhe def2-SVP basis set for all the atoms.[4] Frequency analysis was conducted at the same level of theory on the optimized geometries to determine whether the stationary points are minima. Using the Linear

Synchronous Transit (LST)[5] method, transition state guesses were searched on the potential energy surface, and the subsequent optimization was performed using the Berny algorithm. The transition states and the adjacent intermediates were connected by performing Intrinsic reaction coordinates (IRC)[6-9] calculations. Furthermore, to refine the energetics of the system single-point energy calculations were carried out on the optimized structures using the same functional B3LYP-D3 for all structures employing a higher valence triple-zeta polarization valence basis set def2-TZVP. Solvation energies in *N,N*-dimethylformamide(DMF) solvent was evaluated by a self-consistent reaction field (SCRF) approach using the SMD continuum solvation model [10] as conducted in the experimental setup. Tight wave function convergence criteria were used during single-point energy calculations. The figures and 3D images of the optimized geometries were prepared by using ChemDraw Professional 16.0 and CYLview[11] visualization software respectively.

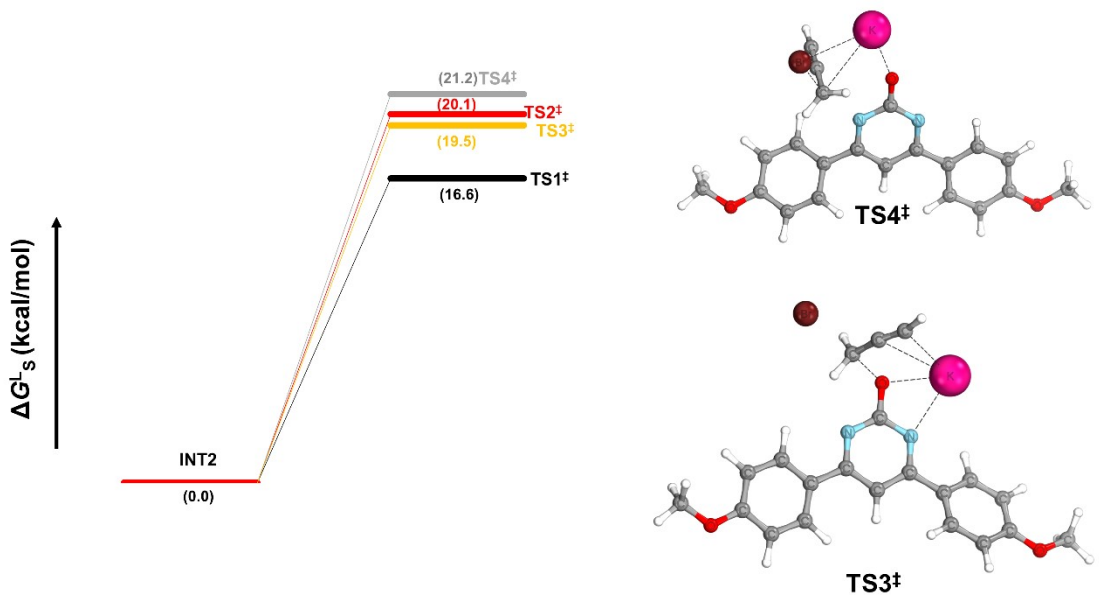

Figure 1: Free energy diagram

Table 1: Absolute Energy values (in hartrees) of all intermediates and transition states are given below. *Ee* = Electronic energy values, GLS = Solvent Gibbs Free energy values, ELS = Solvent Electronic Energy values, HLS = Solvent Enthalpy values.

Species	**E_e**	**E^L_S**	**G^L_S**	**H^L_S**	**Imaginary Mode**
Cs_2CO_3	-304.04091	-304.413651	-304.434767	-304.389512	0

$CsHCO_3$	-284.44153	-284.79695	-284.80079	-284.76262	0
CsBr	-2594.1181	-2594.4775	-2594.50362	-2594.47321	0
KBr	-3173.8101	-3174.23265	-3174.25675	-3174.22832	0
P_Br	-2689.8357	-2690.29033	-2690.27232	-2690.23805	0
R	-1030.0206	-1031.19104	-1030.9318	-1030.86137	0
2a	-1145.3788	-1146.66641	-1146.37523	-1146.29632	0
3a	-1145.3832	-1146.67713	-1146.38519	-1146.30702	0
INT1	-1334.1351	-1335.63892	-1335.37939	-1335.28453	0
INT2	-1049.6422	-1050.82953	-1050.58863	-1050.51061	0
TS1‡	-3739.4656	-3741.11204	-3740.83452	-3740.7398	1
TS2‡	-3739.4802	-3741.1081	-3740.82899	-3740.73582	1
TS3‡	-4319.1615	-4320.86771	-4320.58791	-4320.49547	1
TS4‡	-4319.1751	-4320.86658	-4320.58516	-4320.4942	1

Crystallographic Data

Crystal of compound 2a (CCDC: 2262808) was mounted on Hampton cryoloops. All geometric and intensity data for the crystal were collected using a Super-Nova (Mo) X-ray diffractometer equipped with a micro-focus sealed X-ray tube Mo-Kα (λ = 0.71073 Å) X-ray source, and HyPix3000 detector of with increasing ω (width of 0.3 per frame) at a scan speed of either 5 or 10 s/frame. The CrysAlisPro software was used for data acquisition, and data extraction. Using Olex2[12], the structure was solved with the SIR2004[13] structure solution program using Direct Methods and refined with the ShelXL[14] refinement package using Least Squares minimisation. All non-hydrogen atoms were refined with anisotropic thermal parameters. Detailed crystallographic data and structural refinement parameters are summarized in Table S1-S3. These data can be obtained free of charge from The Cambridge Crystallographic Data Centre.

Table 2: Crystal data and refinement parameters for compound 2a.

CCDC	2262808
Empirical formula	C21H18N2O3
Formula weight	346.39
Temperature/K	293(2)

Crystal system	monoclinic
Space group	P21/c
a/Å	5.2375(5),
b/Å	18.6453(21)
c/Å	17.8444(13)
β/°	90.182(8)
Volume/Å^3	1742.6(2)
Z	4
ρ_{calcg}/cm^3	1.320
μ/mm-1	0.089
F(000)	728.0
Crystal size/mm^3	0.018 × 0.15 × 0.01
Radiation M_oK_α	(λ = 0.71073)
2Θ range for data collection/°	6.32 to 52.74
Index ranges	-6 ≤ h ≤ 6, -22 ≤ k ≤ 23, -22 ≤ l ≤ 21
Reflections collected	16485
Independent reflections	3428
[R_{int} = R_{sigma} =]	0.1006, 0.1269
Data/restraints/parameters	3428/0/237
Goodness-of-fit on F2	0.975
Final R indexes [I>=2σ (I)]	R1 = 0.0636, wR2 = 0.1278
Final R indexes [all data]	R1 = 0.1914, wR2 = 0.1764
Largest diff. peak/hole / e Å^{-3}	0.60/-0.59

Table 2: Bond Lengths for Compound 2a.

Atom	Atom	Length/Å	Atom	Atom	Length/Å
O3	C15	1.364(3)	C3	C4	1.386(4)
O3	C18	1.423(3)	C12	C13	1.383(4)
O1	C1	1.364(3)	C12	C17	1.394(4)
O1	C19	1.438(4)	C2	C10	1.377(4)
O2	C6	1.368(3)	C13	C14	1.383(4)
O2	C9	1.433(3)	C14	C15	1.382(4)
N1	C2	1.350(3)	C15	C16	1.382(4)
N1	C1	1.322(3)	C6	C5	1.380(4)

N2	C11	1.346(3)	C6	C7	1.375(4)
N2	C1	1.326(3)	C8	C7	1.385(4)
C11	C12	1.474(4)	C17	C16	1.364(4)
C11	C10	1.384(4)	C4	C5	1.373(4)
C3	C2	1.476(4)	C20	C19	1.460(4)
C3	C8	1.380(4)	C20	C21	1.150(4)

Table 3: Bond Angles for Compound 2a.

Atom	**Atom**	**Atom**	**Angle/°**	**Atom**	**Atom**	**Atom**	**Angle/°**
C18	O3	C15	118.3(3)	N2	C1	N1	129.6(3)
C19	O1	C1	117.0(2)	C14	C13	C12	121.9(3)
C9	O2	C6	118.4(3)	C15	C14	C13	119.8(3)
C1	N1	C2	115.0(3)	C14	C15	O3	125.1(3)
C1	N2	C11	115.0(3)	C16	C15	O3	116.0(3)
C12	C11	N2	116.4(3)	C16	C15	C14	118.9(3)
C10	C11	N2	120.2(3)	C2	C10	C11	119.8(3)
C10	C11	C12	123.3(3)	C5	C6	O2	116.0(3)
C8	C3	C2	121.3(3)	C7	C6	O2	124.3(3)
C4	C3	C2	121.4(3)	C7	C6	C5	119.7(3)
C4	C3	C8	117.3(3)	C7	C8	C3	121.7(3)
C13	C12	C11	121.2(3)	C16	C17	C12	121.5(3)
C17	C12	C11	121.7(3)	C5	C4	C3	121.9(3)
C17	C12	C13	117.0(3)	C4	C5	C6	119.8(3)

C3	C2	N1	116.7(3)	C8	C7	C6	119.6(3)
C10	C2	N1	120.3(3)	C17	C16	C15	120.8(3)
C10	C2	C3	123.0(3)	C21	C20	C19	177.5(4)
N1	C1	O1	118.2(3)	C20	C19	O1	113.3(3)

Refrences

1. Frisch, M. J.; Trucks, G. W.; Schlegel, H. B.; Scuseria, G. E.; Robb, M. A.; Cheeseman, J. R.; Scalmani, G.; Barone, V.; Petersson, G. A.; Nakatsuji, H.; Li, X.; Caricato, M.; Marenich, A. V.; Bloino, J.; Janesko, B. G.; Gomperts, R.; Mennucci, B.; Hratchian, H. P.; Ortiz, J. V.; Izmaylov, A. F.; Sonnenberg, J. L.; Williams-Young, D.; Ding, F.; Lipparini, F.; Egidi, F.; Goings, J.; Peng, B.; Petrone, A.; Henderson, T.; Ranasinghe, D.; Zakrzewski, V. G.; Gao, J.; Rega, N.; Zheng, G.; Liang, W.; Hada, M.; Ehara, M.; Toyota, K.; Fukuda, R.; Hasegawa, J.; Ishida, M.; Nakajima, T.; Honda, Y.; Kitao, O.; Nakai, H.; Vreven, T.; Throssell, K.; Montgomery, J. A., Jr.; Peralta, J. E.; Ogliaro, F.; Bearpark, M. J.; Heyd, J. J.; Brothers, E. N.; Kudin, K. N.; Staroverov, V. N.; Keith, T. A.; Kobayashi, R.; Normand, J.; Raghavachari, K.; Rendell, A. P.; Burant, J. C.; Iyengar, S. S.; Tomasi, J.; Cossi, M.; Millam, J. M.; Klene, M.; Adamo, C.; Cammi, R.; Ochterski, J. W.; Martin, R. L.; Morokuma, K.; Farkas, O.; Foresman, J. B.; Fox, D. J. *Gaussian 16*, revision C.01; Gaussian, Inc.: Wallingford CT, 2016.

2. Goldstein, E.; Brett Beno; and K. N. Houk. Density functional theory prediction of the relative energies and isotope effects for the concerted and stepwise mechanisms of the Diels−Alder reaction of butadiene and ethylene. *Journal of the American Chemical Society* **1996**, *118*(25), 6036-6043.

3. Grimme, S.; Ehrlich, S.; Goerigk, L. Effect of the Damping Function in Dispersion Corrected Density Functional Theory. *J. Comput. Chem.* **2011**, 32, 1456−1465.

4. Hehre W. J.; Ditchfield R.; Pople J. A., *J. Chem. Phys*. **1972**, 56, 2257.

5. Halgren, T. A.; Lipscomb, W. N. The Synchronous-Transit Method for Determining Reaction Pathways and Locating Molecular Transition States. Chem. Phys. Lett. 1977, 49, 225−232.

6. Hratchian, H. P.; Schlegel, H. B. Finding Minima, Transition States, and Following Reaction Pathways on Ab Initio Potential Energy Surfaces. In *Theory and Applications of Computational Chemistry: The First 40 Years*; Dykstra, C. E.; Frenking, G.; Kim, K. S.; Scuseria, G., Eds.; Elsevier: Amsterdam, 2005; pp. 195−249.

7. Hratchian, H. P.; Schlegel, H. B. Using Hessian Updating to Increase the Efficiency of a Hessian Based Predictor-Corrector Reaction Path Following Method. *J. Chem. Theory Comput*. **2005**, 1, 61−69.

8. Hratchian, H. P.; Schlegel, H. B. Accurate Reaction Paths Using a Hessian Based Predictor-Corrector Integrator. *J. Chem. Phys*. **2004**, 120, 9918−9924.

9. Fukui, K. The path of Chemical Reactions - The IRC approach. *Acc. Chem. Res*. **1981**, 14, 363−368.

10. Marenich, A. V.; Cramer, C. J.; Truhlar, D. G. Universal Solvation Model Based on Solute Electron Density and on a Continuum Model of the Solvent Defined by the Bulk Dielectric Constant and Atomic Surface Tensions. *J. Phys. Chem. B* **2009**, 113, 6378−6396.

11. Legault, C. Y. CYLview 20, Université de Sherbrooke; **2020**. See http://www.cylview.org.

12. Dolomanov, O. V.; Bourhis, L. J.; Gildea, R. J.; Howard, J. A.; Puschmann, H. OLEX2: a complete structure solution, refinement and analysis program. J. Appl. Crystallogr. 2009, 42, 339−341.

13. Burla, M. C.; Caliandro, R.; Camalli, M.; Carrozzini, B.; Cascarano, G. L.; De Caro, L.; Giacovazzo, C.; Polidori, G.; Siliqi, D.; Spagna, R. IL MILIONE: a suite of computer programs for crystal structure solution of proteins. J. Appl. Crystallogr. 2007, 40, 609−613.

14. Sheldrick, G. M. SHELXT−Integrated space-group and crystalstructure determination. Acta Crystallogr., Sect. C: Struct. Chem. 2015, 71, 3−8.

Spectral data

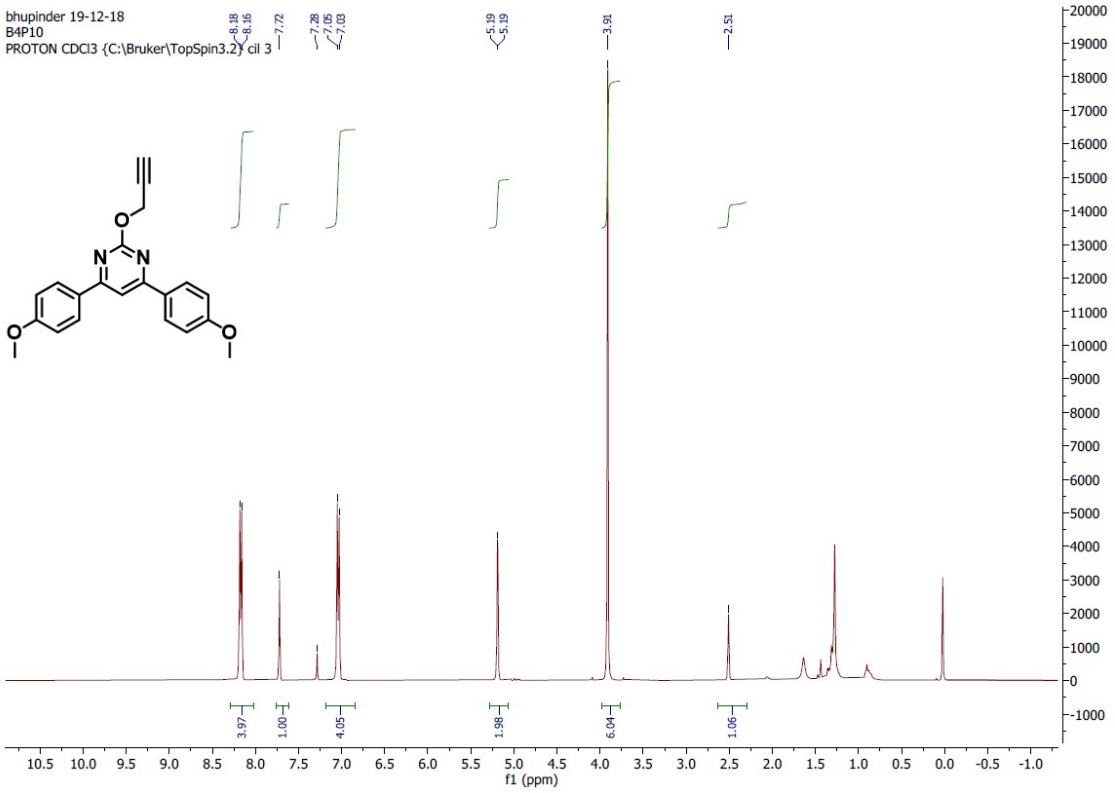

Figure 2: [1]H NMR spectra of 2a

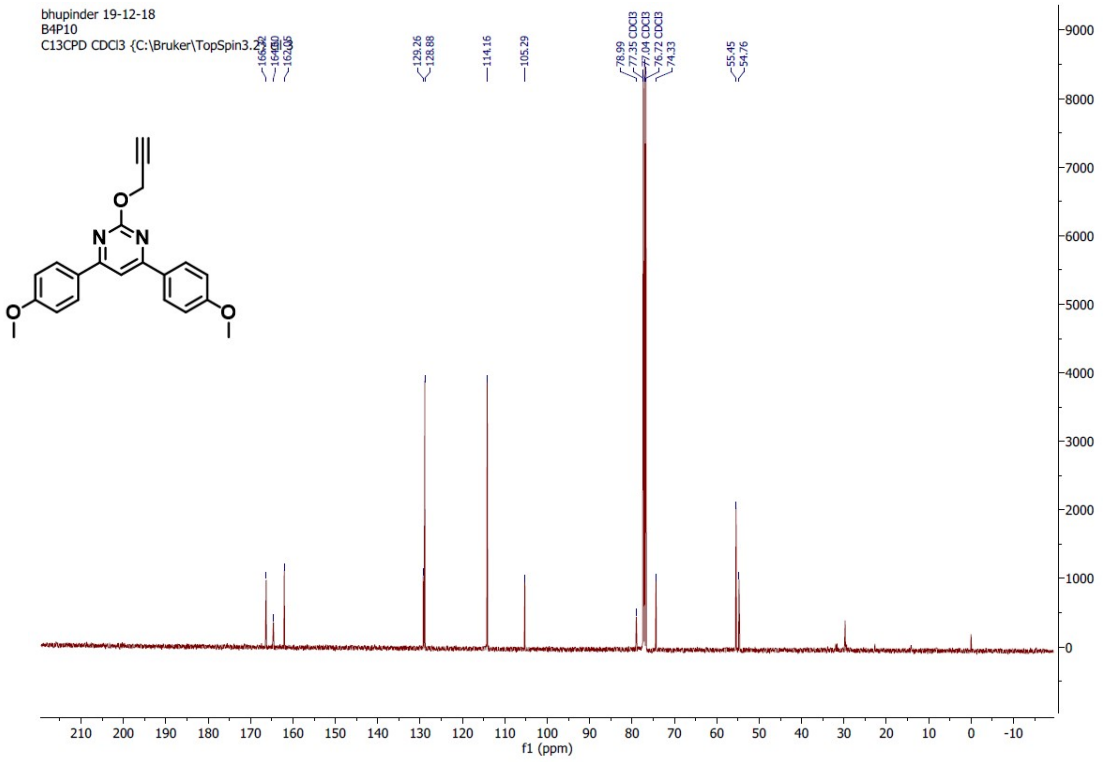

Figure 3: [13]C NMR spectra of 2a

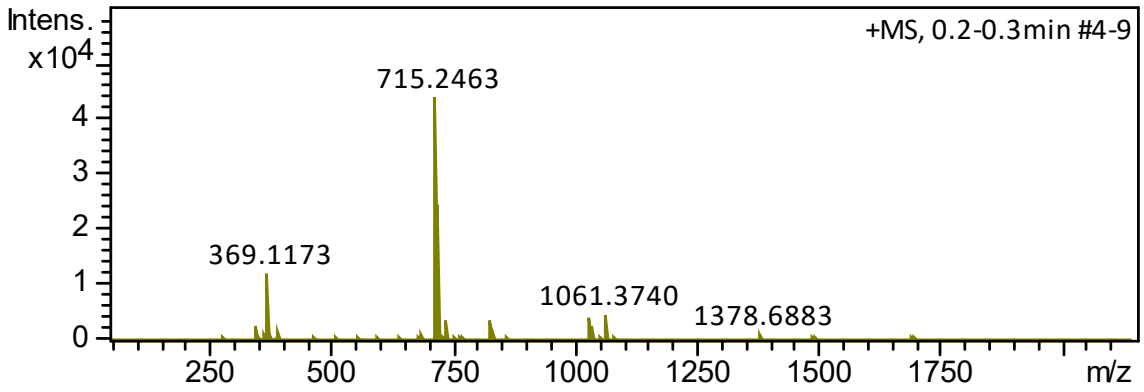

Figure 4: HRMS of 2a: m/z [M+ Na]$^+$ $C_{21}H_{18}N_2NaO_3^+$ calculated 369.1210; observed: 369.1173

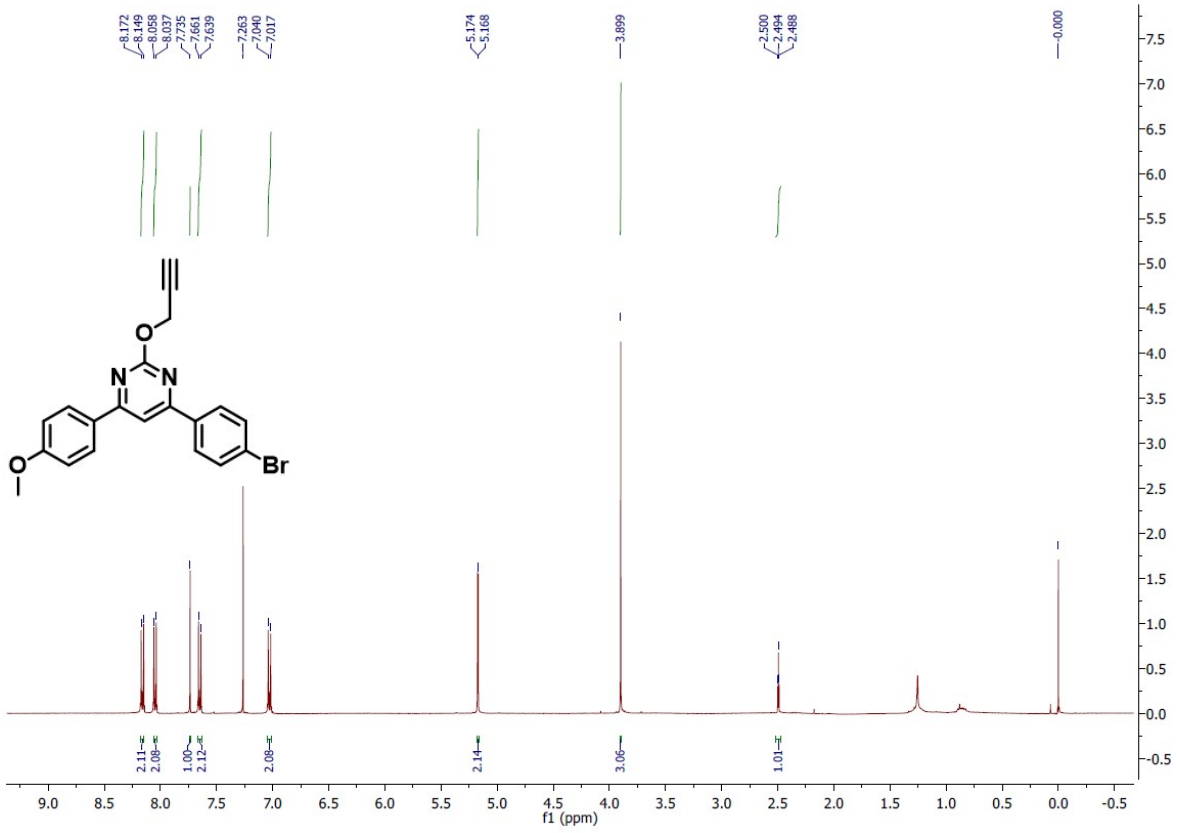

Figure 5: ^{1}H NMR spectra of 2b

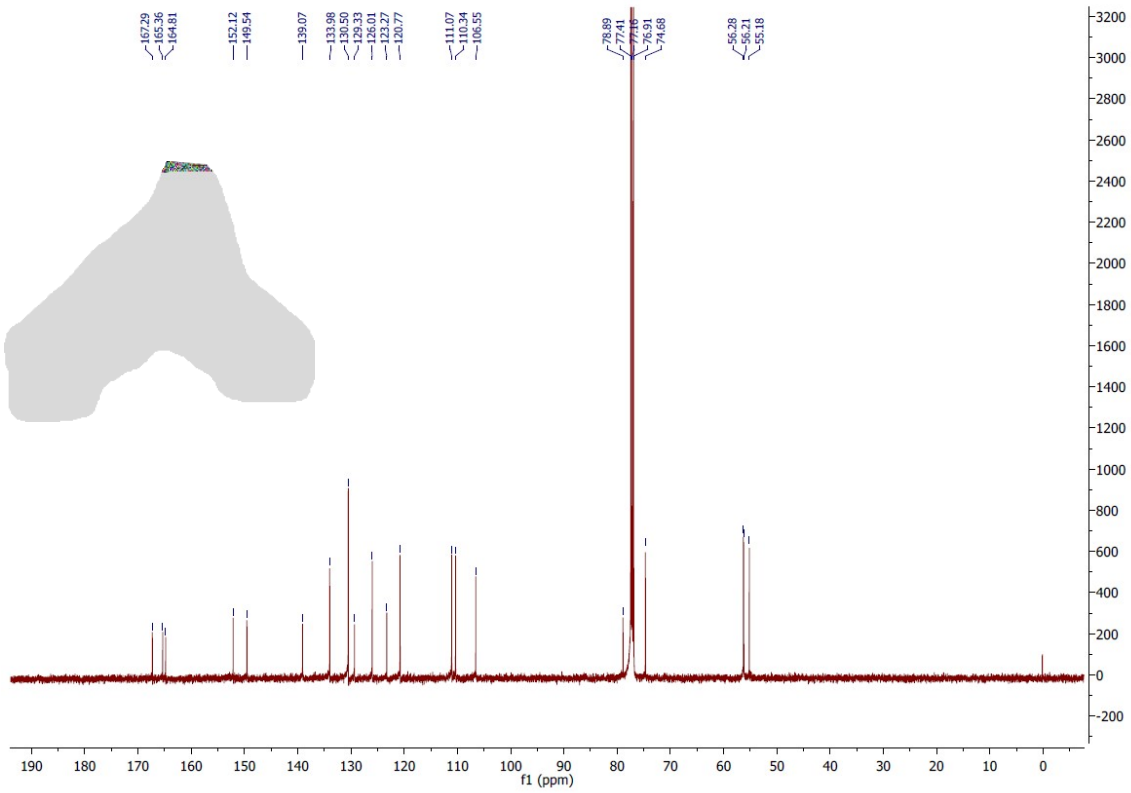

Figure 6: ^{13}C NMR spectra of 2b

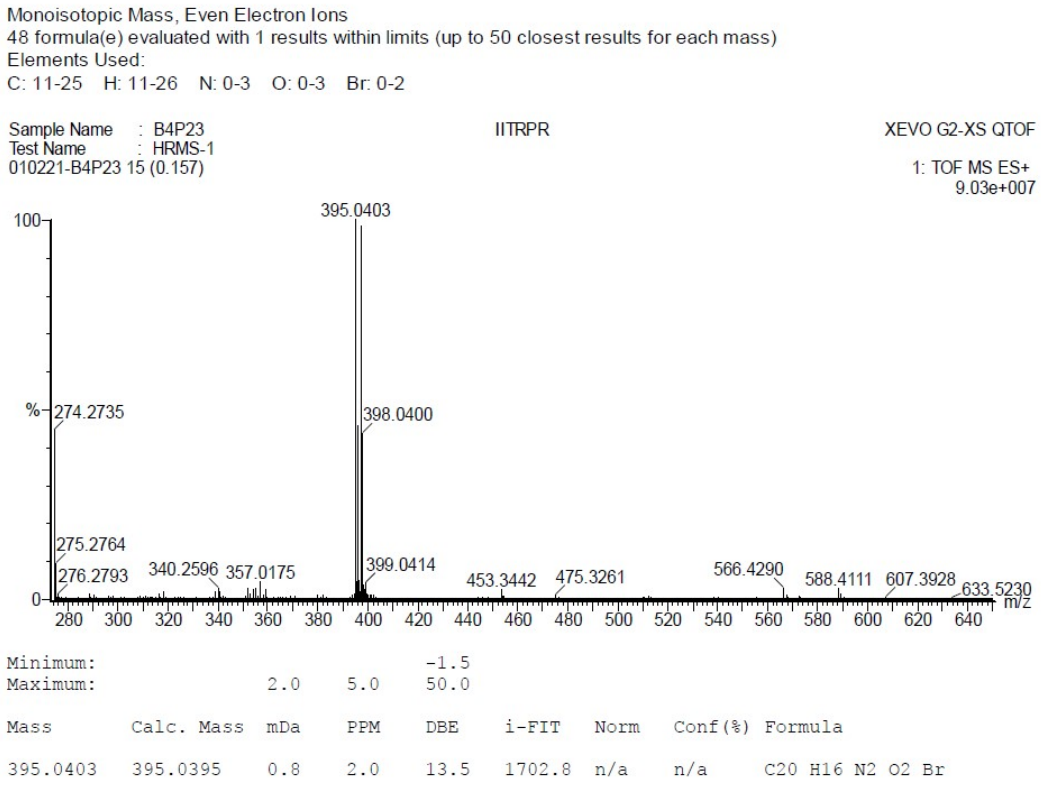

Figure 7: HRMS of 2b: m/z $[M+H]^+$ for $C_{20}H_{16}BrN_2O_2^+$, calculated 395.0395; observed: 395.0403

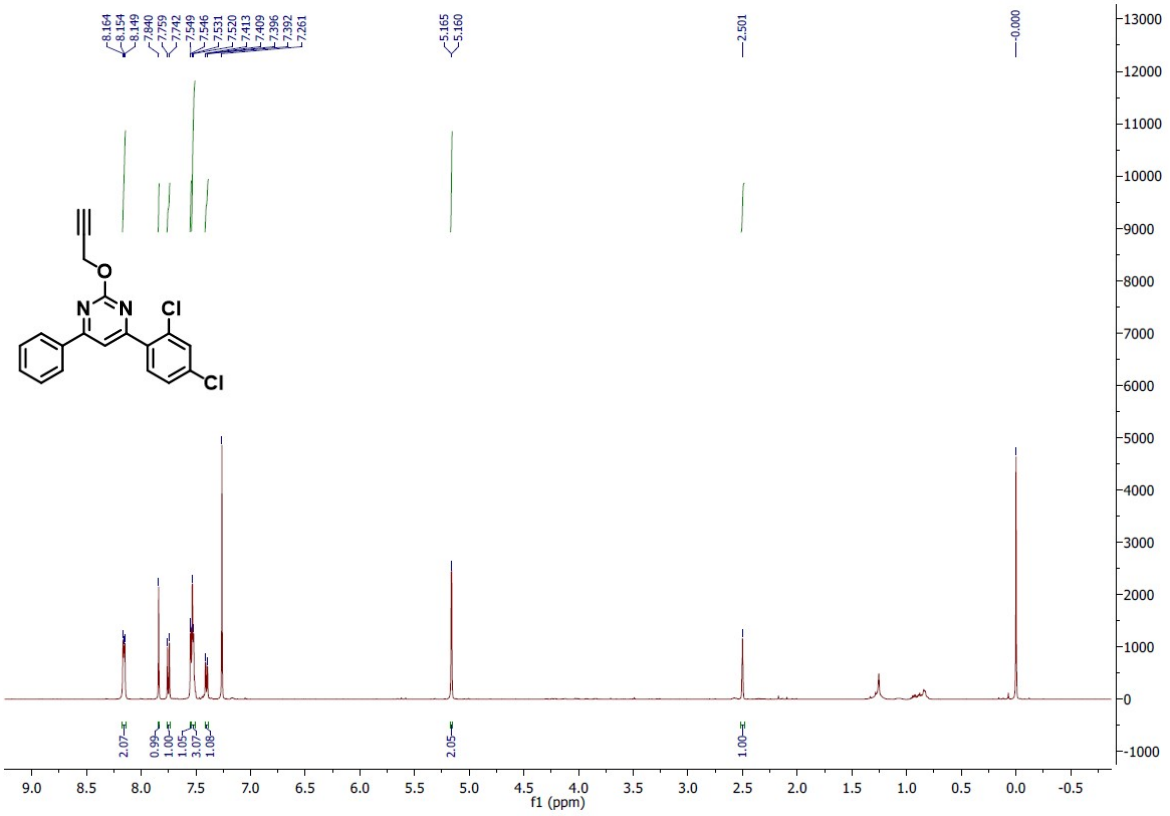

Figure 8: [1]H NMR spectra of 2c

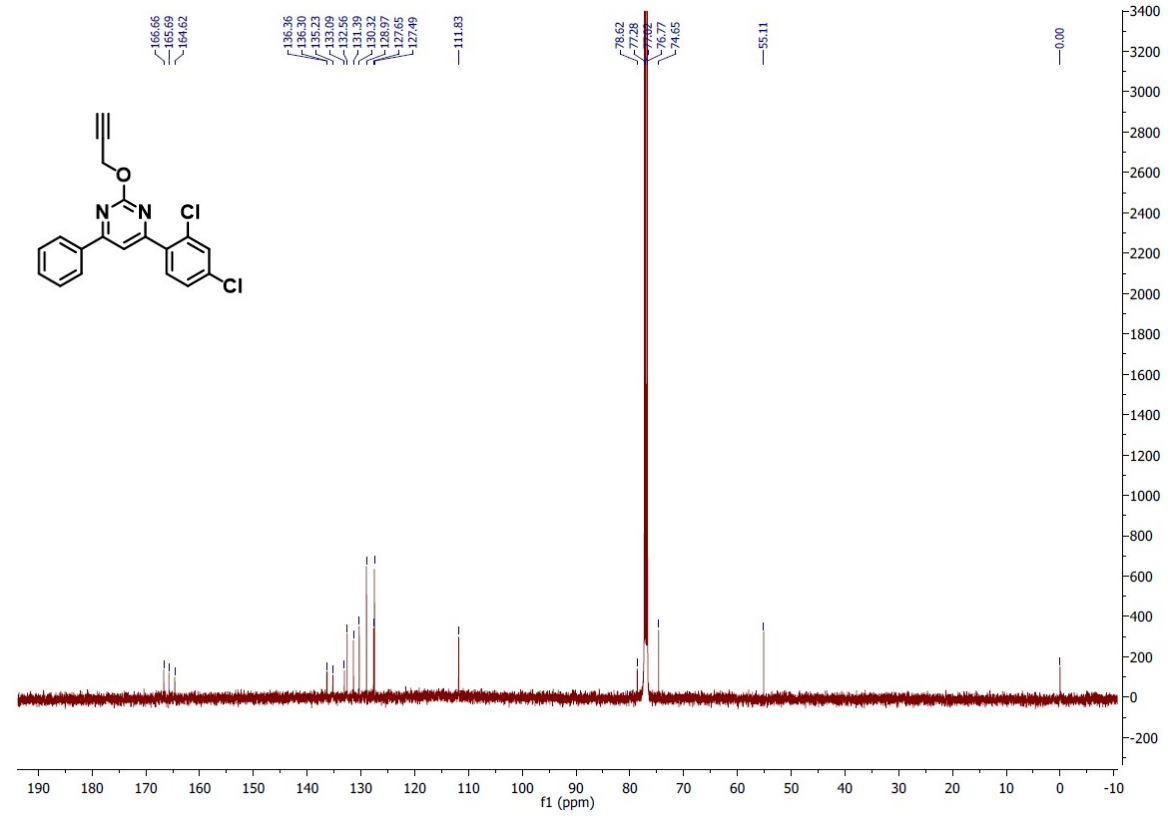

Figure 9: [13]C NMR spectra of 2c

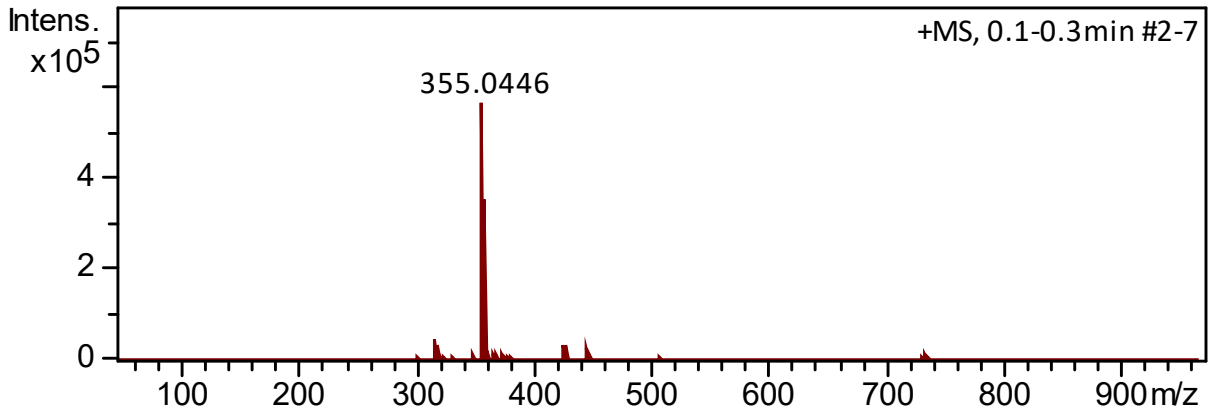

Figure 10: HRMS of 2c: m/z $[M+H]^+$ for $C_{19}H_{13}Cl_2N_2O^+$, calculated 355.0405; observed: 355.0446

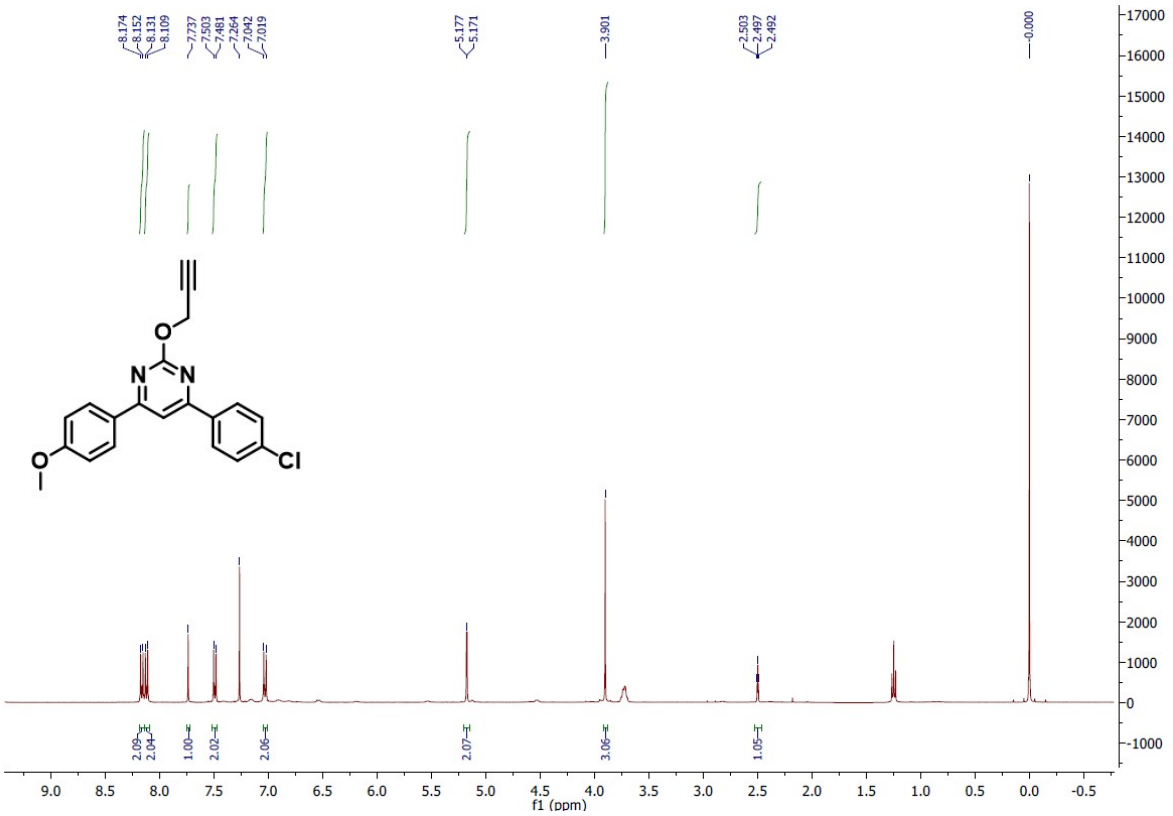

Figure 11: ^1H NMR spectra of 2d

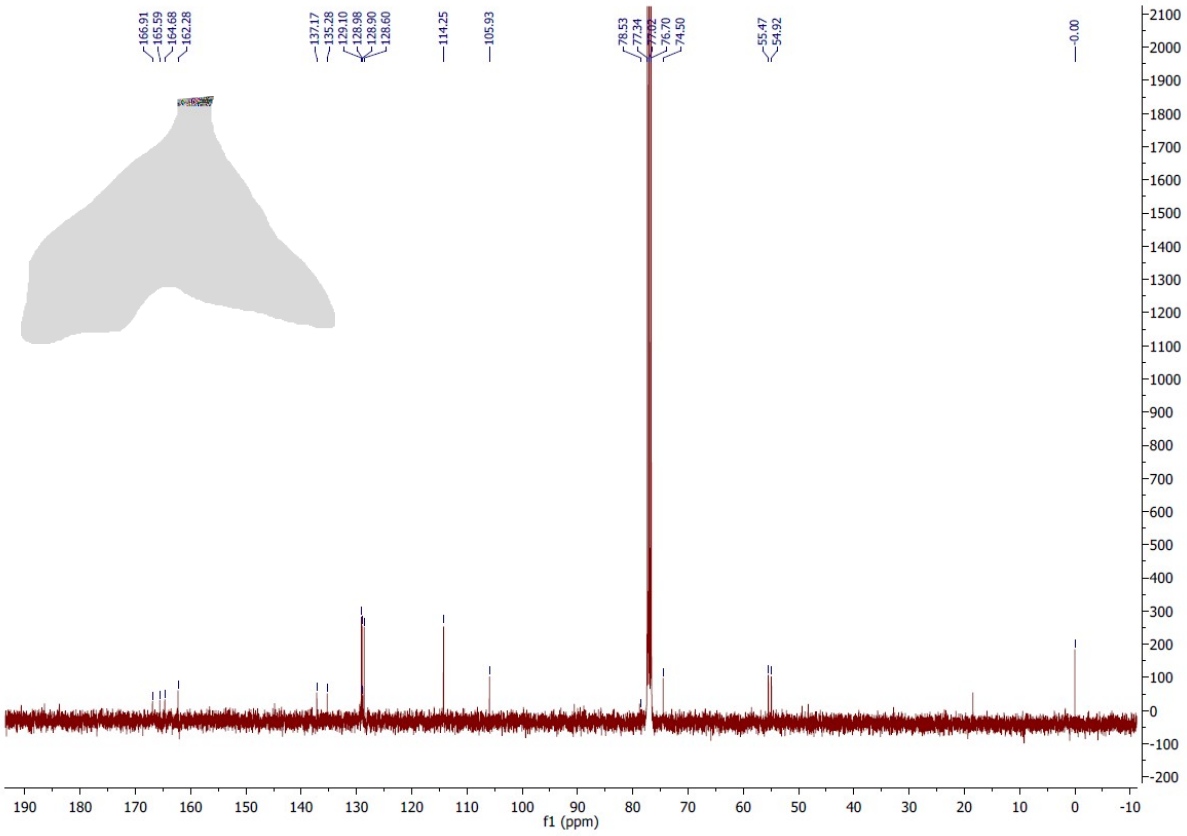

Figure 12: ^{13}C NMR spectra of 2d

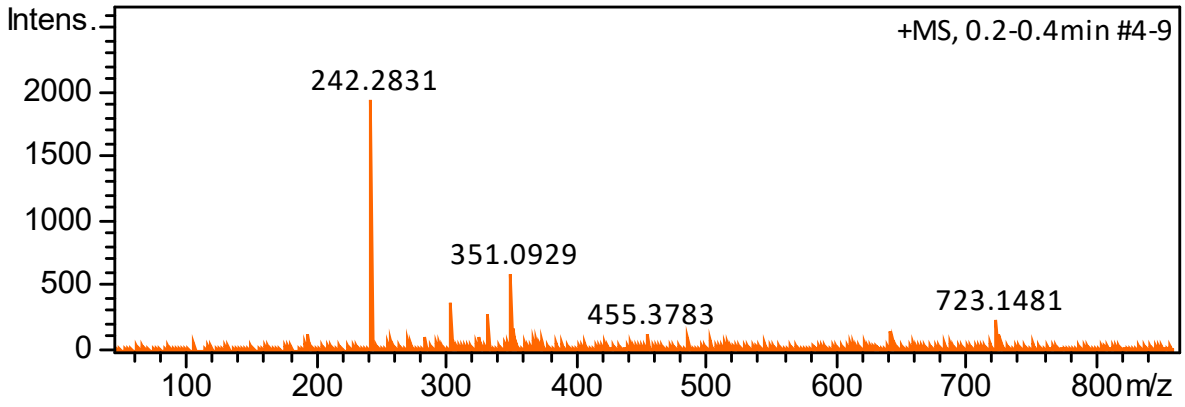

Figure 13: HRMS of 2d: m/z $[M+H]^+$ for $C_{20}H_{16}ClN_2O_2^+$, calculated 351.0900; observed: 351.0929

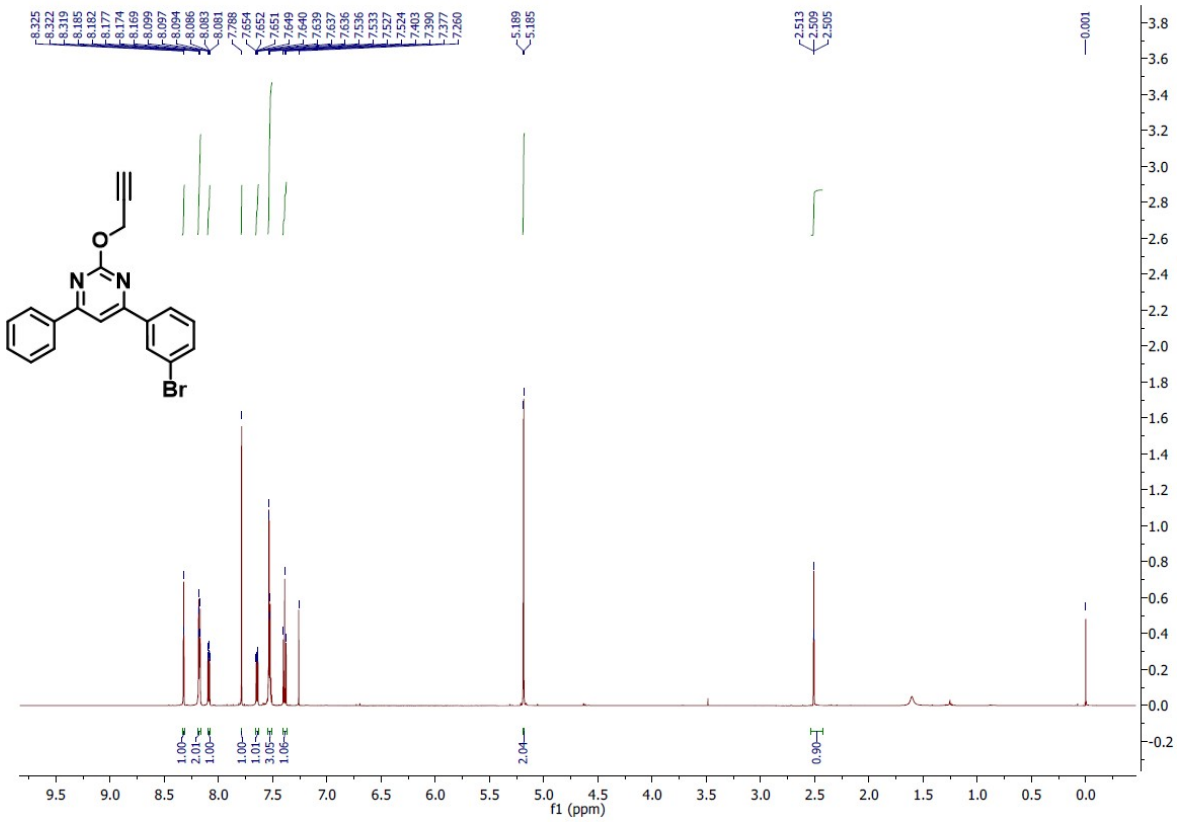

Figure 14: [1]H NMR spectra of 2e

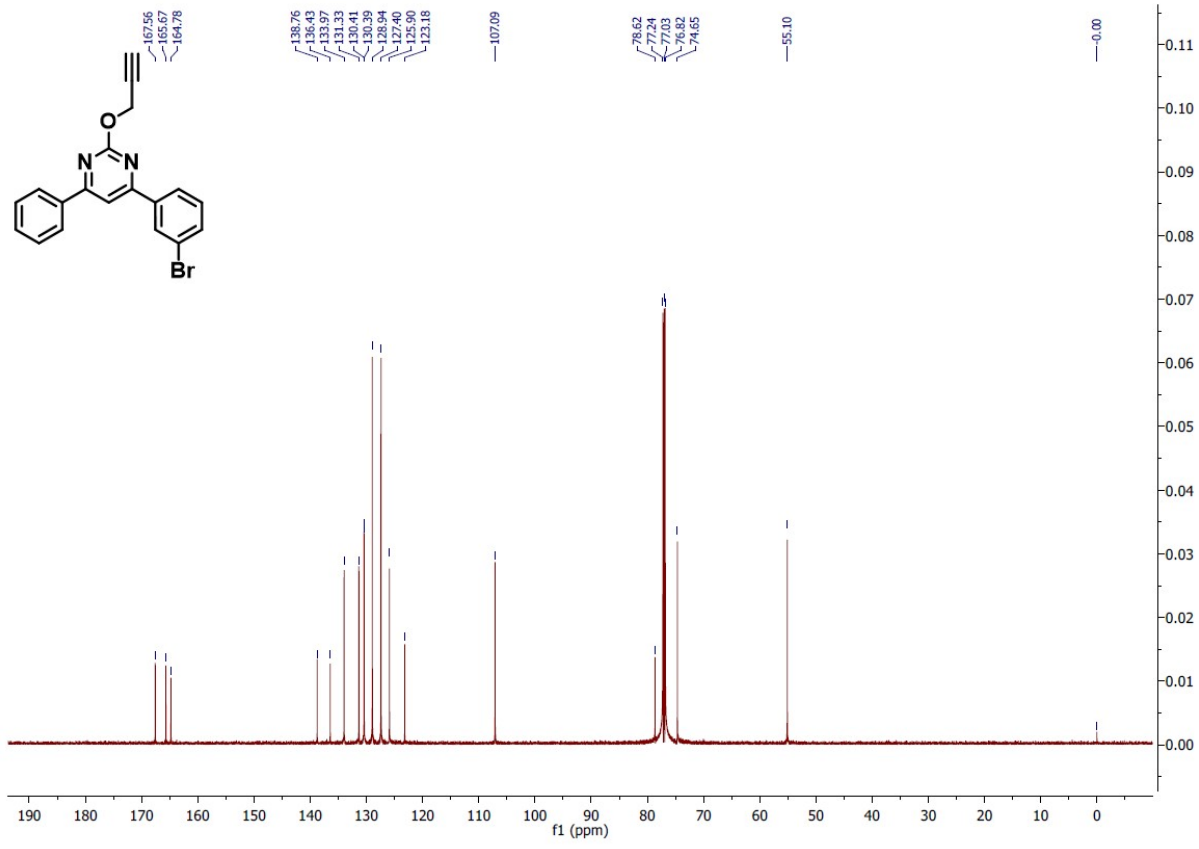

Figure 15: [13]C NMR spectra of 2e

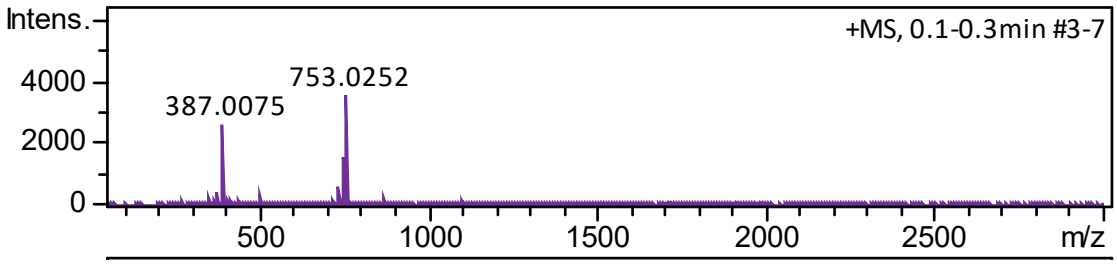

Figure 16: HRMS of 2e: m/z $[M+Na]^+$ for $C_{19}H_{13}BrN_2NaO^+$, calculated 387.0104; observed: 387.0075

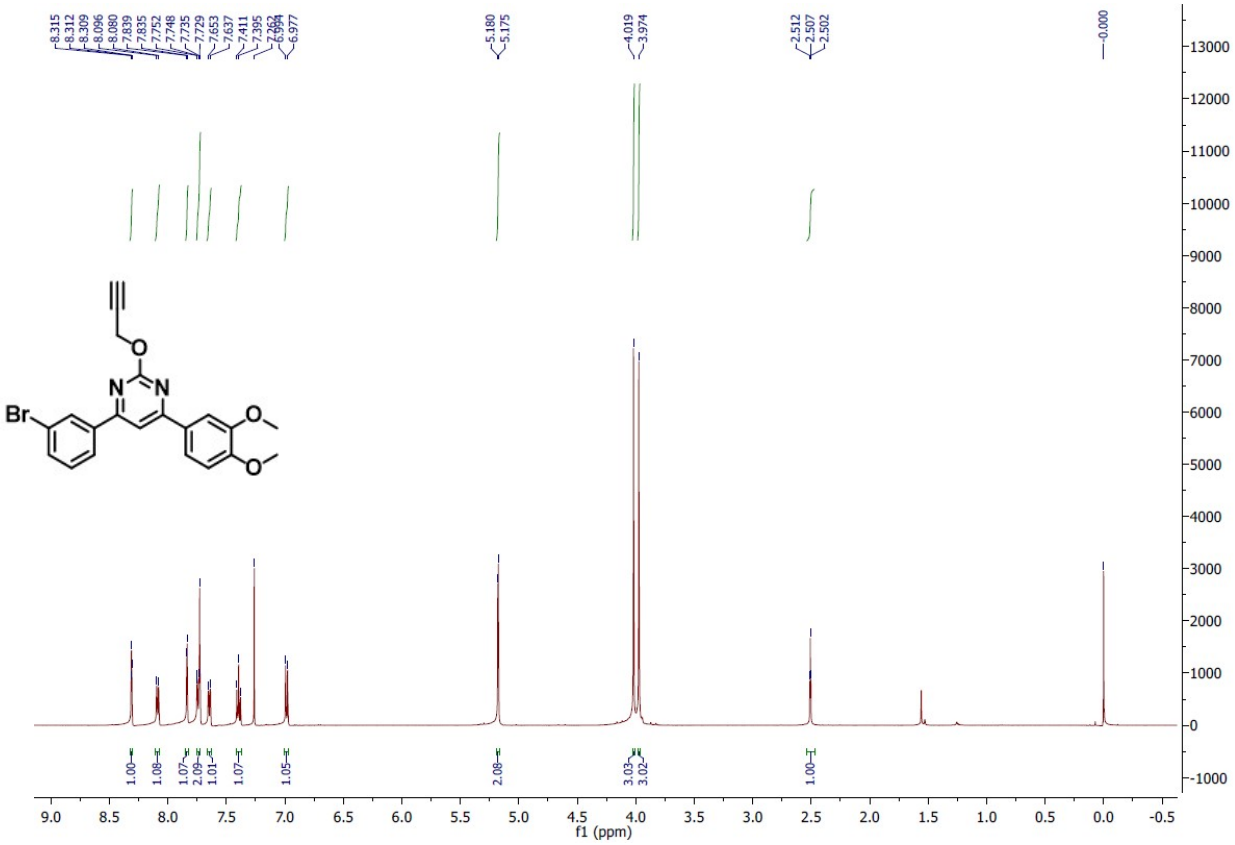

Figure 17: ^1H NMR spectra of 2f

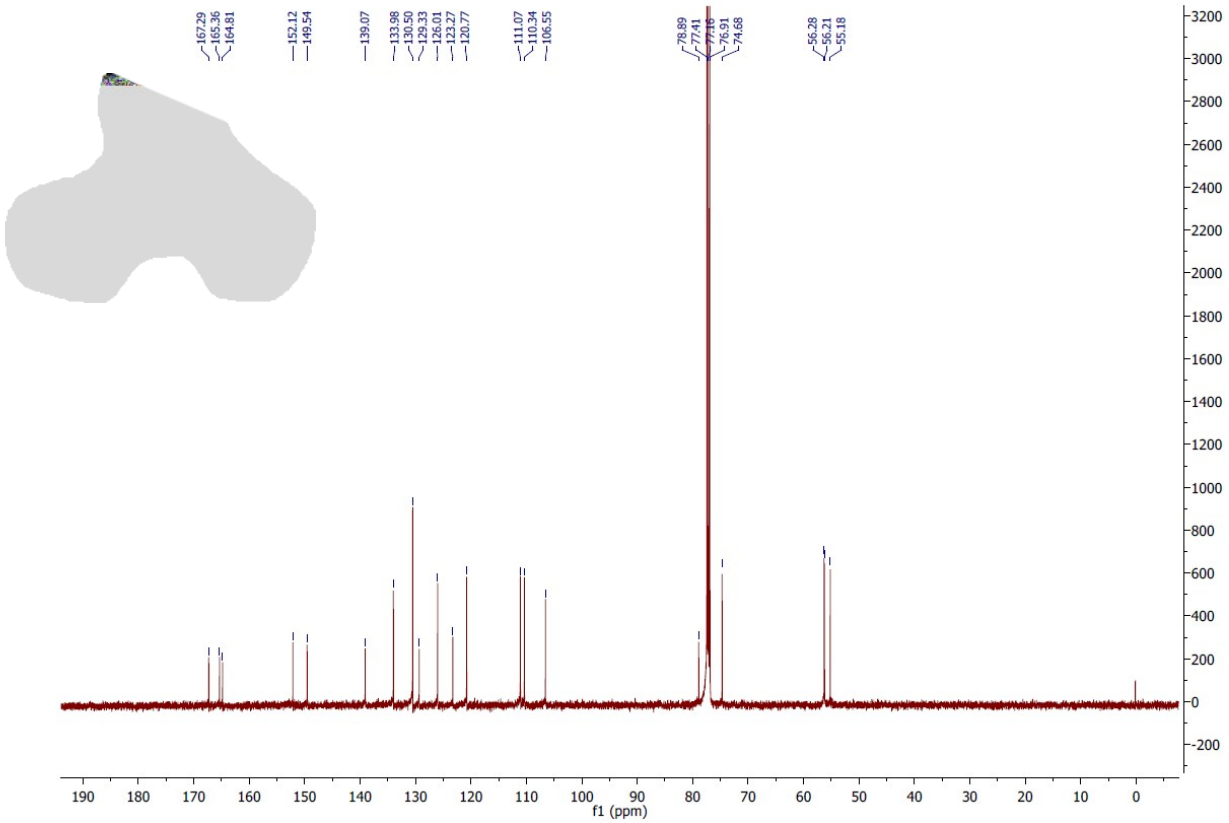

Figure 18: ^{13}C NMR spectra of 2f

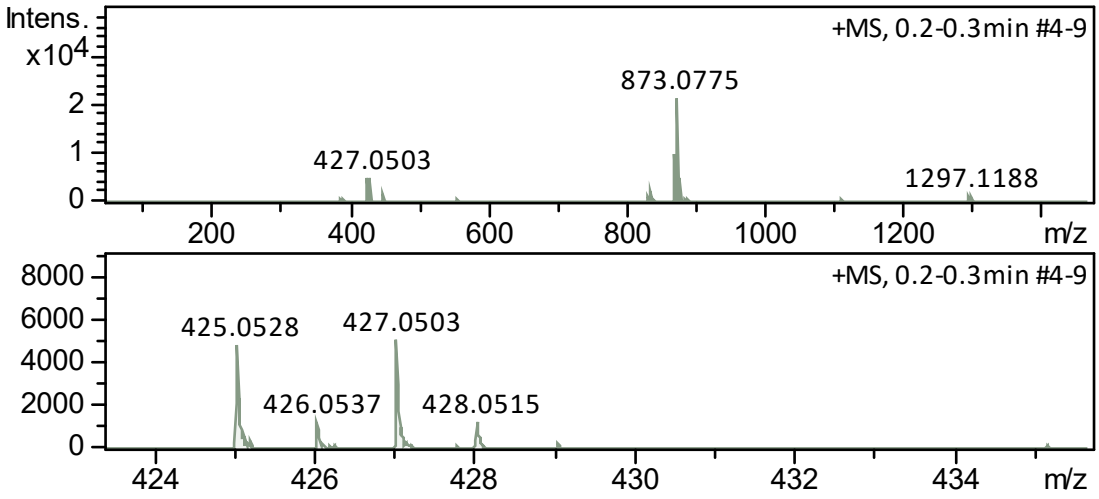

Figure 19: HRMS of 2f: m/z $[M+H]^+$ for $C_{21}H_{18}BrN_2O_3^+$, calculated 425.0500; observed: 425.528

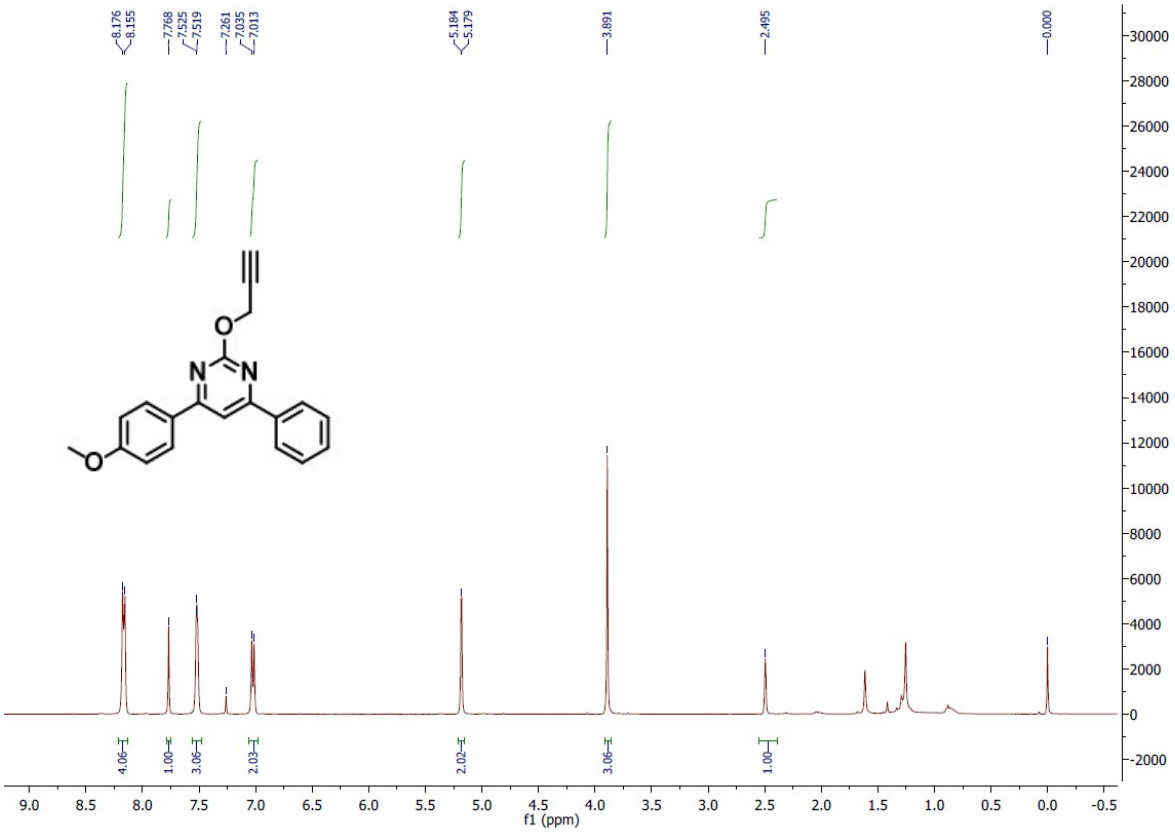

Figure 20: [1]H NMR spectra of 2g

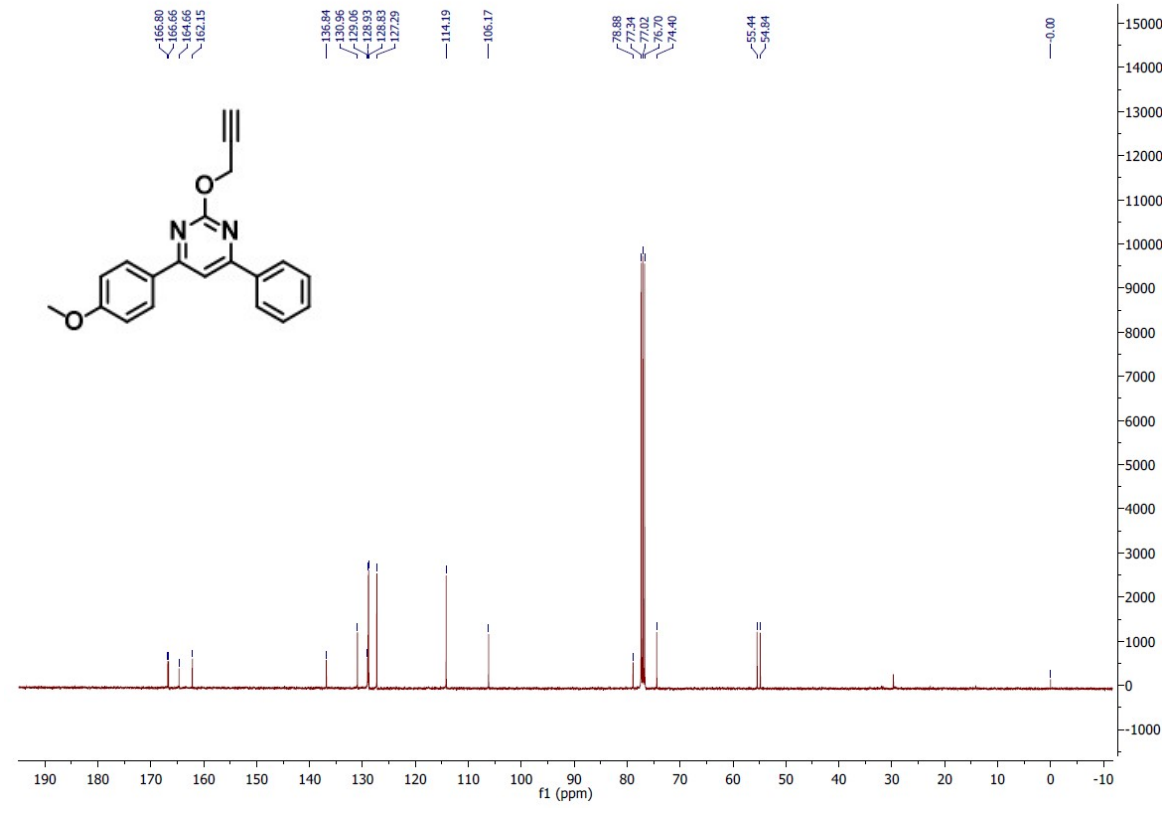

Figure 21: [13]C NMR spectra of 2g

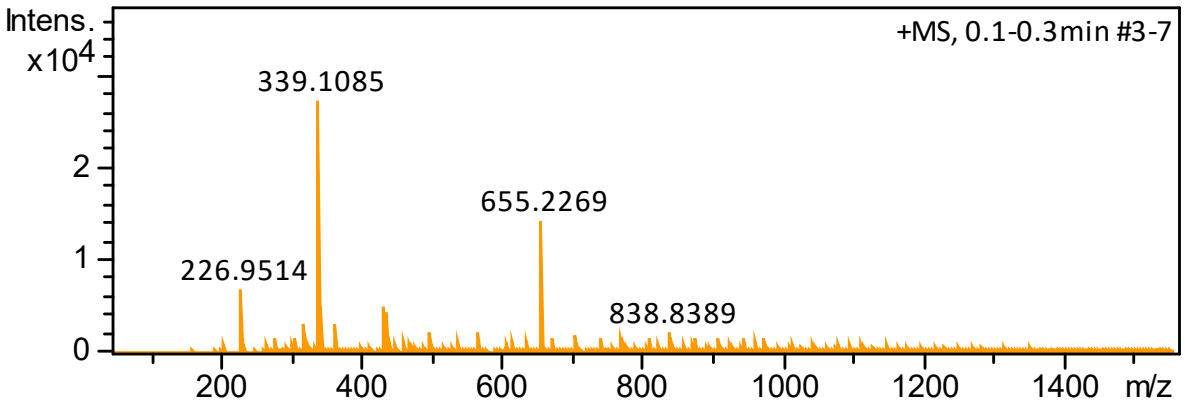

Figure 22: HRMS of 2g: m/z $[M+Na]^+$ for $C_{20}H_{16}N_2NaO_2^+$, calculated 339.1109; observed: 339.1085.

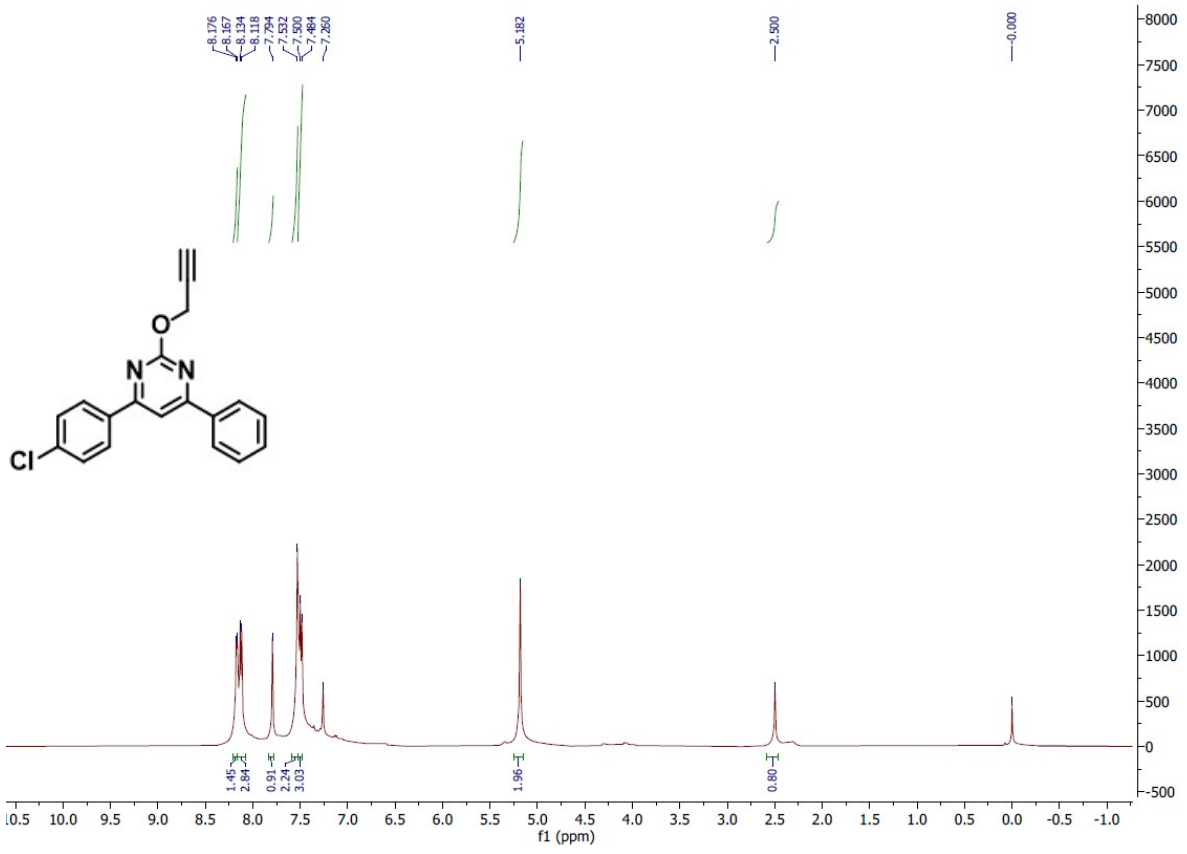

Figure 23: ^1H NMR spectra of 2h

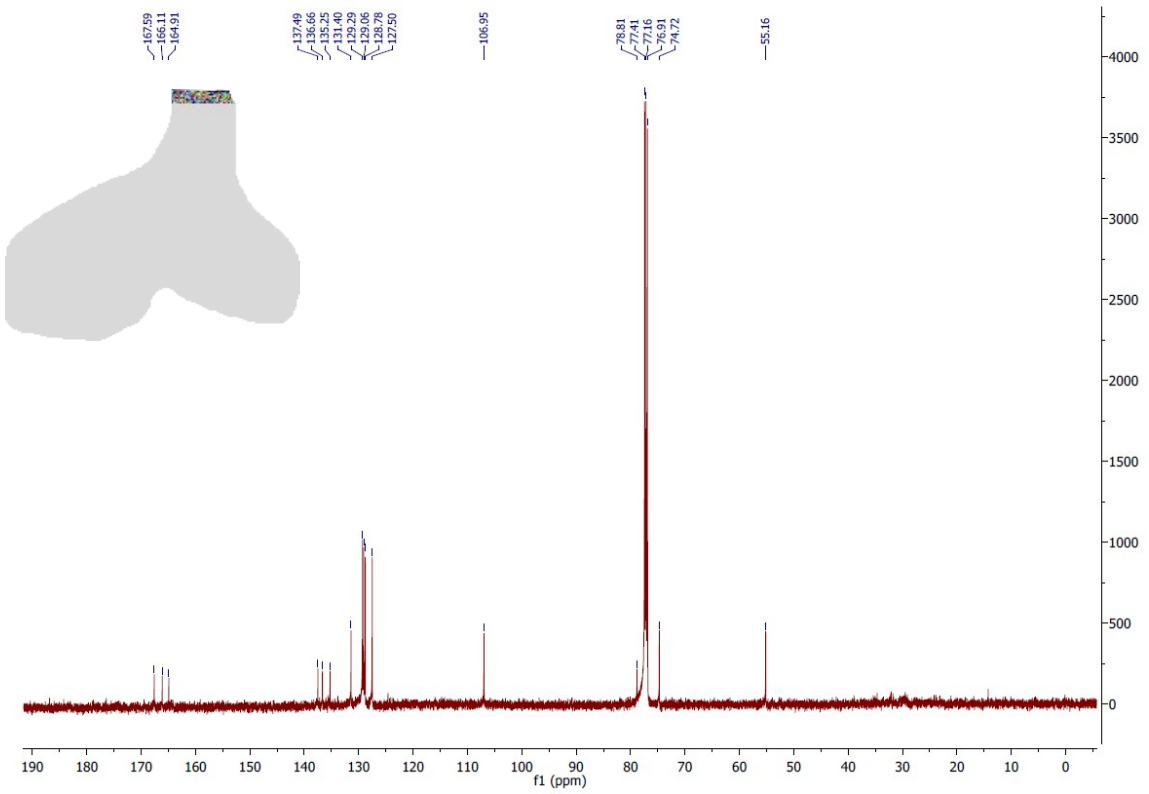

Figure 24: ^{13}C NMR spectra of 2h

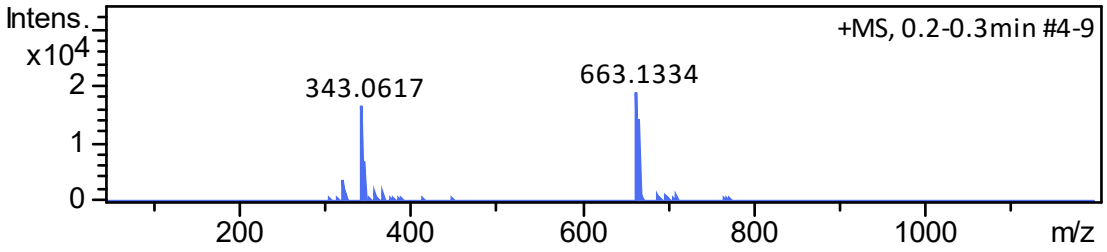

Figure 25: HRMS of 2h: m/z $[M+Na]^+$ for $C_{19}H_{13}ClN_2NaO^+$, calculated 343.0614; observed: 343.0617.

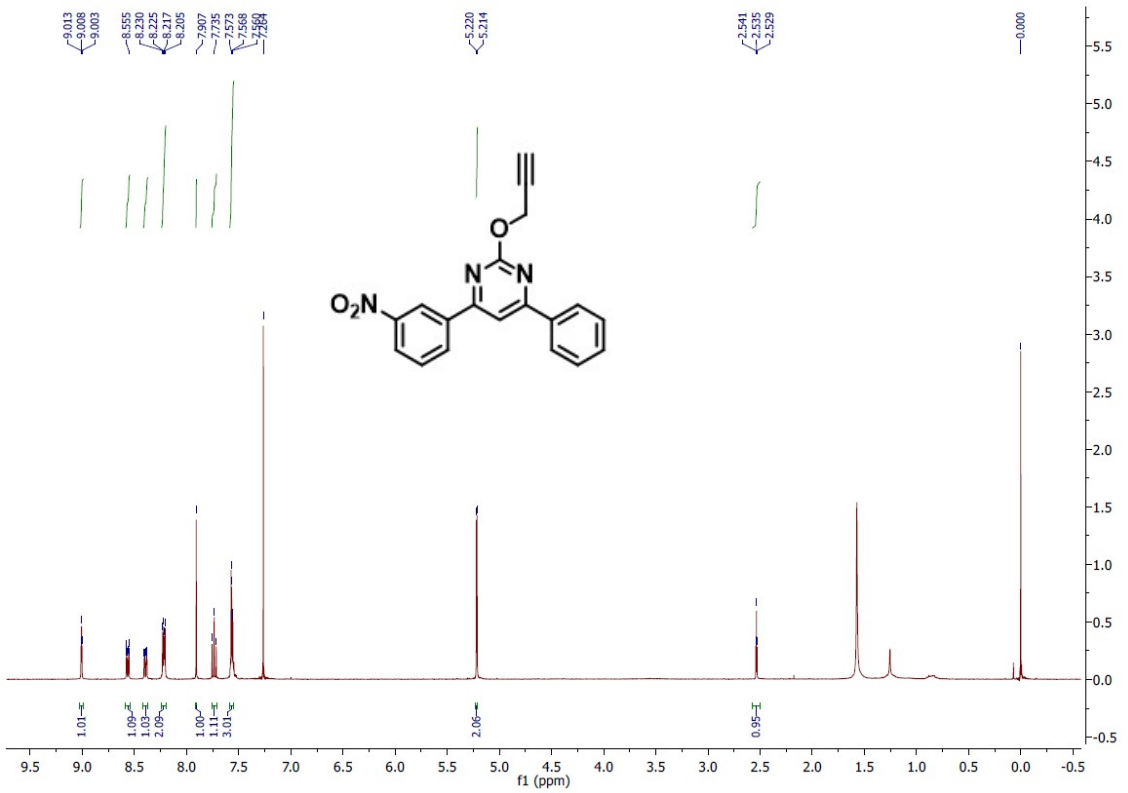

Figure 26: [1]H NMR spectra of 2i

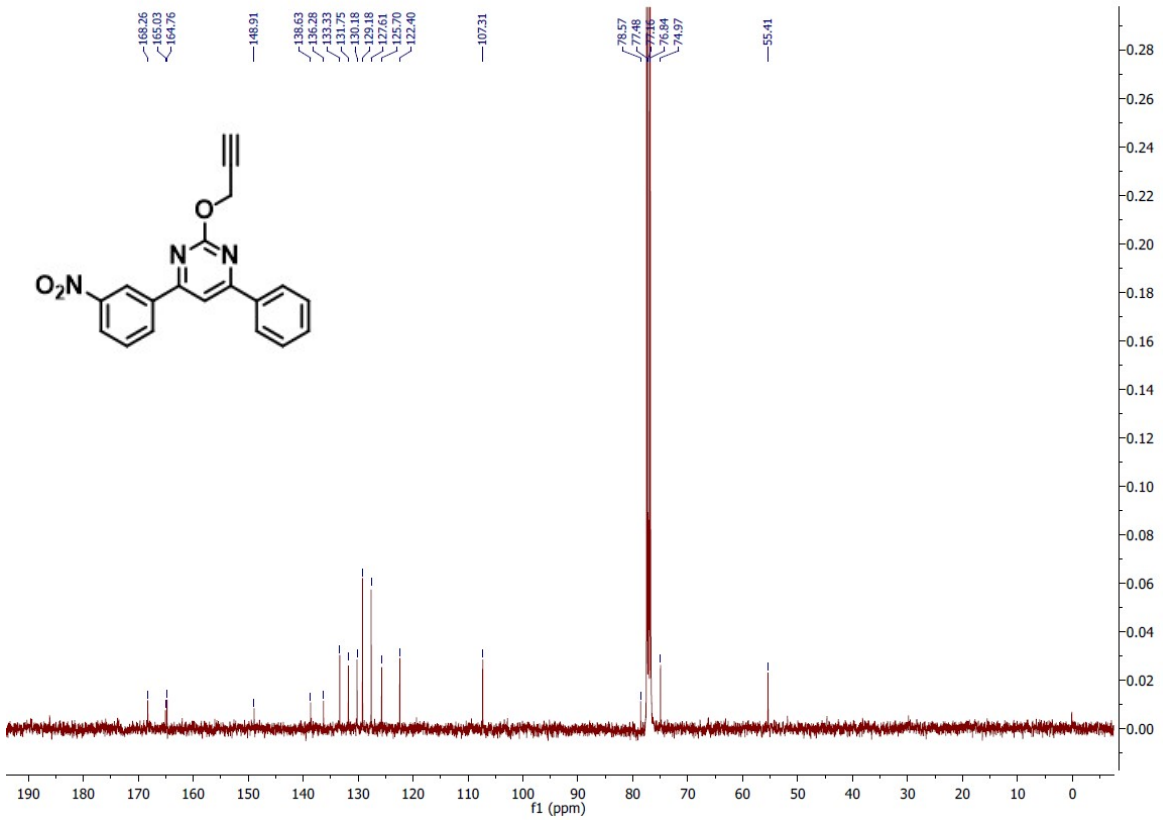

Figure 27: [13]C NMR spectra of 2i

Elemental Composition Report **Page 1**

Single Mass Analysis
Tolerance = 5.0 PPM / DBE: min = -1.5, max = 50.0
Element prediction: Off
Number of isotope peaks used for i-FIT = 5

Monoisotopic Mass, Even Electron Ions
63 formula(e) evaluated with 1 results within limits (up to 50 closest results for each mass)
Elements Used:
C: 11-25 H: 11-26 N: 0-3 O: 0-3 S: 0-2

Sample Name : NKS-118 IITRPR XEVO G2-XS QTOF
Test Name : HRMS-1
010221-NKS-118 17 (0.174) 1: TOF MS ES+
3.09e+006

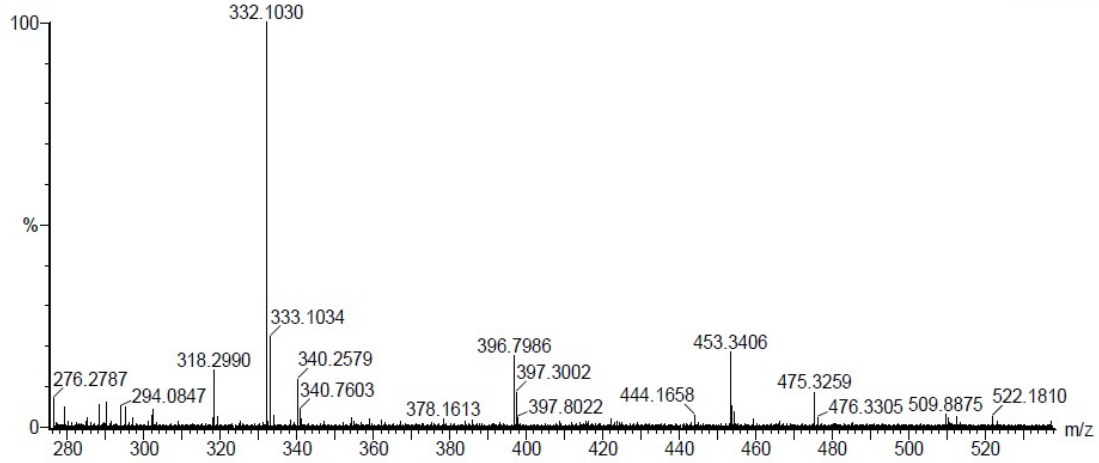

Minimum:				-1.5				
Maximum:		2.0	5.0	50.0				
Mass	Calc. Mass	mDa	PPM	DBE	i-FIT	Norm	Conf(%)	Formula
332.1030	332.1035	-0.5	-1.5	14.5	1291.2	n/a	n/a	C19 H14 N3 O3

Figure 28: HRMS of 2i: m/z $[M+H]^+$ for $C_{19}H_{14}N_3O_3^+$, calculated 332.1035; observed: 332.1030

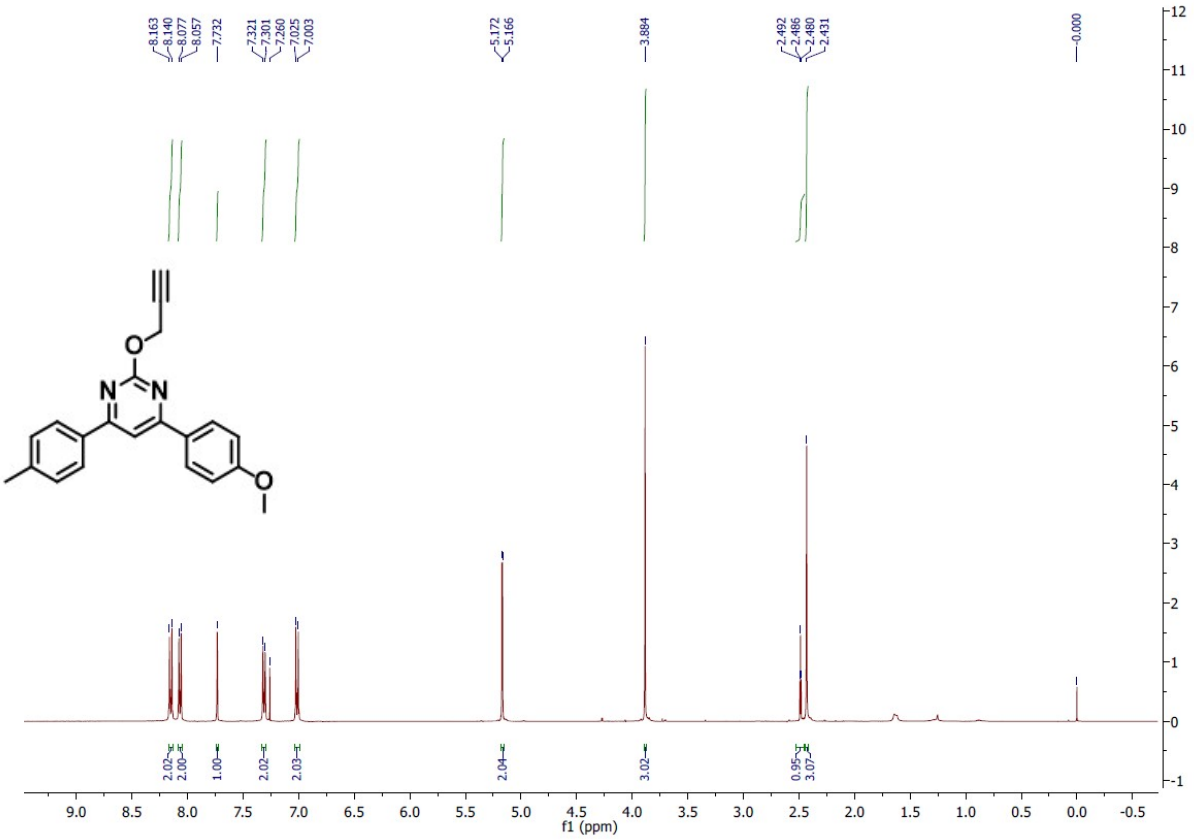

Figure 29: [1]H NMR spectra of 2j

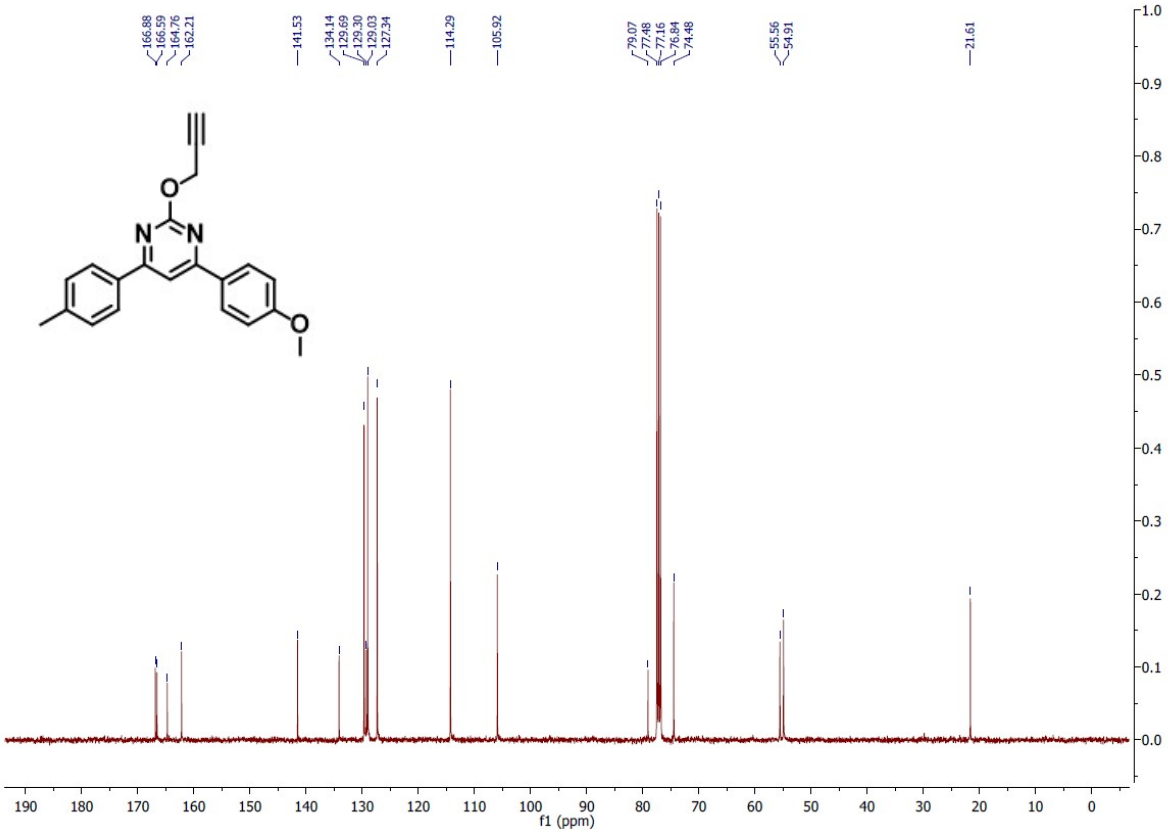

Figure 30: [13]C NMR spectra of 2j

Elemental Composition Report **Page 1**

Single Mass Analysis
Tolerance = 5.0 PPM / DBE: min = -1.5, max = 50.0
Element prediction: Off
Number of isotope peaks used for i-FIT = 5

Monoisotopic Mass, Even Electron Ions
63 formula(e) evaluated with 1 results within limits (up to 50 closest results for each mass)
Elements Used:
C: 11-25 H: 11-26 N: 0-3 O: 0-3 S: 0-2

Sample Name : NKS-114 IITRPR XEVO G2-XS QTOF
Test Name : HRMS-1
010221-NKS-114 18 (0.183) 1: TOF MS ES+
7.90e+007

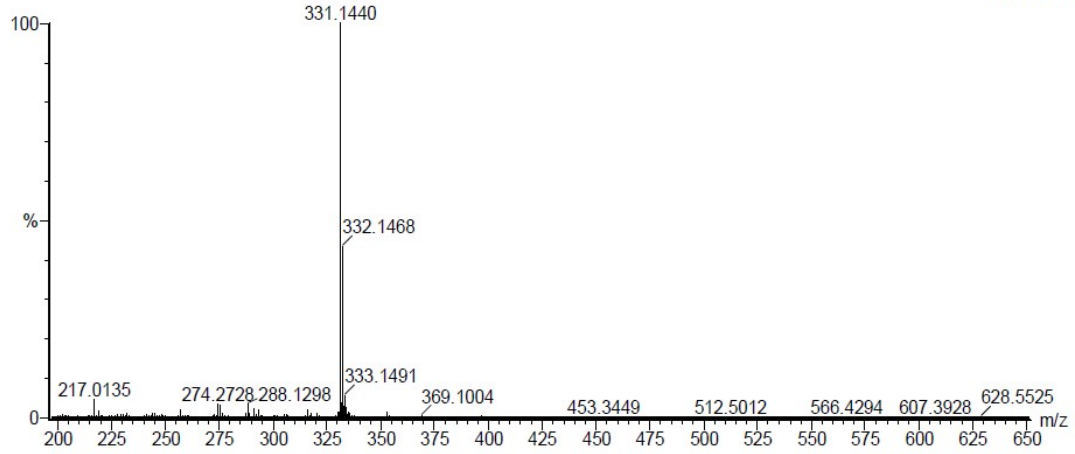

Minimum:				-1.5				
Maximum:		2.0	5.0	50.0				
Mass	Calc. Mass	mDa	PPM	DBE	i-FIT	Norm	Conf(%)	Formula
331.1440	331.1447	-0.7	-2.1	13.5	1798.8	n/a	n/a	C21 H19 N2 O2

Figure 31: HRMS of 2j: m/z $[M+H]^+$ for $C_{21}H_{19}N_2O_2$+, calculated 331.1447; observed: 331.1440

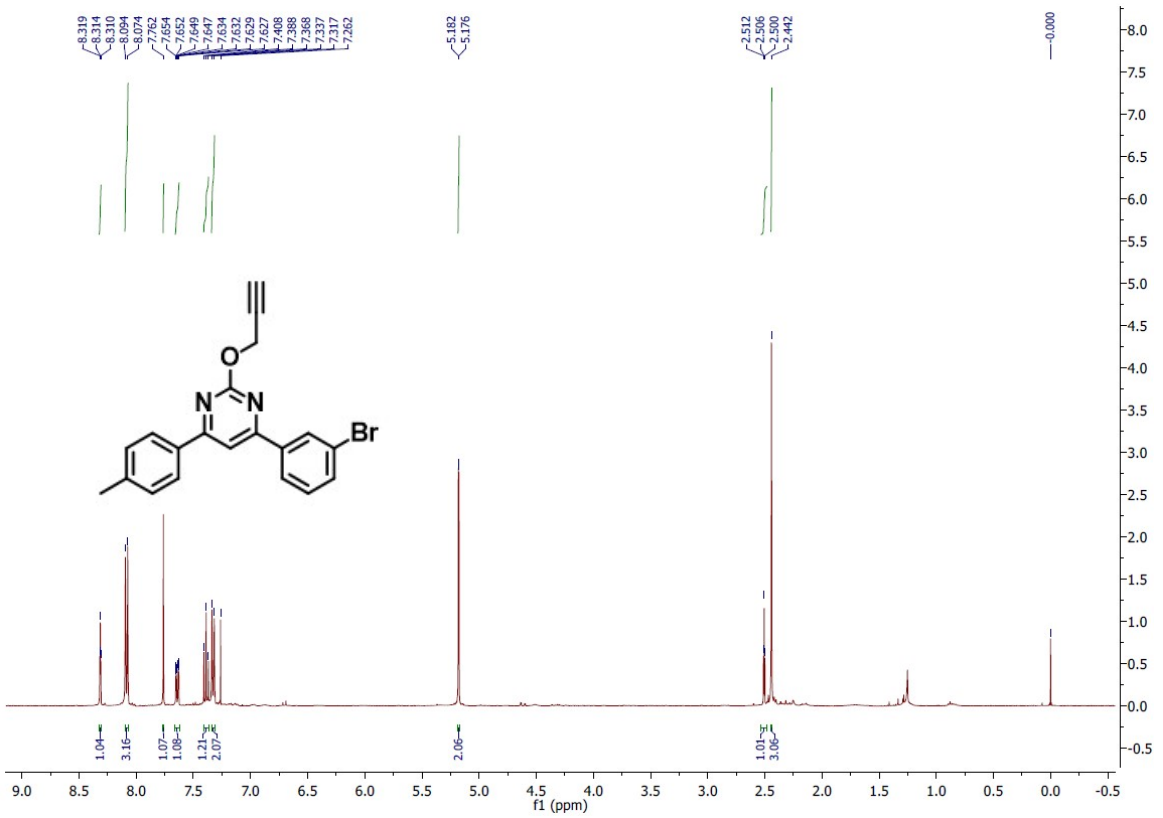

Figure 32: [1]H NMR spectra of 2k

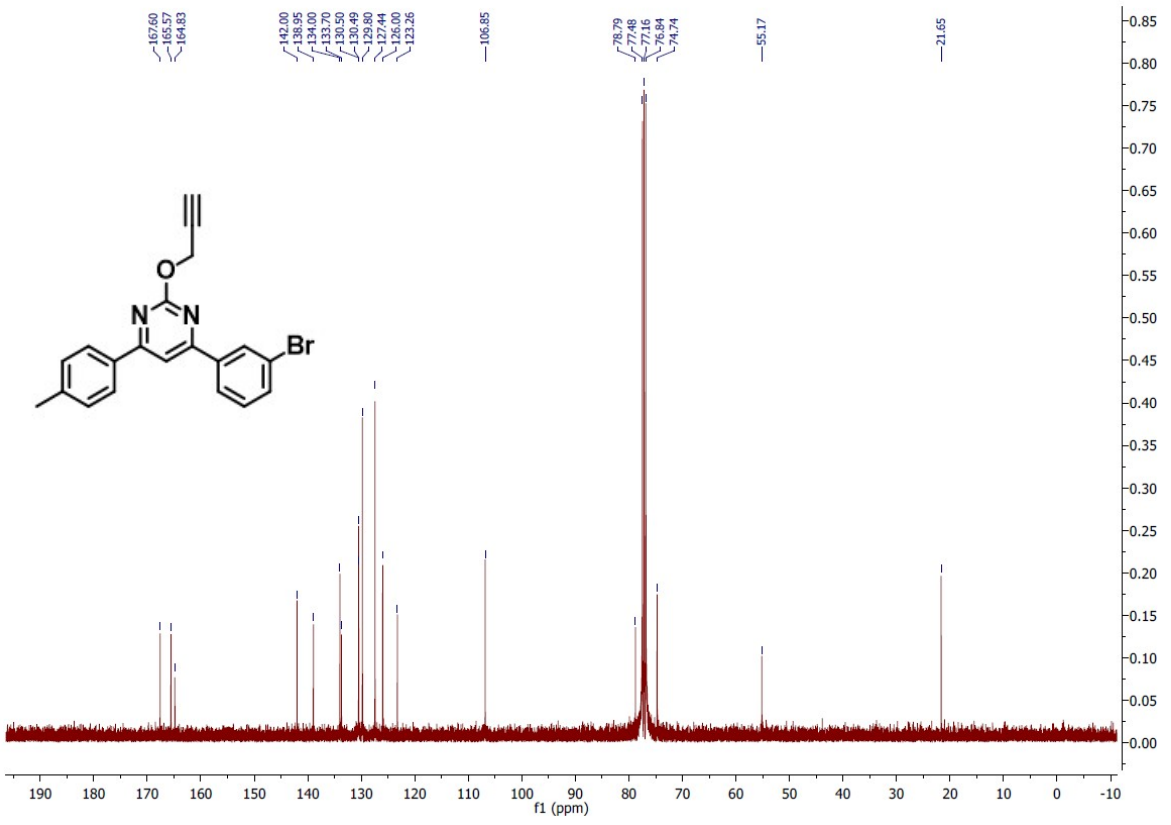

Figure 33: [13]C NMR spectra of 2k

Elemental Composition Report **Page 1**

Single Mass Analysis
Tolerance = 5.0 PPM / DBE: min = -1.5, max = 50.0
Element prediction: Off
Number of isotope peaks used for i-FIT = 5

Monoisotopic Mass, Even Electron Ions
48 formula(e) evaluated with 1 results within limits (up to 50 closest results for each mass)
Elements Used:
C: 11-25 H: 11-26 N: 0-3 O: 0-3 Br: 0-2

Sample Name : NKS-113
Test Name : HRMS-1
010221-NKS-113 19 (0.203)

IITRPR

XEVO G2-XS QTOF
1: TOF MS ES+
3.78e+007

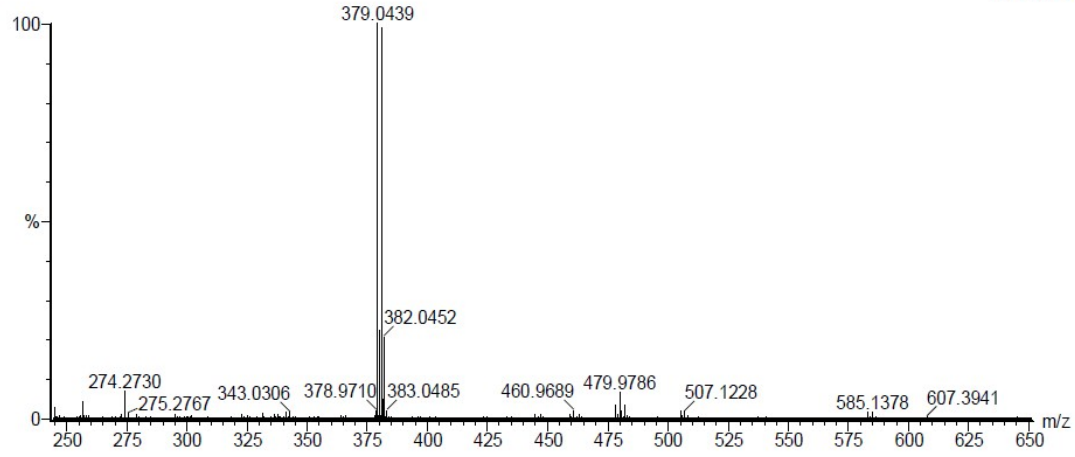

Minimum:				-1.5				
Maximum:		2.0	5.0	50.0				
Mass	Calc. Mass	mDa	PPM	DBE	i-FIT	Norm	Conf(%)	Formula
379.0439	379.0446	-0.7	-1.8	13.5	1567.5	n/a	n/a	C20 H16 N2 O Br

Figure 34:HRMS of 2k: m/z [M+H]$^+$ for $C_{20}H_{16}BrN_2O^+$, calculated 379.0446; observed: 379.0439

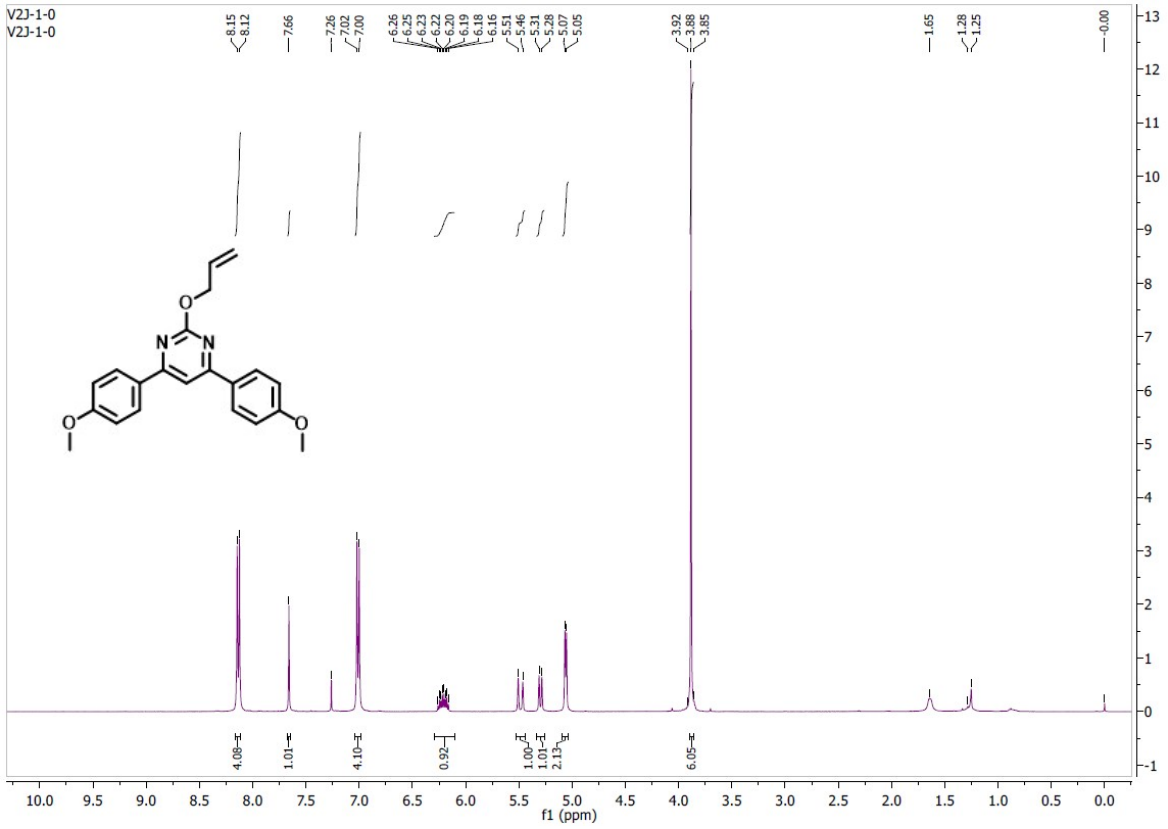

Figure 35: [1]H NMR spectra of 2l

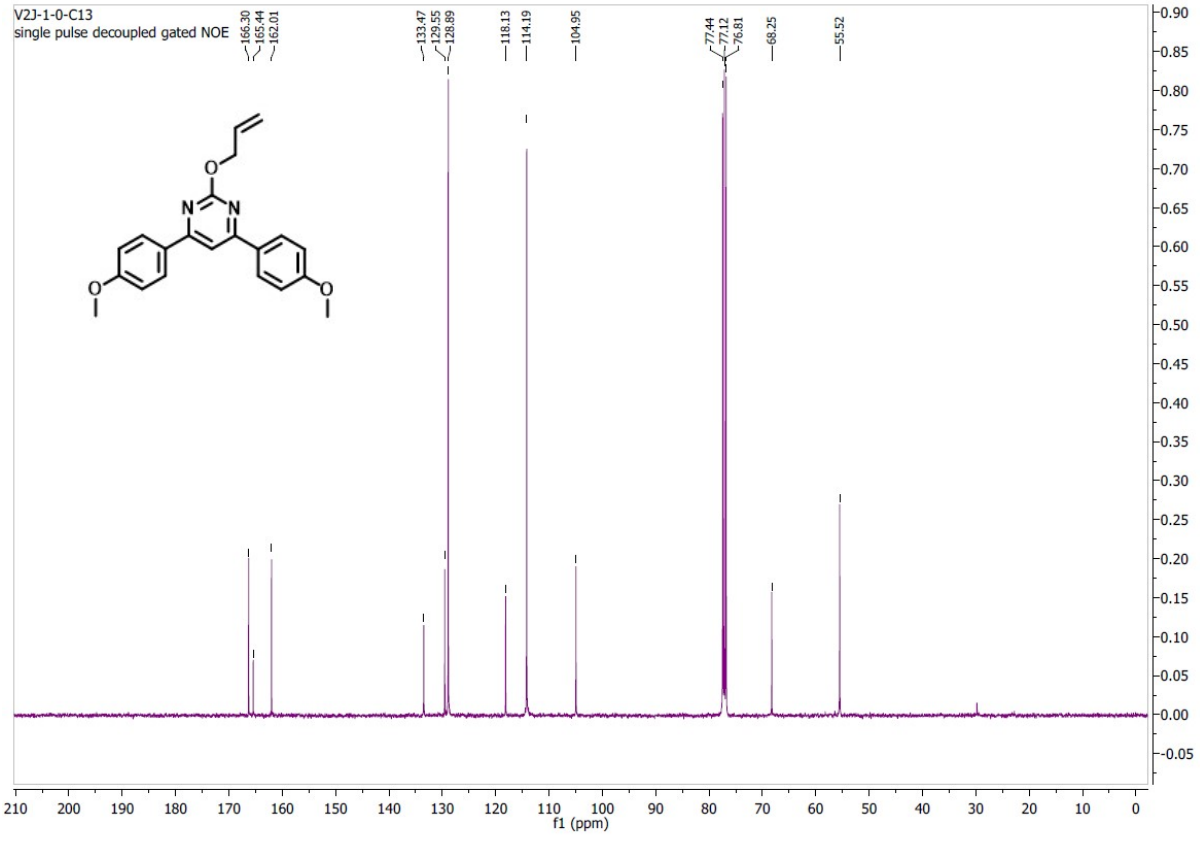

Figure 36: [13]C NMR spectra of 2l

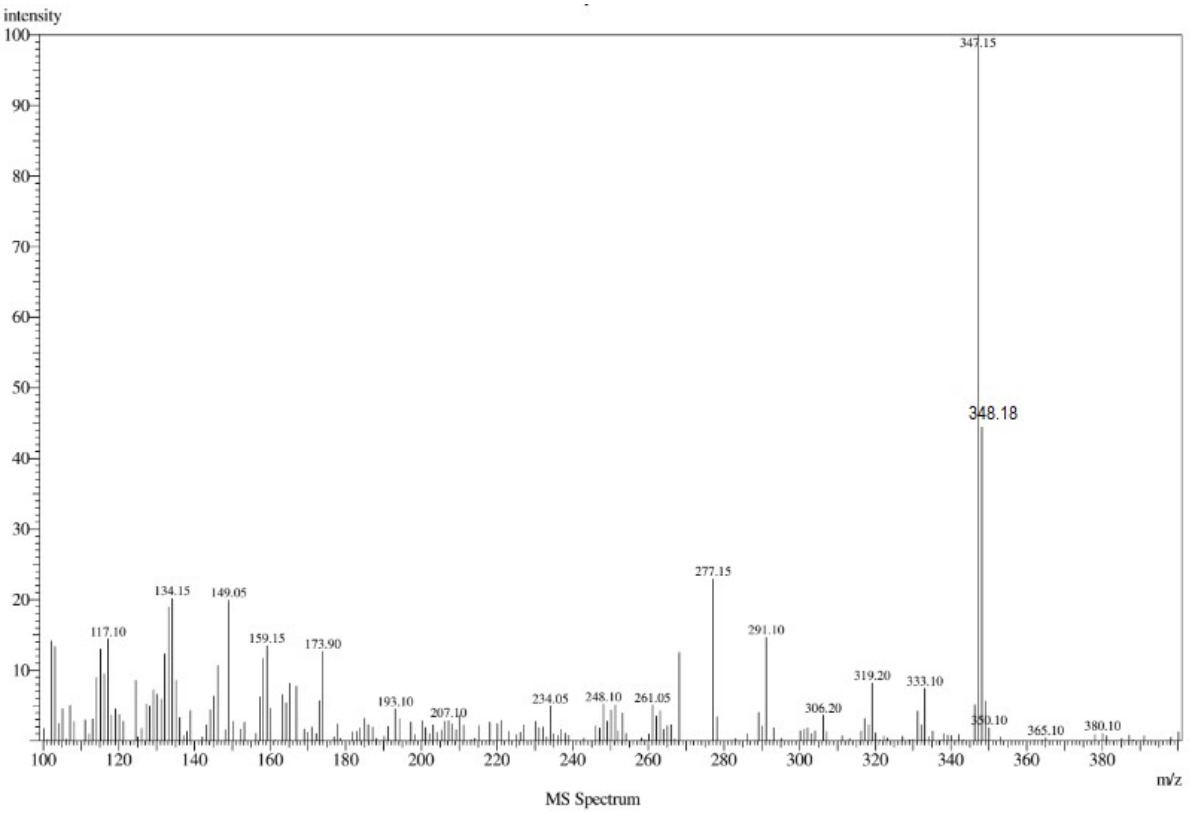

Figure 37: EI-MS of 2l: $[M]^+$ for $C_{21}H_{20}N_2O_3^+$ calculated: 348.15; observed: 347.18.

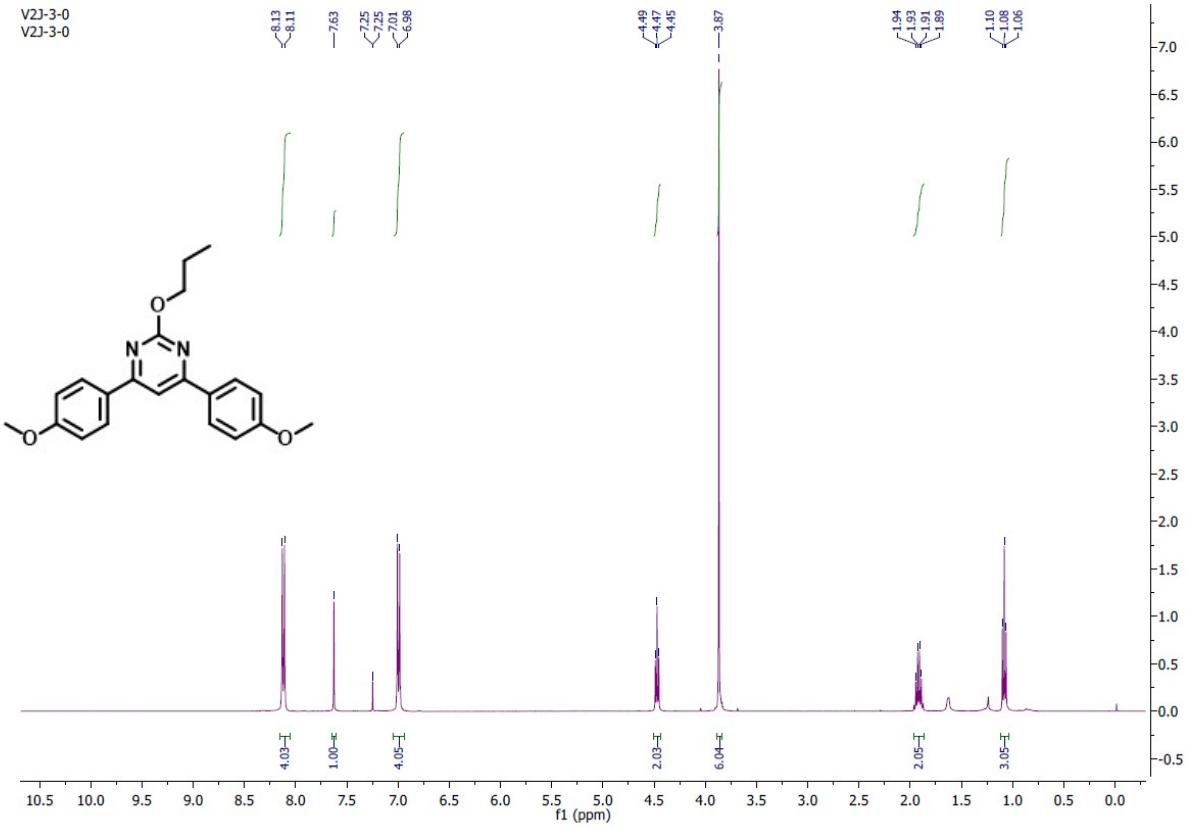

Figure 38: [1]H NMR spectra of 2m

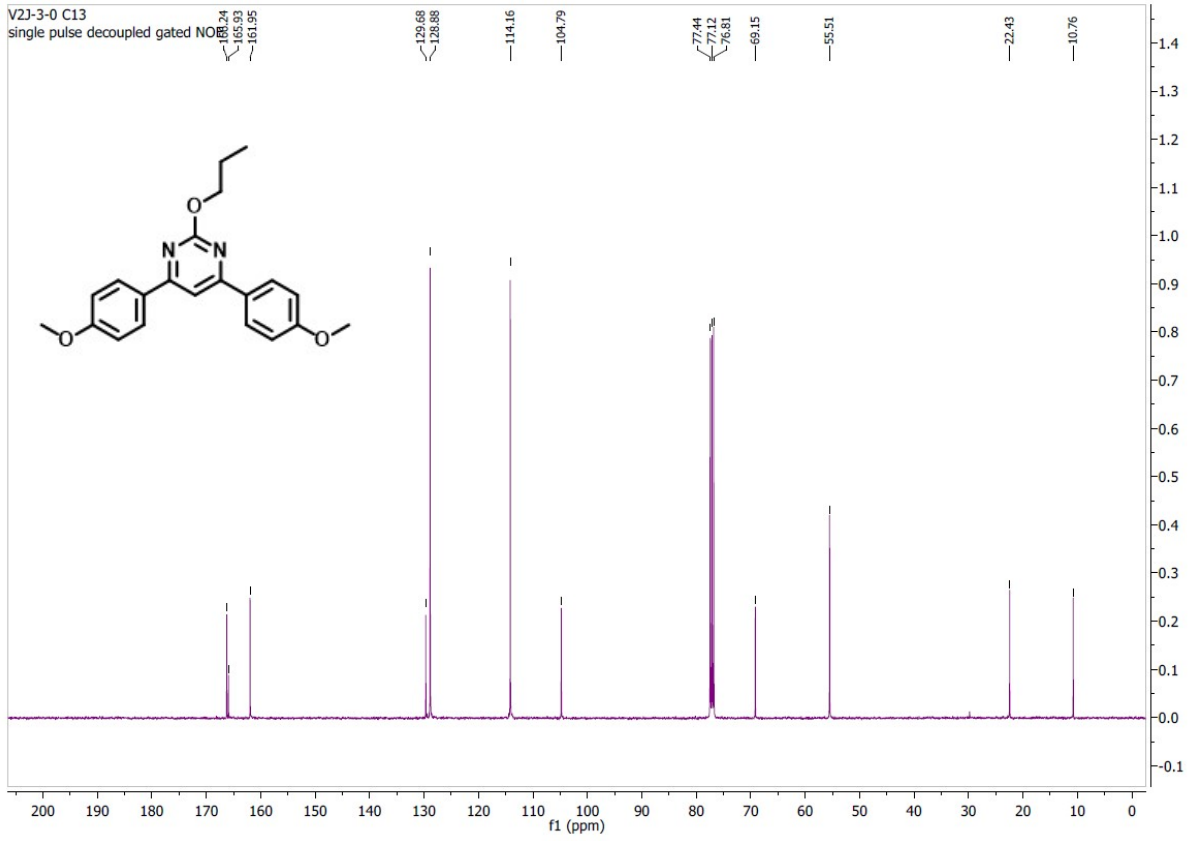

Figure 39: [13]C NMR spectra of 2m

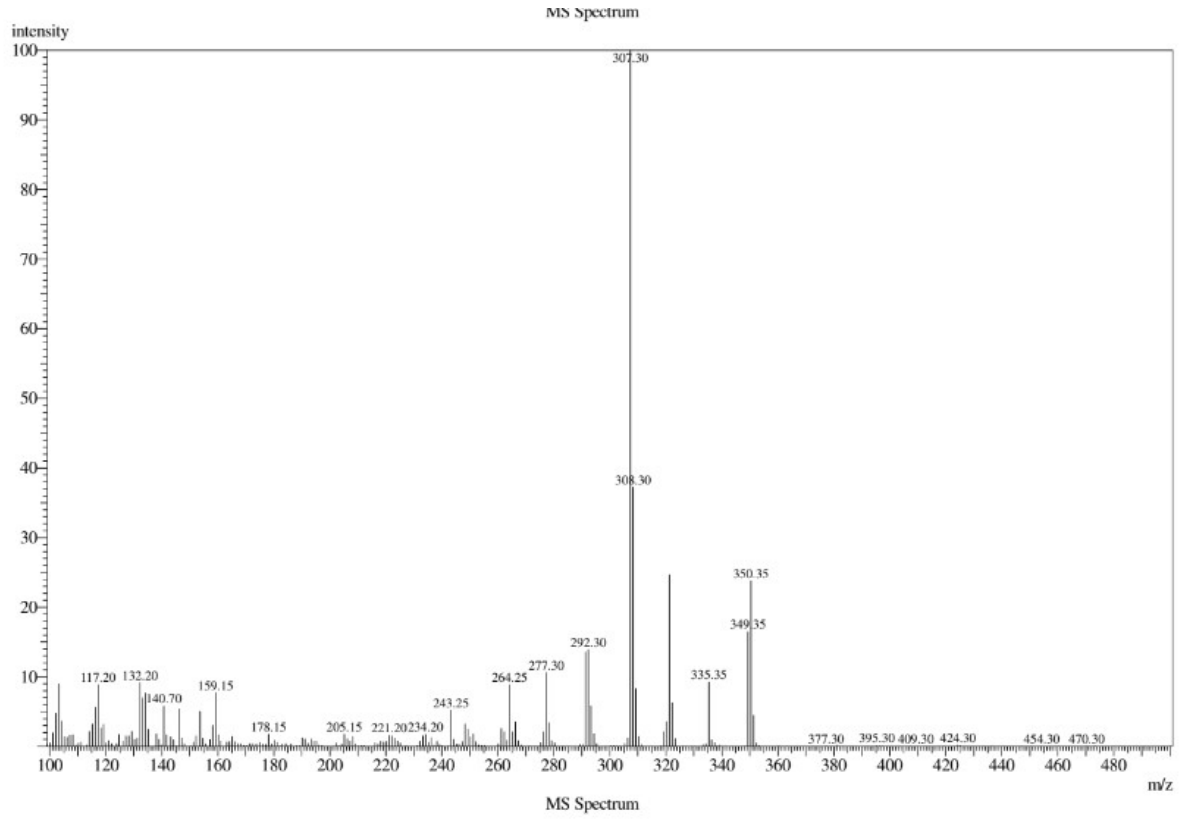

Figure 40: EI-MS of 2m: m/z $[M]^+$ for $C_{21}H_{22}N_2O_3^+$ calculated: 350.16; observed: 350.35.

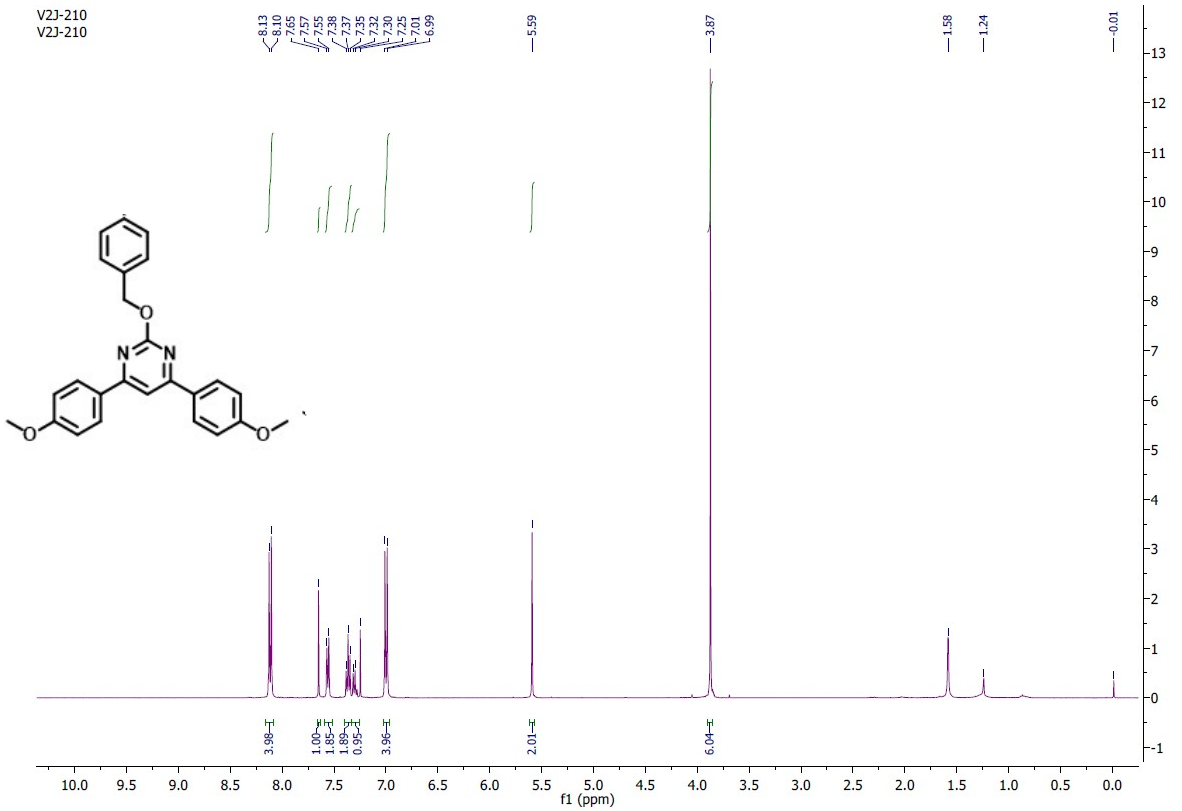

Figure 41: [1]H NMR spectra of 2n

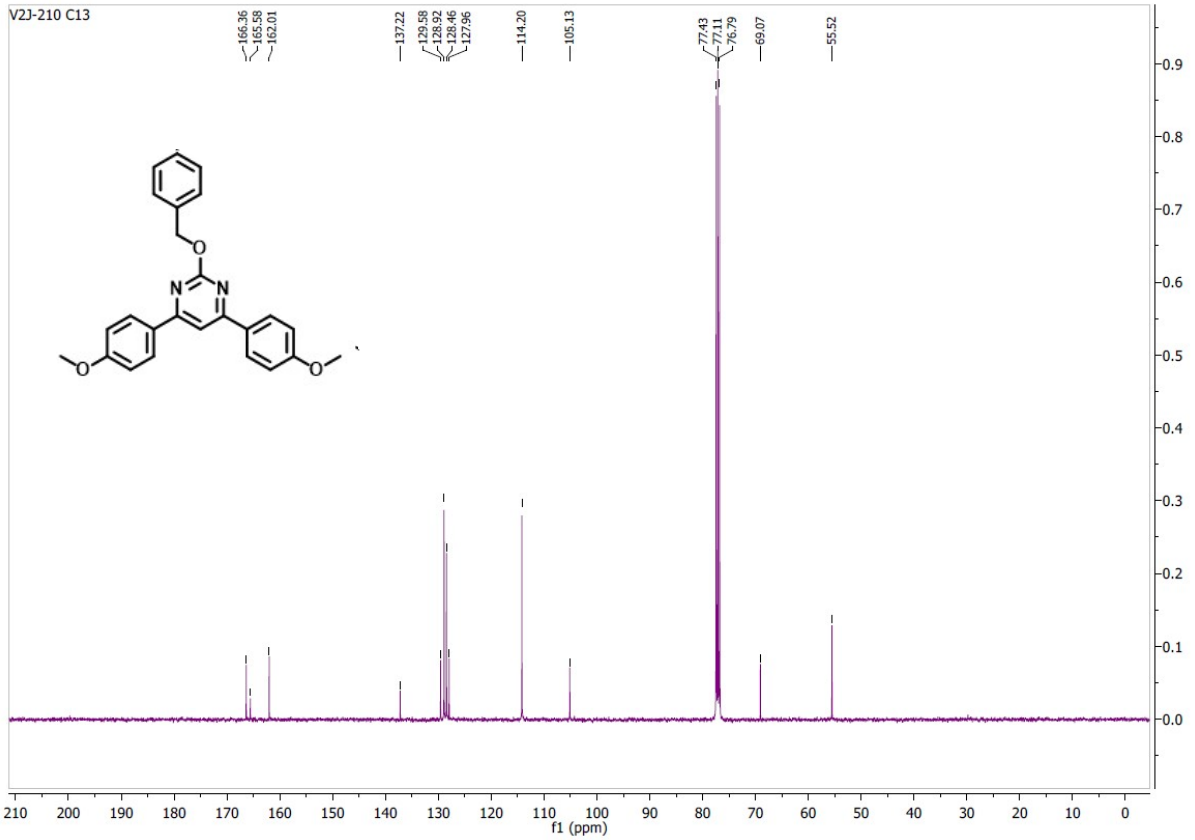

Figure 42: [13]C NMR spectra of 2n

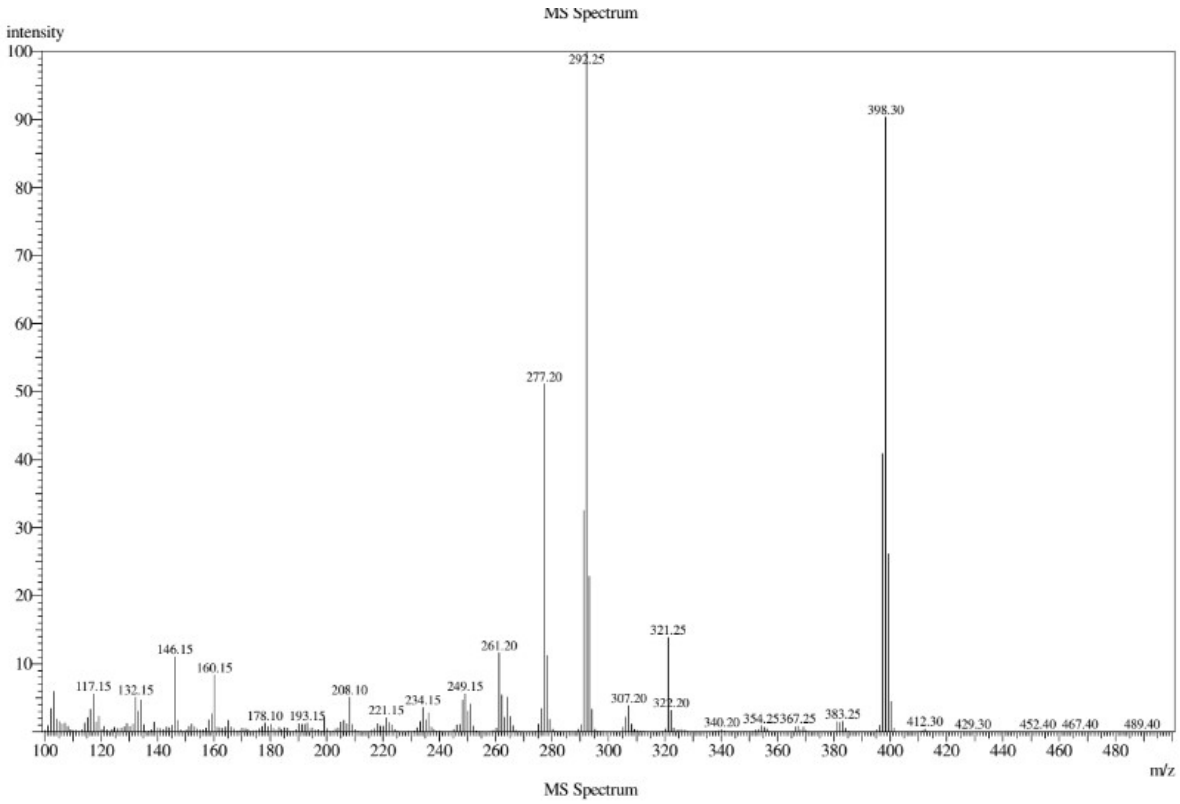

Figure 43: *EI-MS of 2n: m/z [M]$^+$ for $C_{25}H_{22}N_2O_3$ calculated: 398.16; observed: 398.30.*

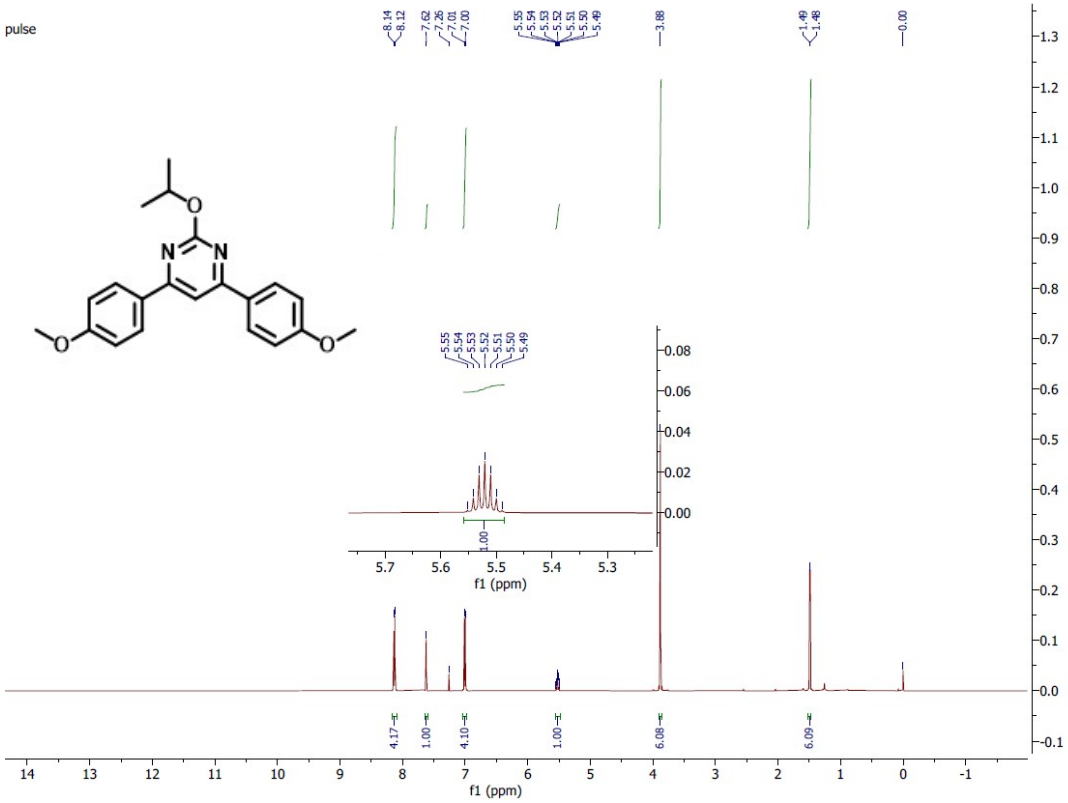

Figure 44: ^{1}H NMR spectra of 2o

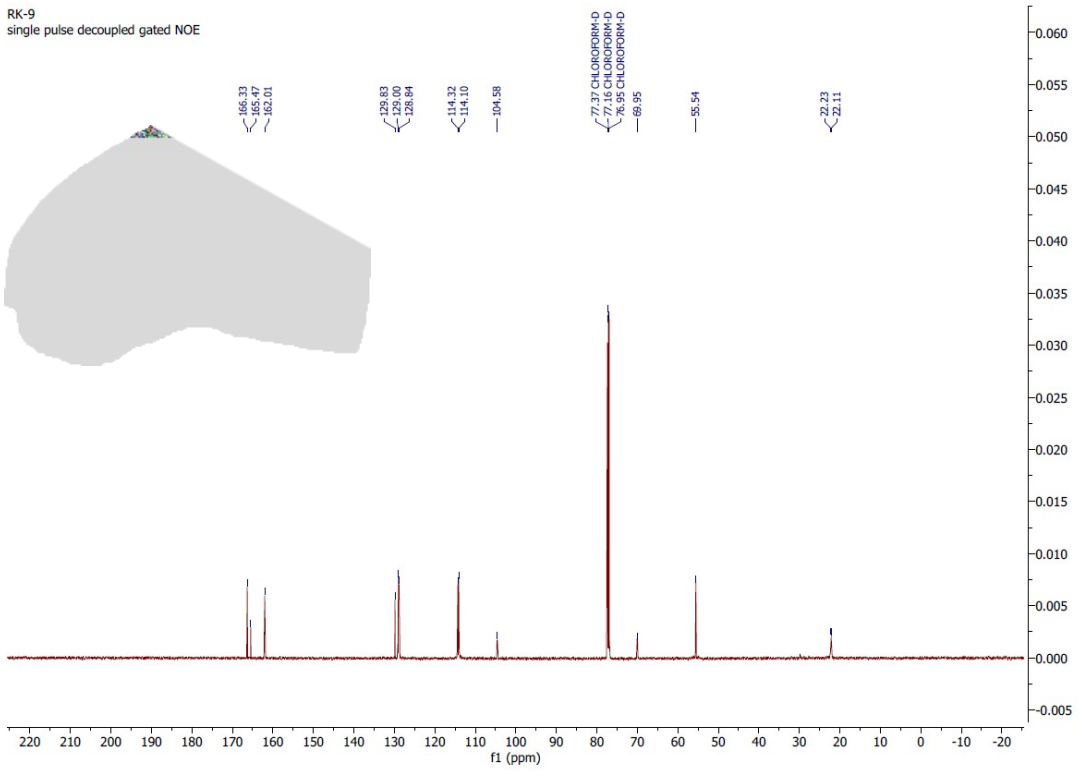

Figure 45: ^{13}C NMR spectra of 2o

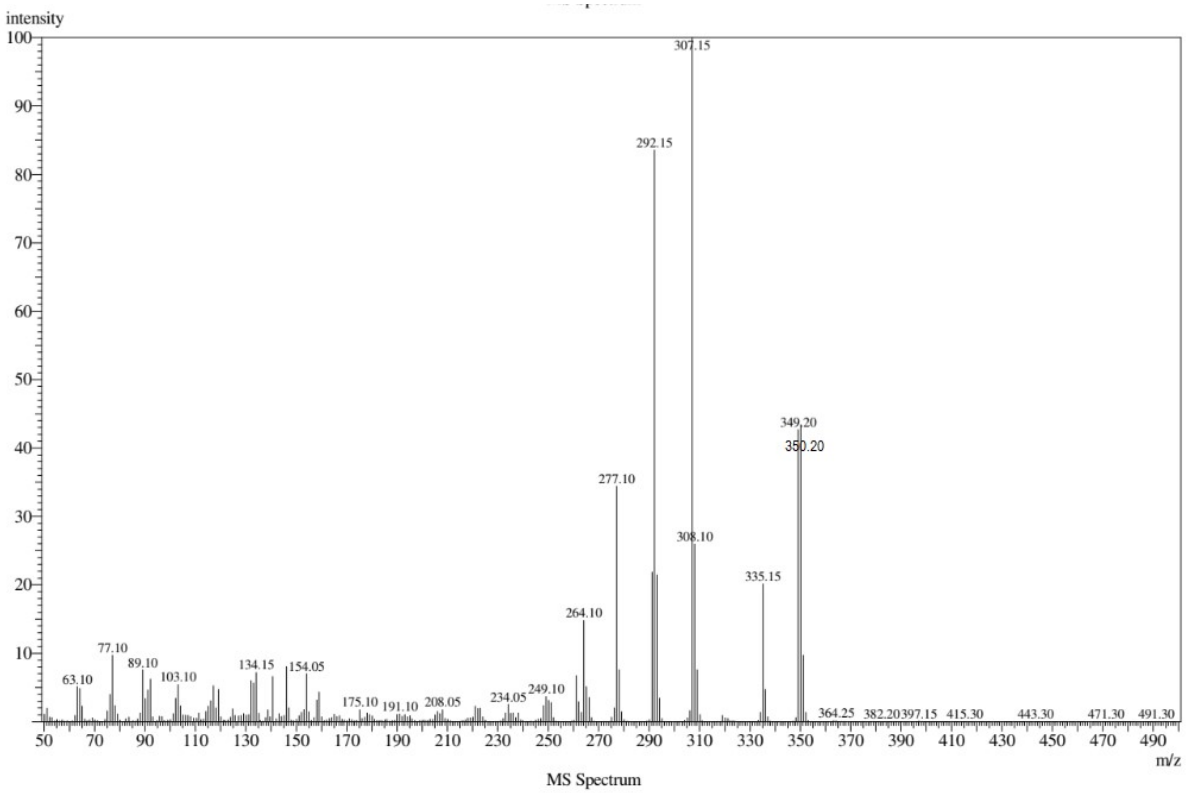

Figure 46: EI-MS of 2o: m/z $[M]^+$ for $C_{21}H_{22}N_2O_3^+$ calculated: 350.16; observed: 350.20.

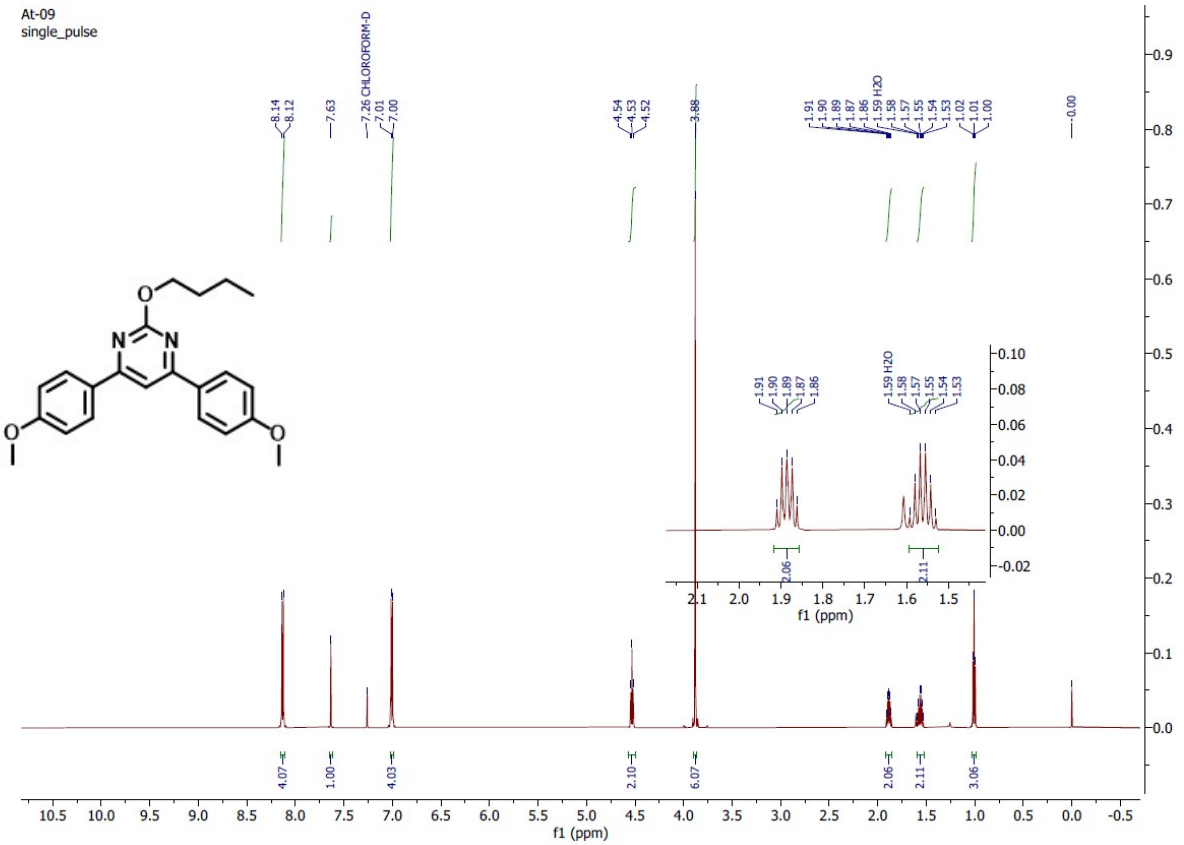

Figure 47: [1]H NMR spectra of 2p

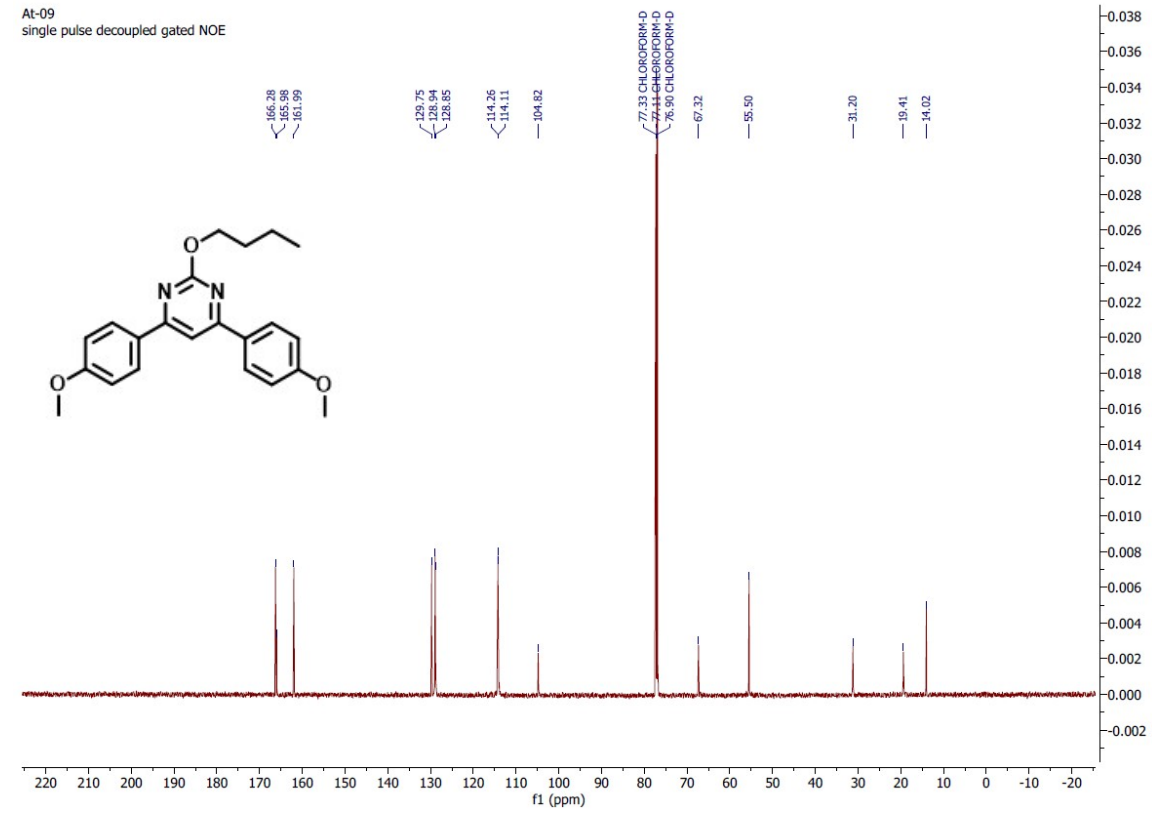

Figure 48: [13]C NMR spectra of 2p

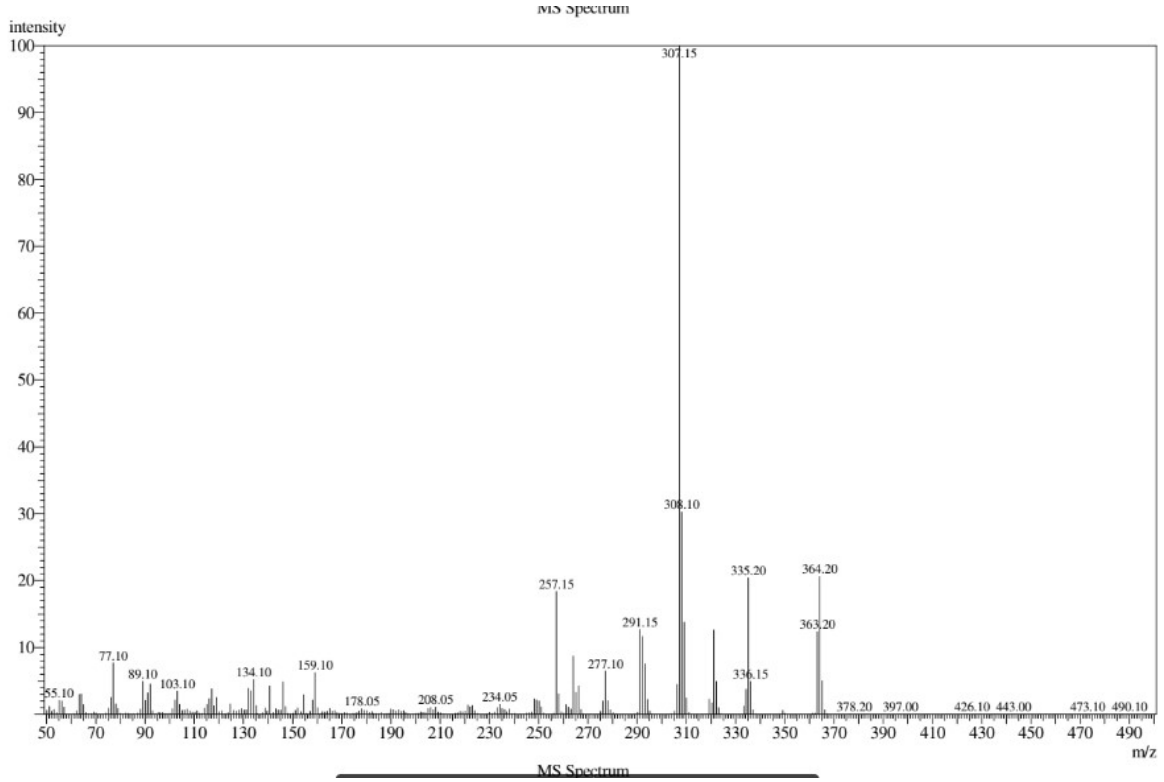

Figure 49: EI-MS of 2p: m/z [M]$^+$ for $C_{22}H_{24}N_2O_3^+$ calculated: 364.45; observed: 364.20.

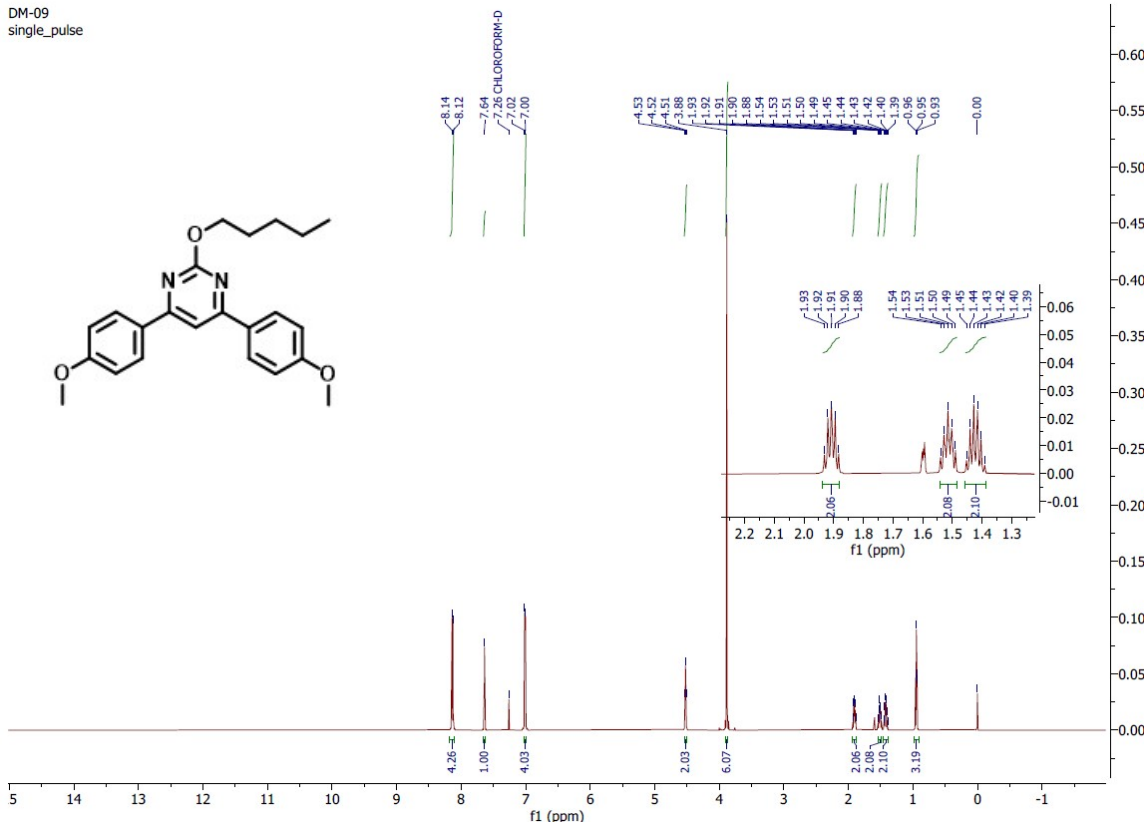

Figure 50: ^{1}H NMR spectra of 2q

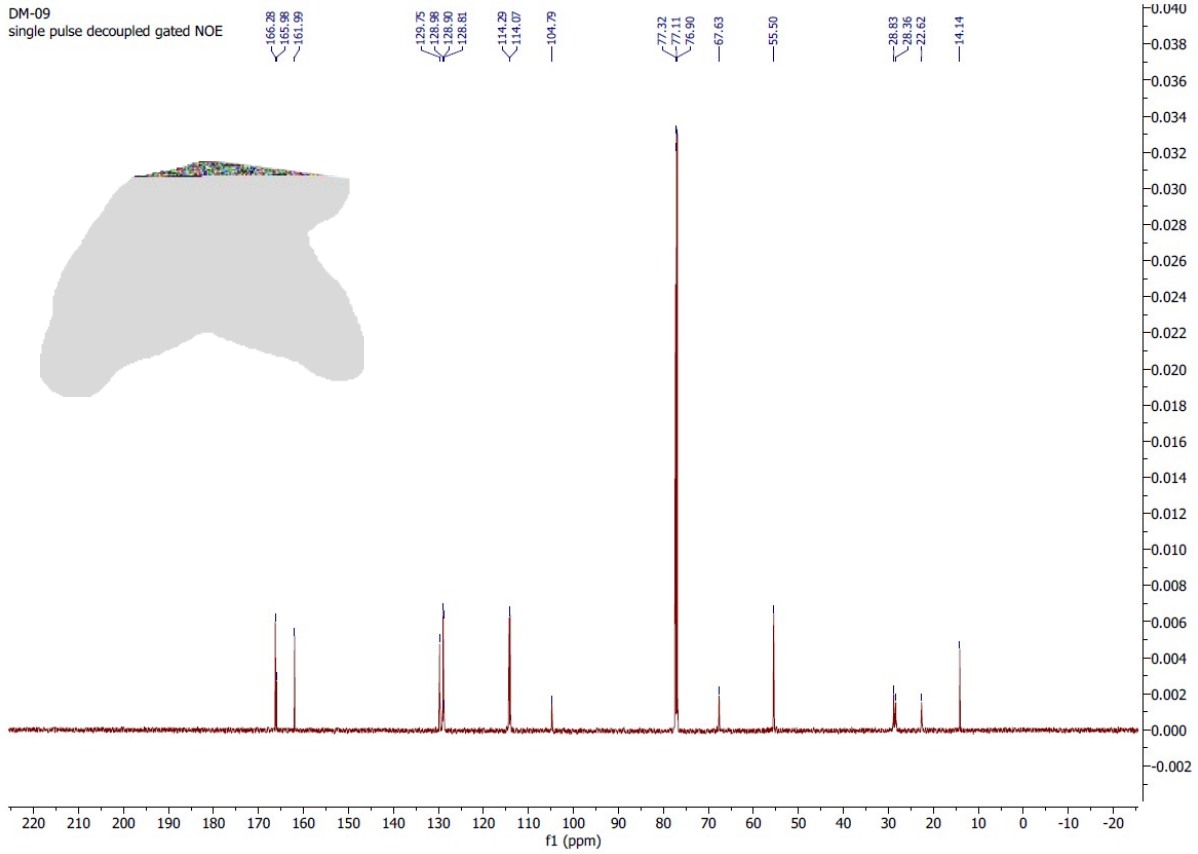

Figure 51: ^{13}C NMR spectra of 2q

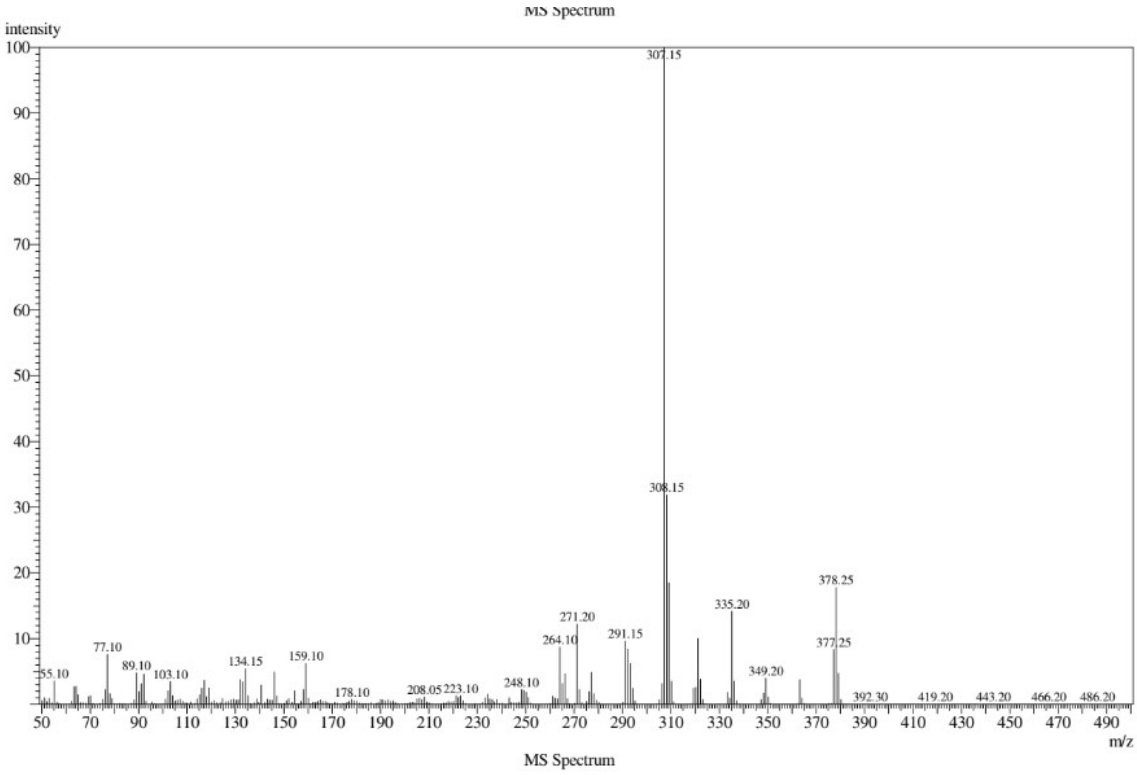

Figure 52: EI-MS of 2q: m/z $[M]^+$ for $C_{23}H_{26}N_2O_3^+$ calculated: 348.47; observed: 378.25.

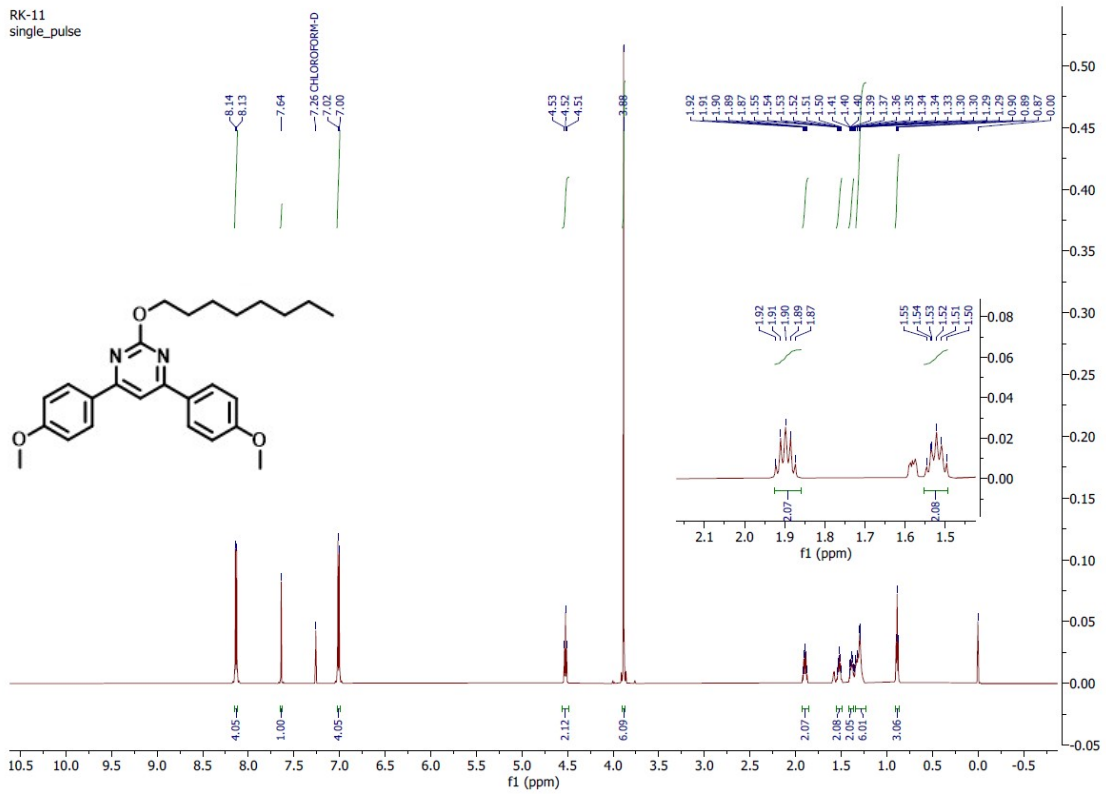

Figure 53: [1]H NMR spectra of 2r

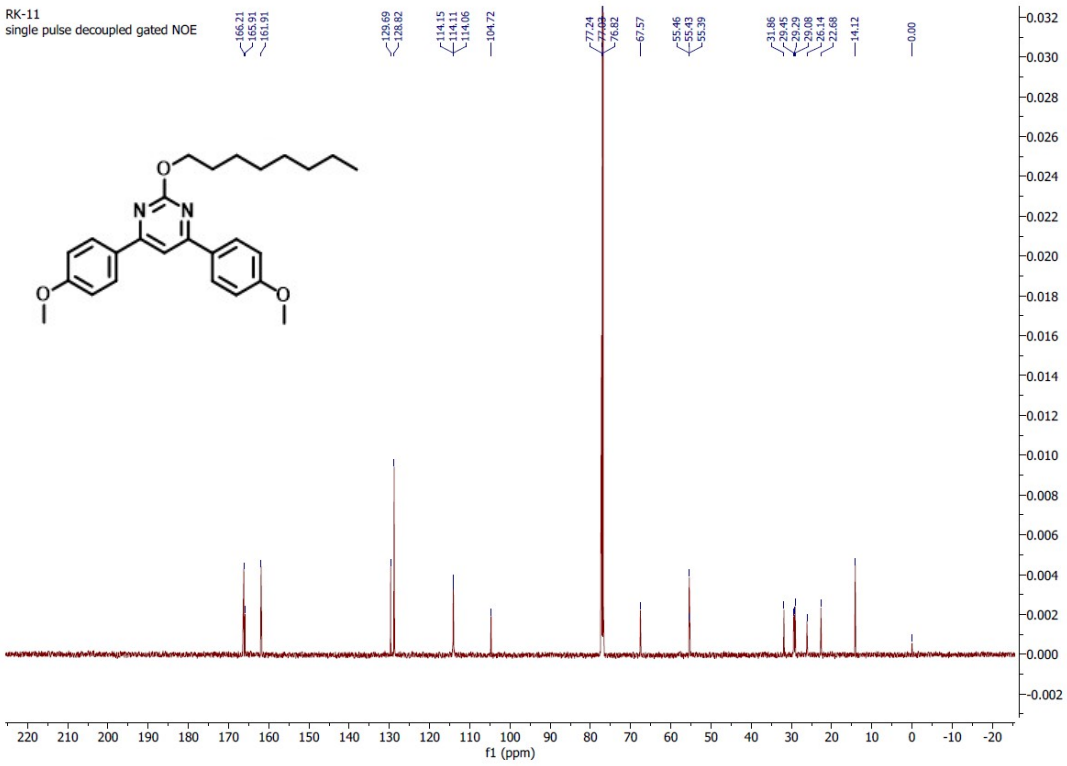

Figure 54: [13]C NMR spectra of 2r

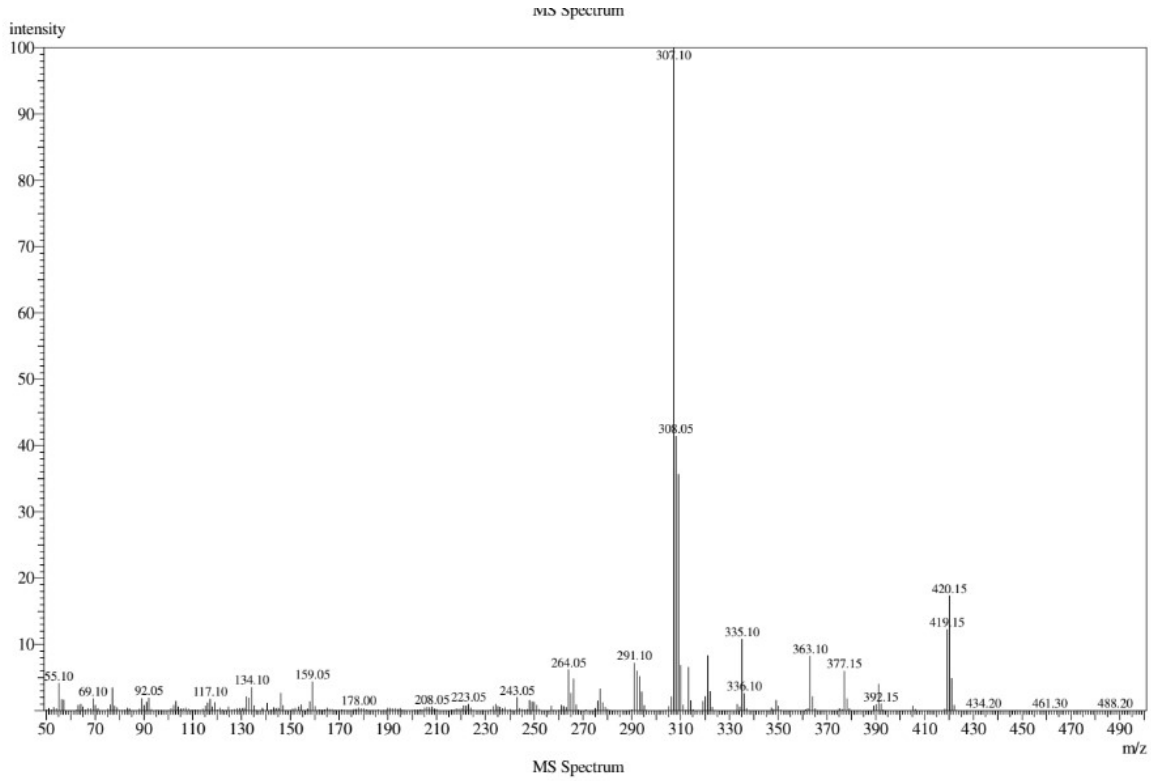

Figure 55: EI-MS of 2r: m/z [M]$^+$ for $C_{26}H_{32}N_2O_3^+$ calculated: 420.55; observed: 420.15.

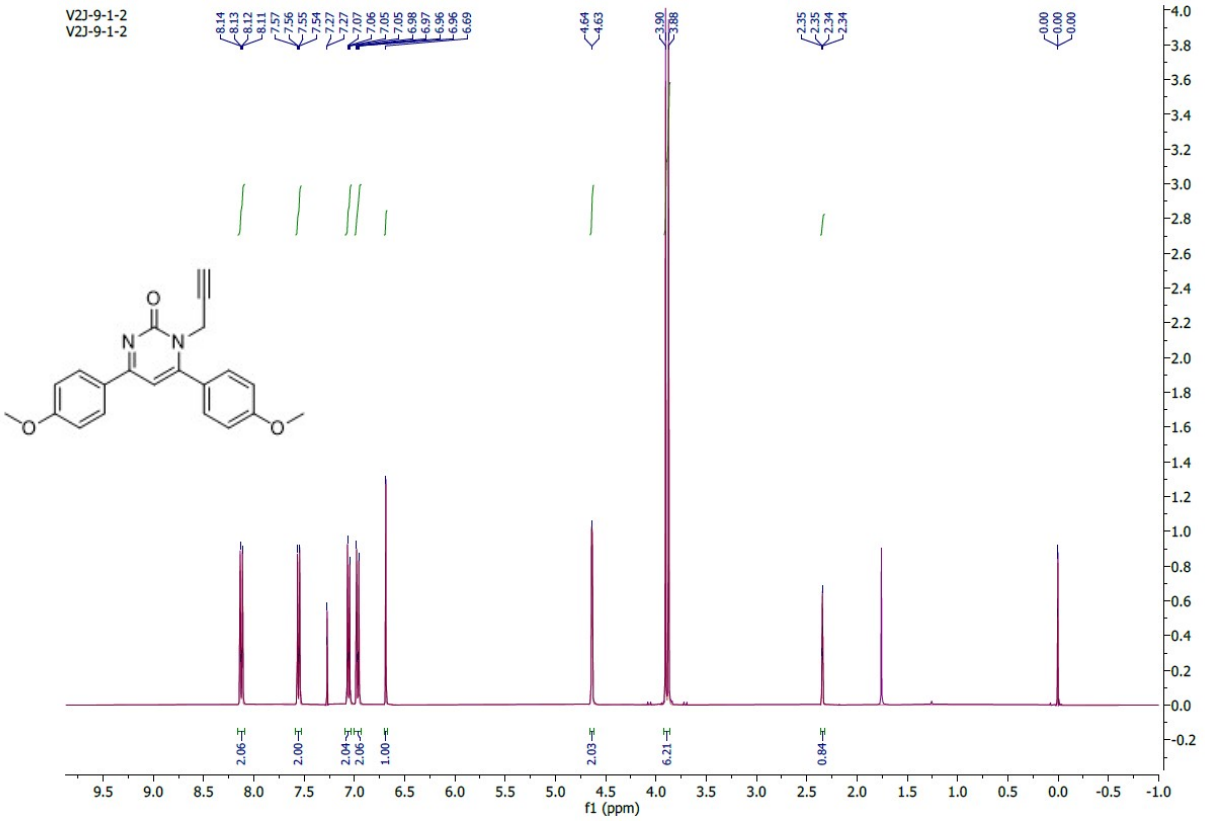

Figure 56: ^{1}H NMR spectra of 3a

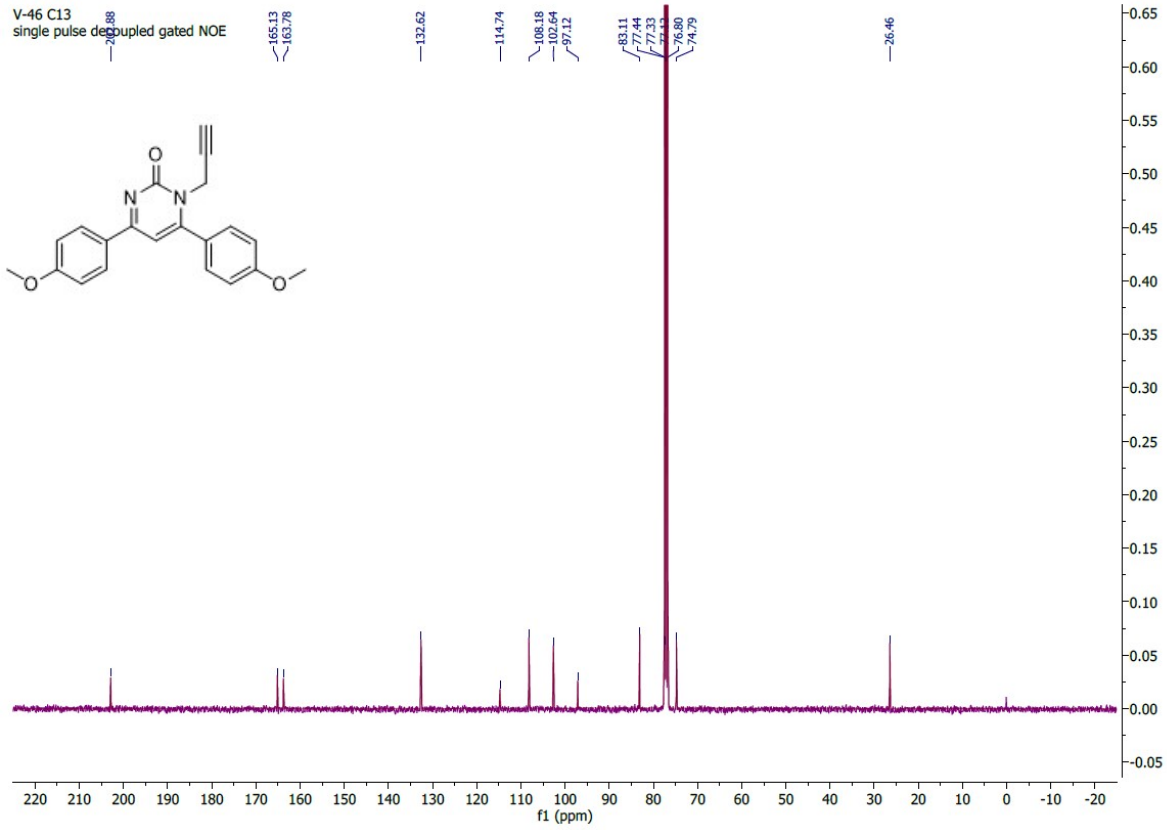

Figure 57: ^{13}C NMR spectra of 3a

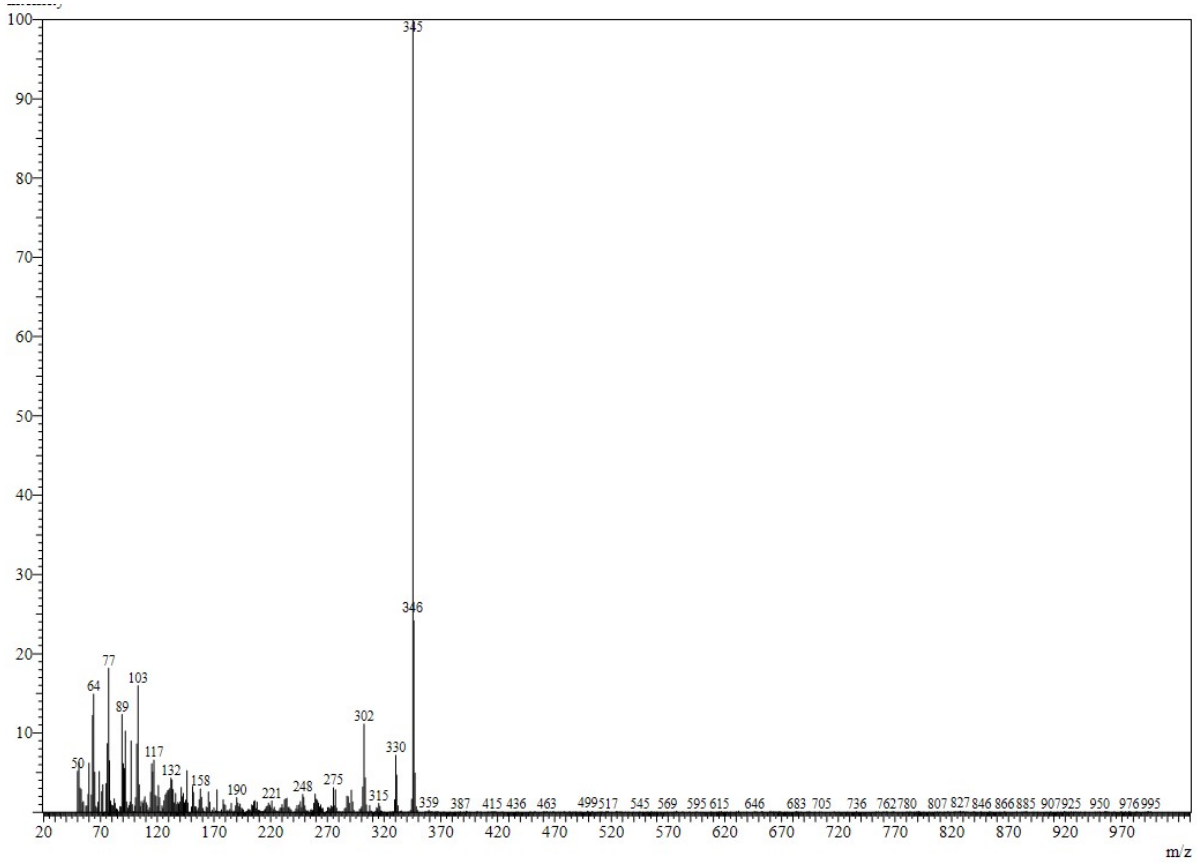

Figure 58: EI-MS of 3a: m/z [M]⁺ for $C_{21}H_{18}N_2O_3^+$ calculated: 346; observed: 346.

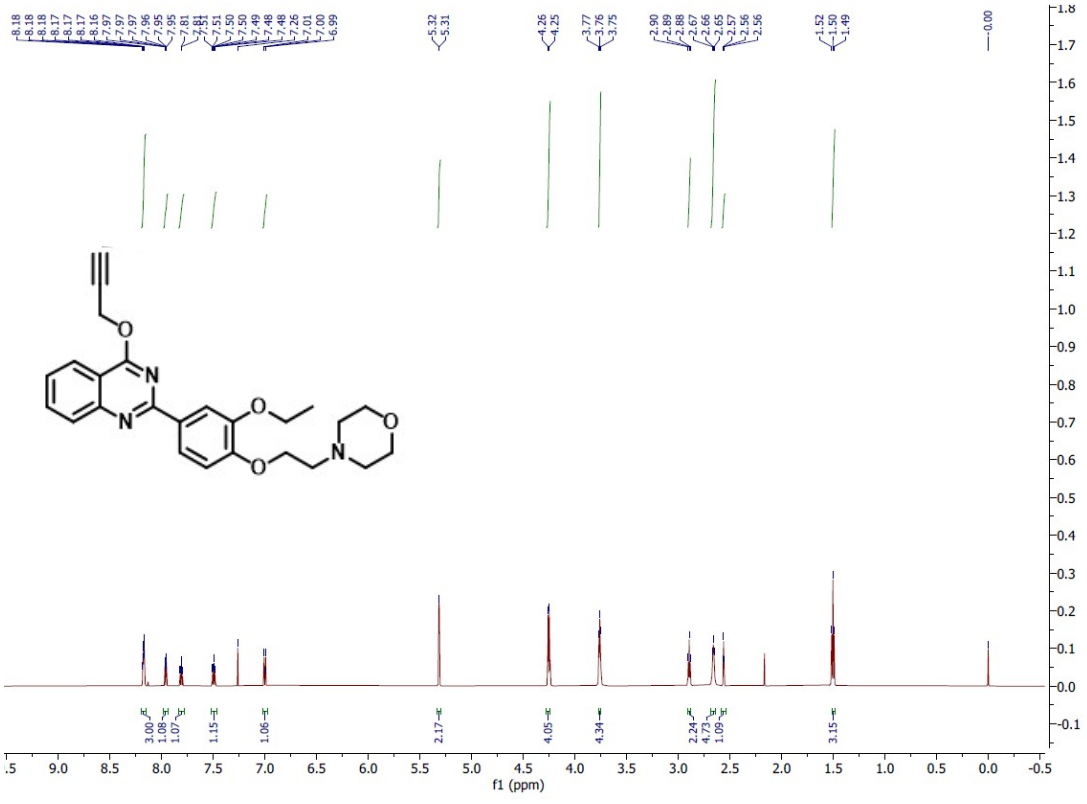

Figure 59: ^1H NMR spectra of 5a

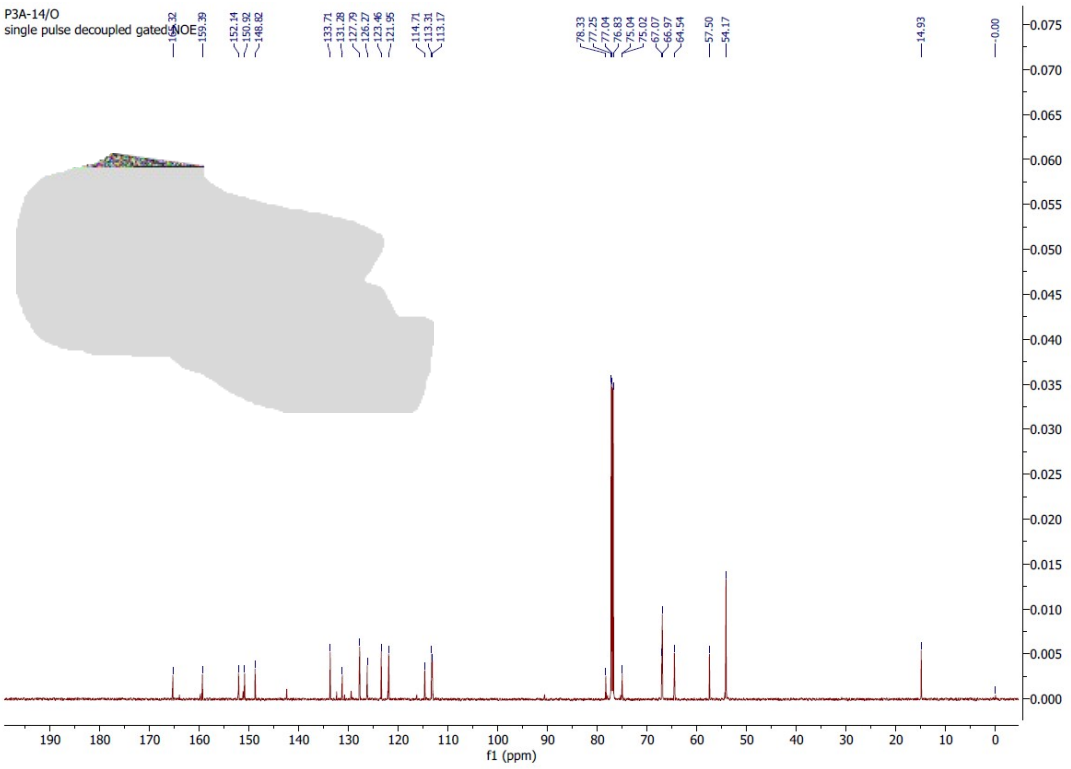

Figure 60: ^{13}CNMR spectra of 5a

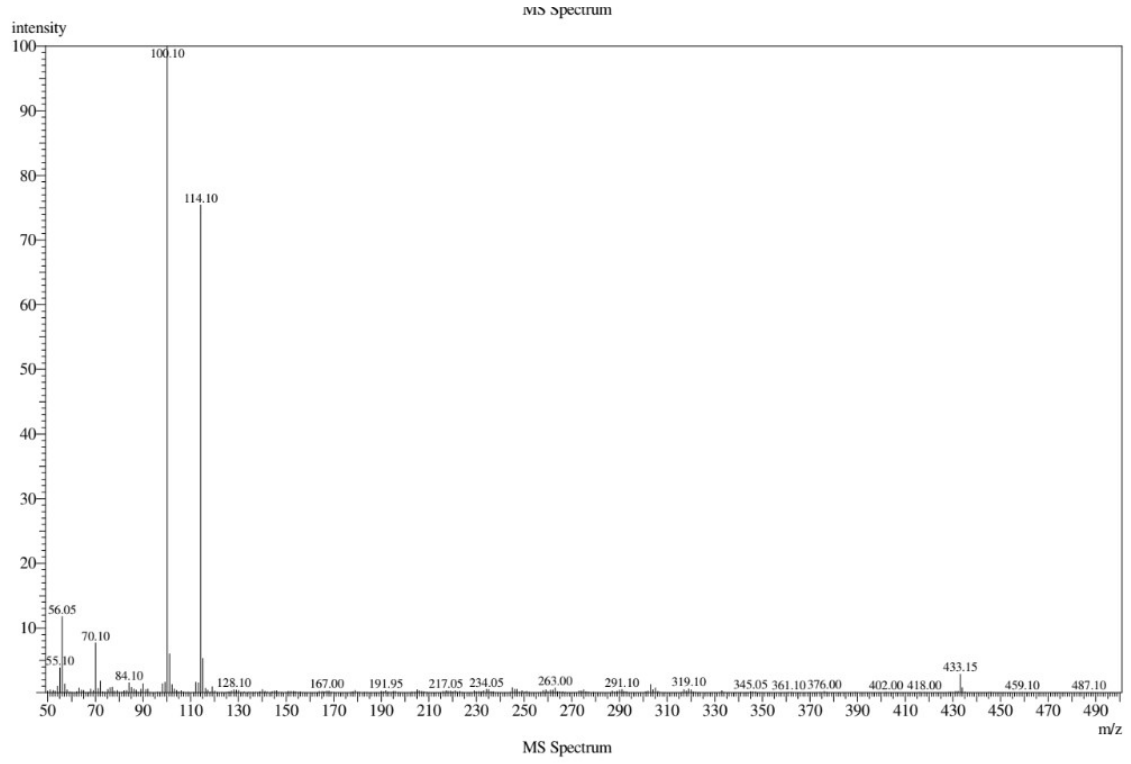

Figure 61: EI-MS of 5a: m/z $[M]^+$ for $C_{25}H_{27}N_3O_4^+$ calculated: 433.20; observed: 433.15.

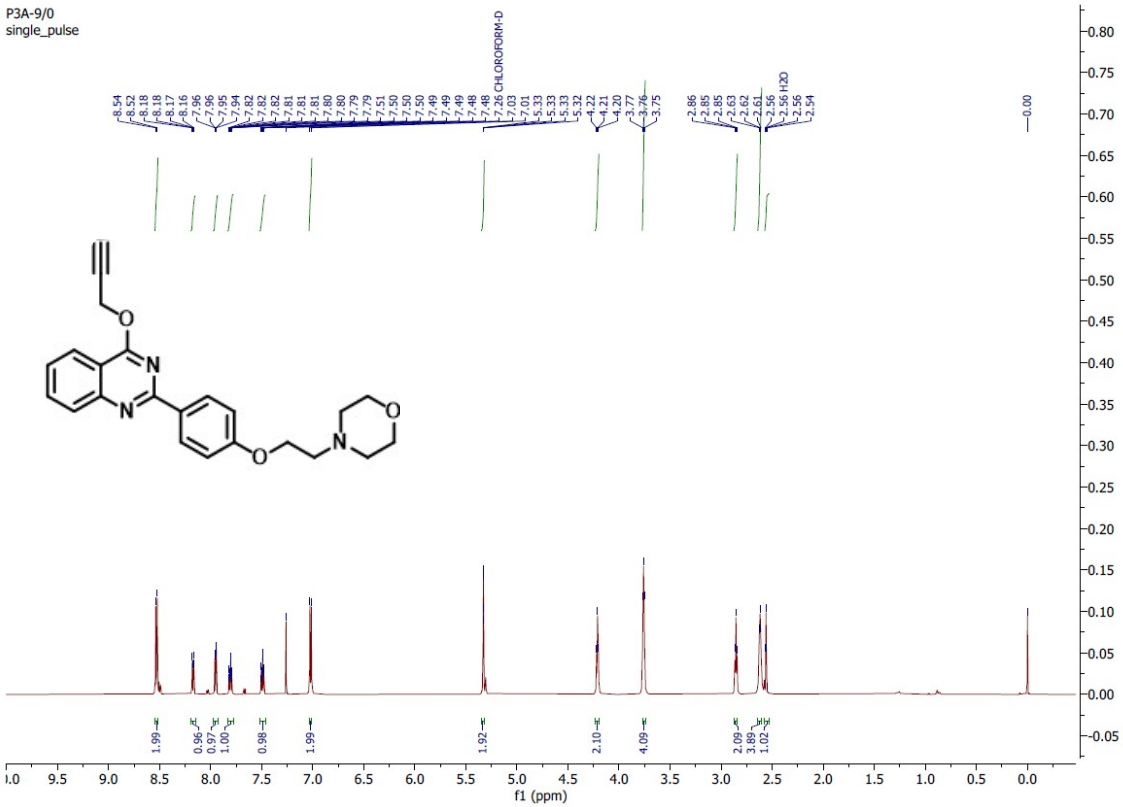

Figure 62: [1]H NMR spectra of 5b

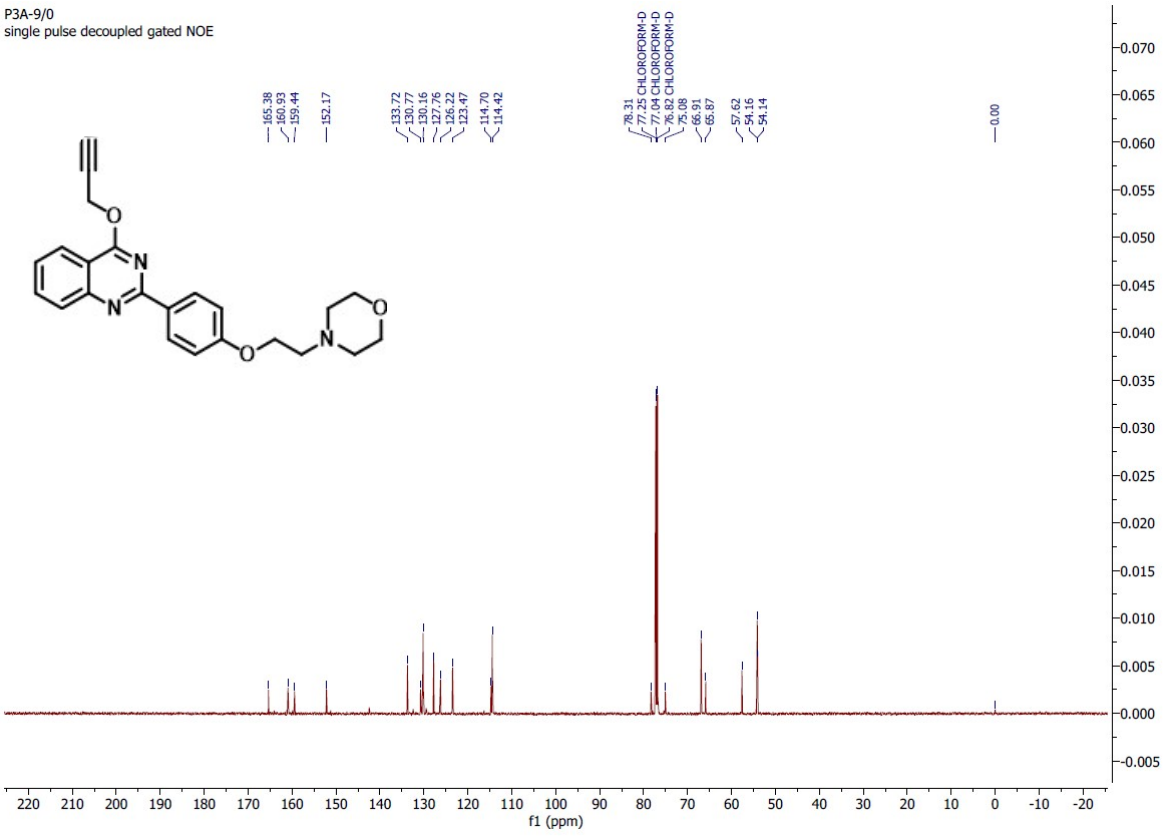

Figure 63: [13]CNMR spectra of 5b

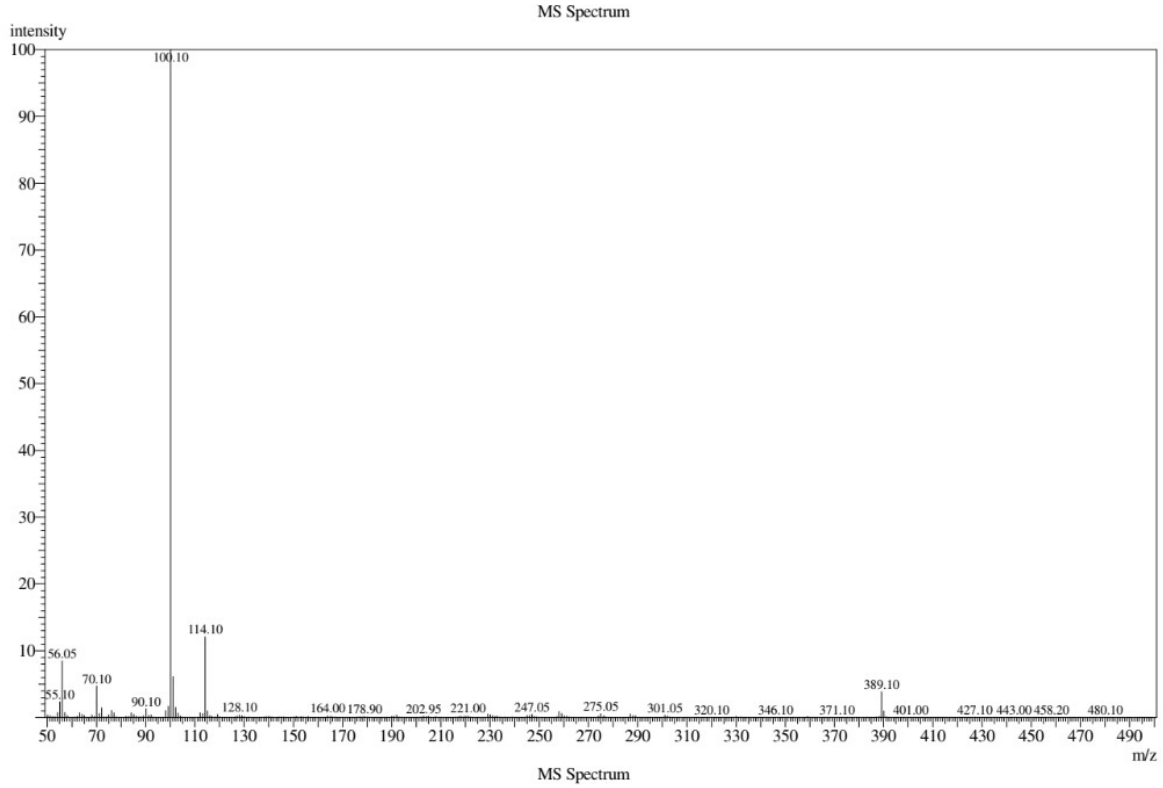

Figure 64: EI-MS of 5b: m/z [M]$^+$ for $C_{23}H_{23}N_3O_3^+$ calculated: 389.17; observed: 389.10.

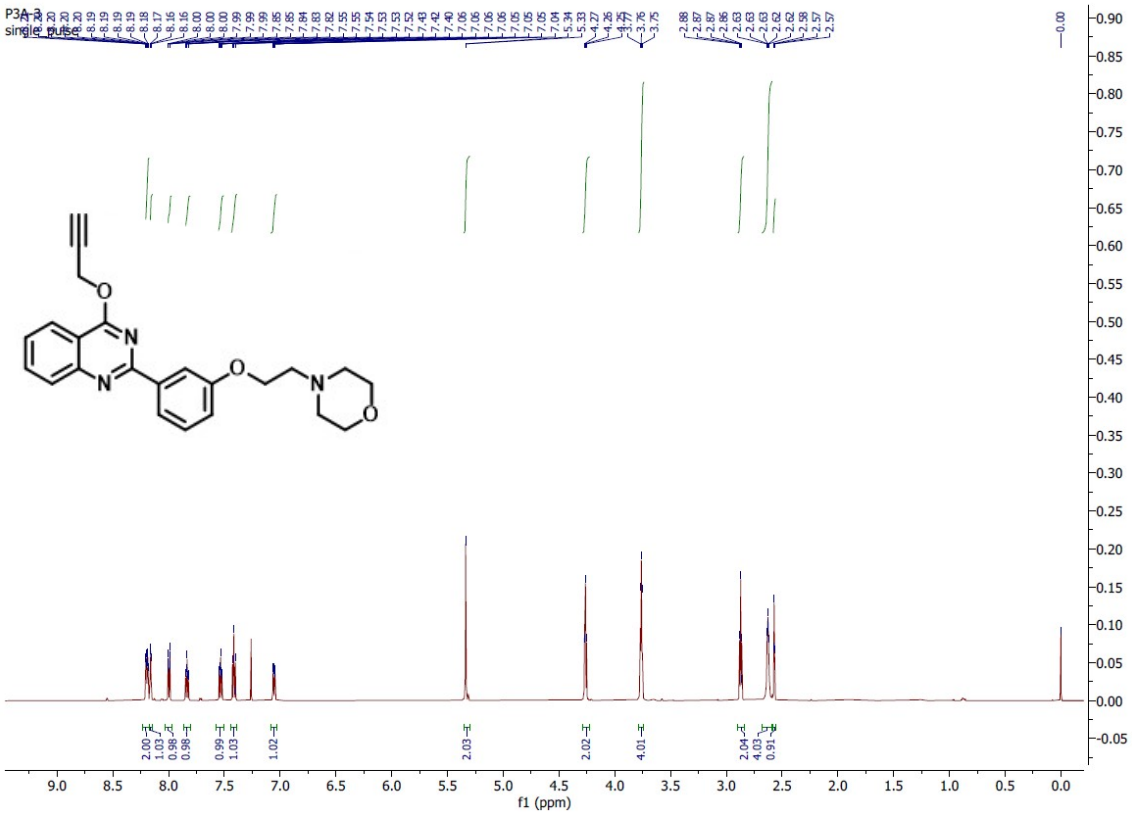

Figure 65:^{1}H NMR spectra of 5c

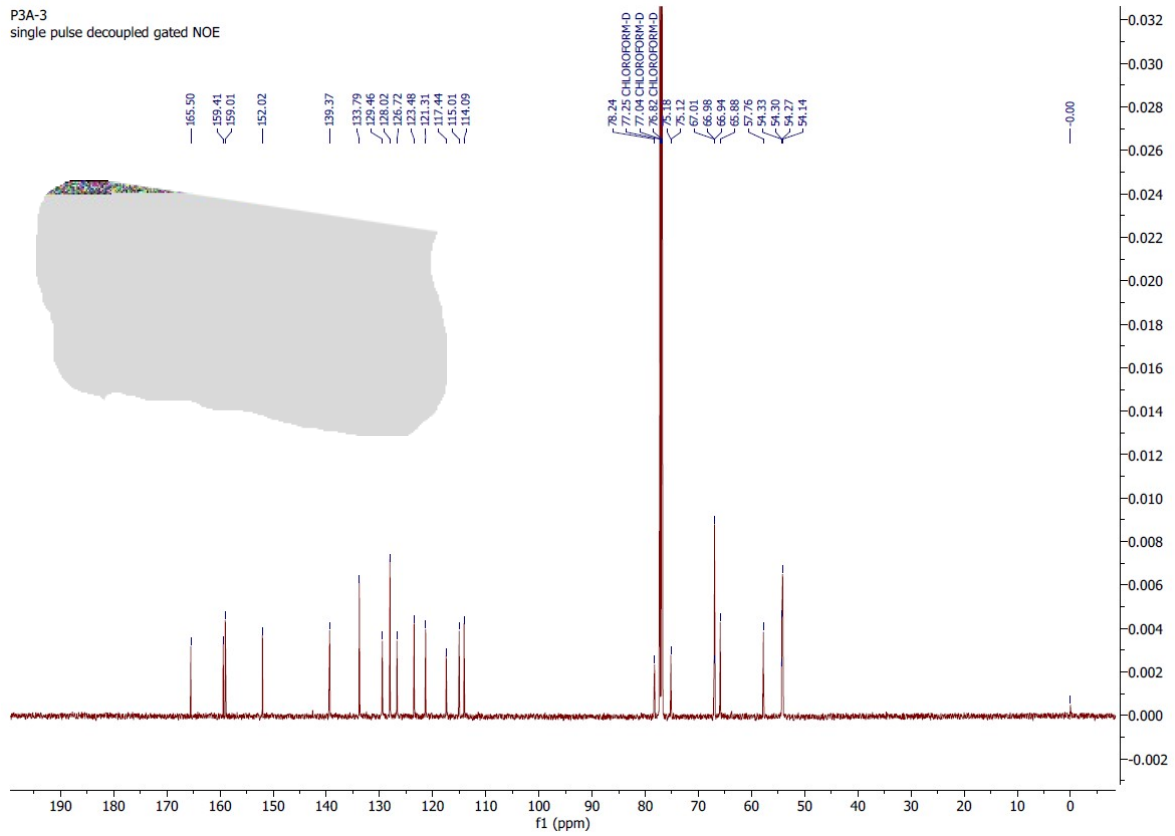

Figure 66: ^{13}C NMR spectra of 5c

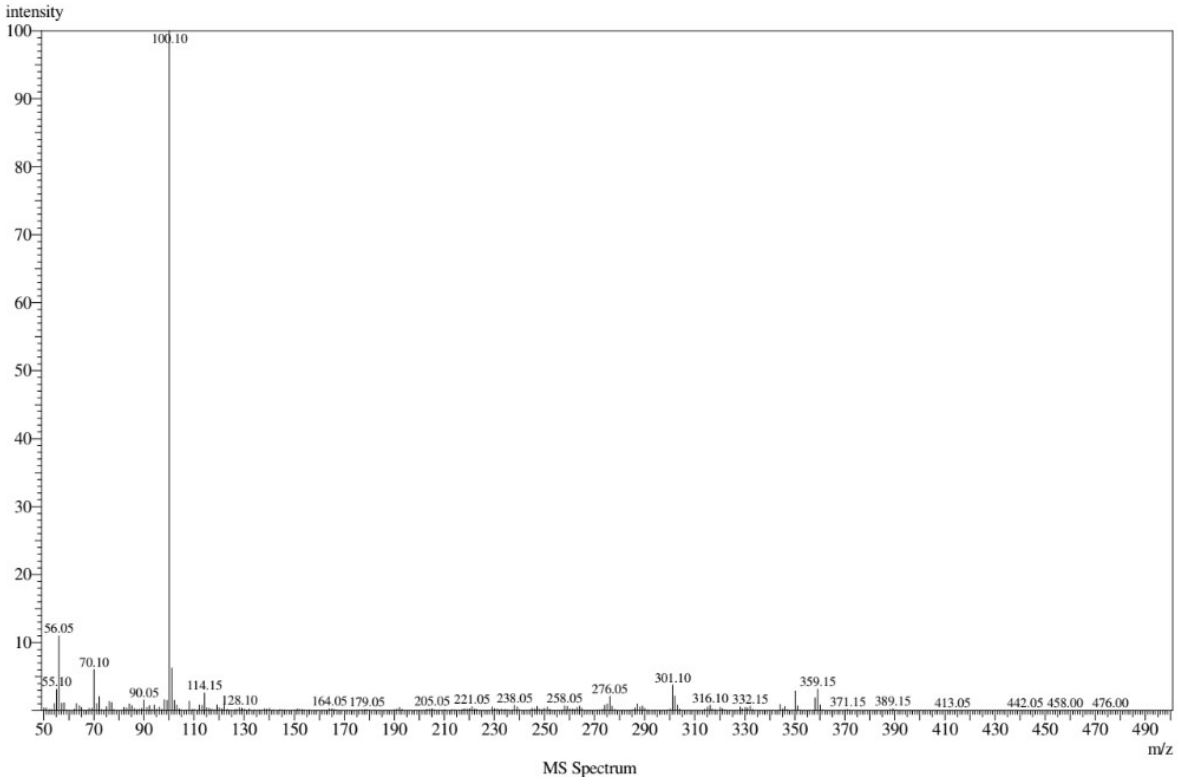

Figure 67: EI-MS of 5c: m/z $[M]^+$ for $C_{23}H_{23}N_3O_3^+$ calculated: 389.17; observed: 389.10.

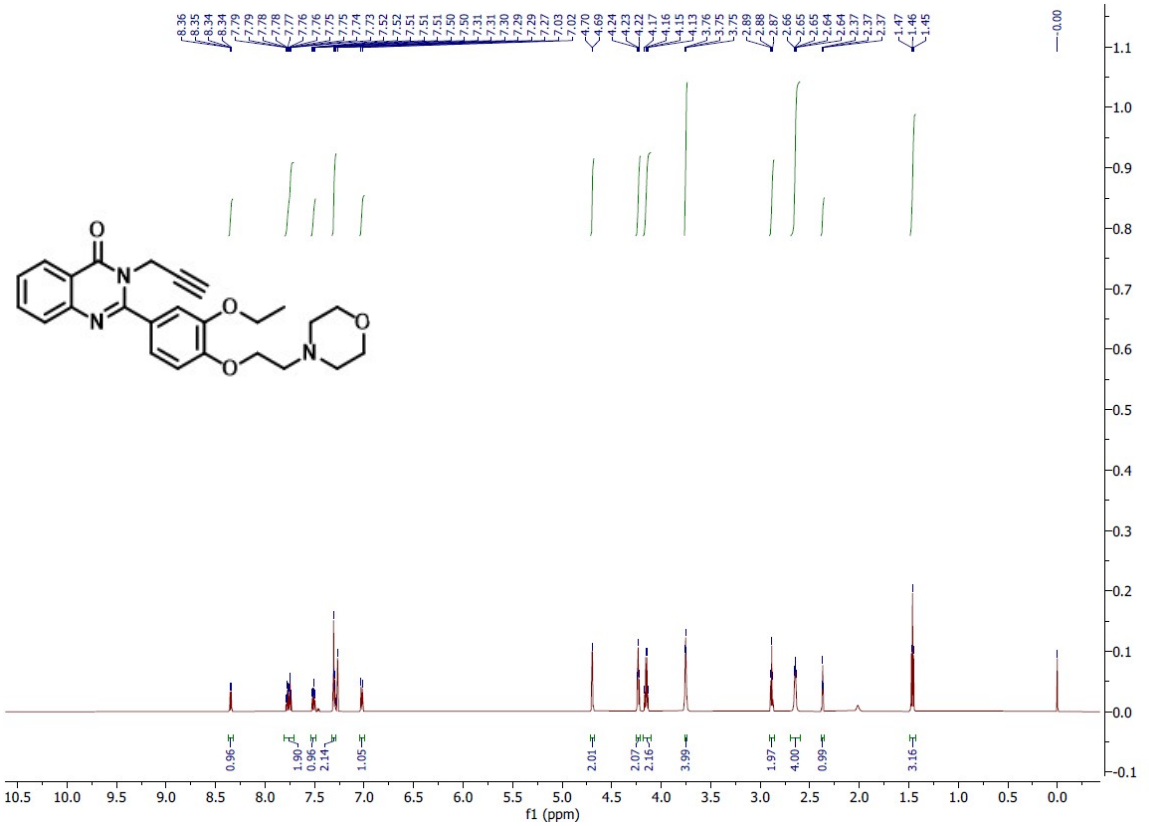

Figure 68: [1]H NMR spectra of 6a

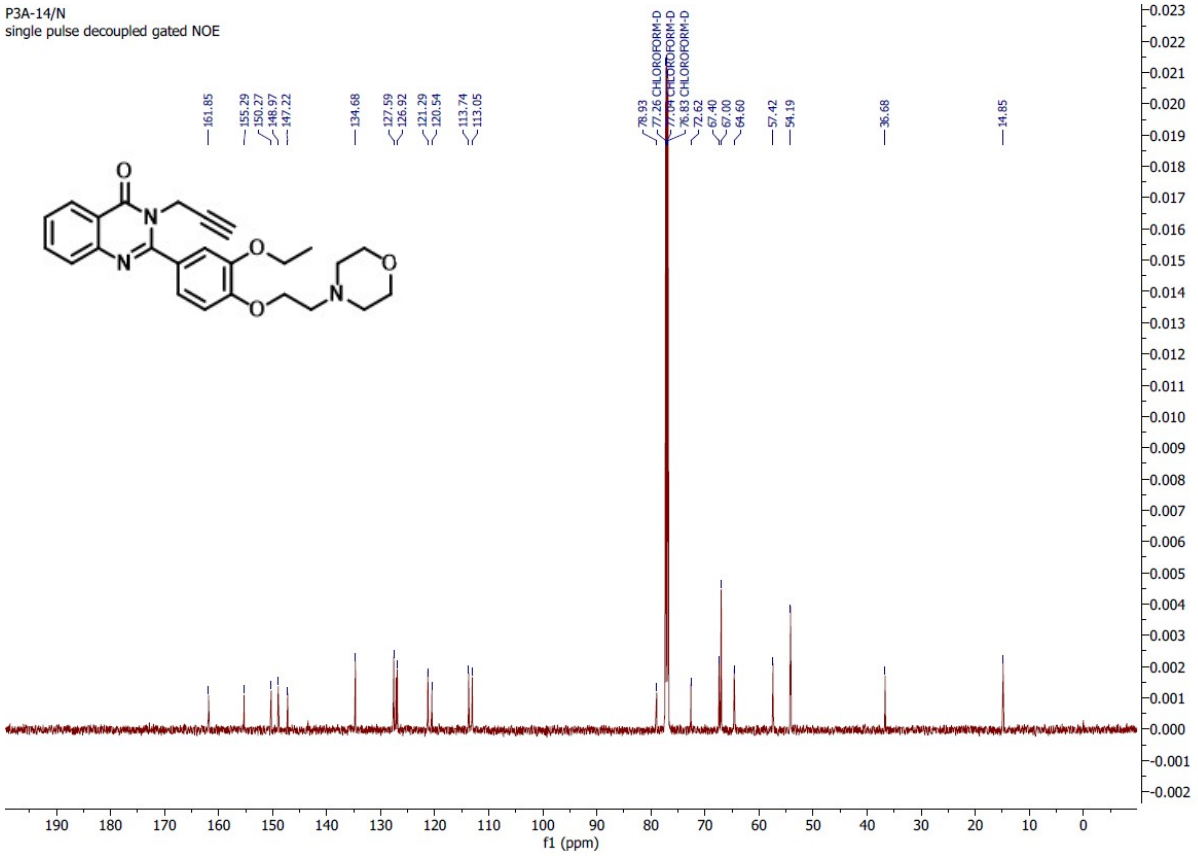

Figure 69: [13]C NMR spectra of 6a

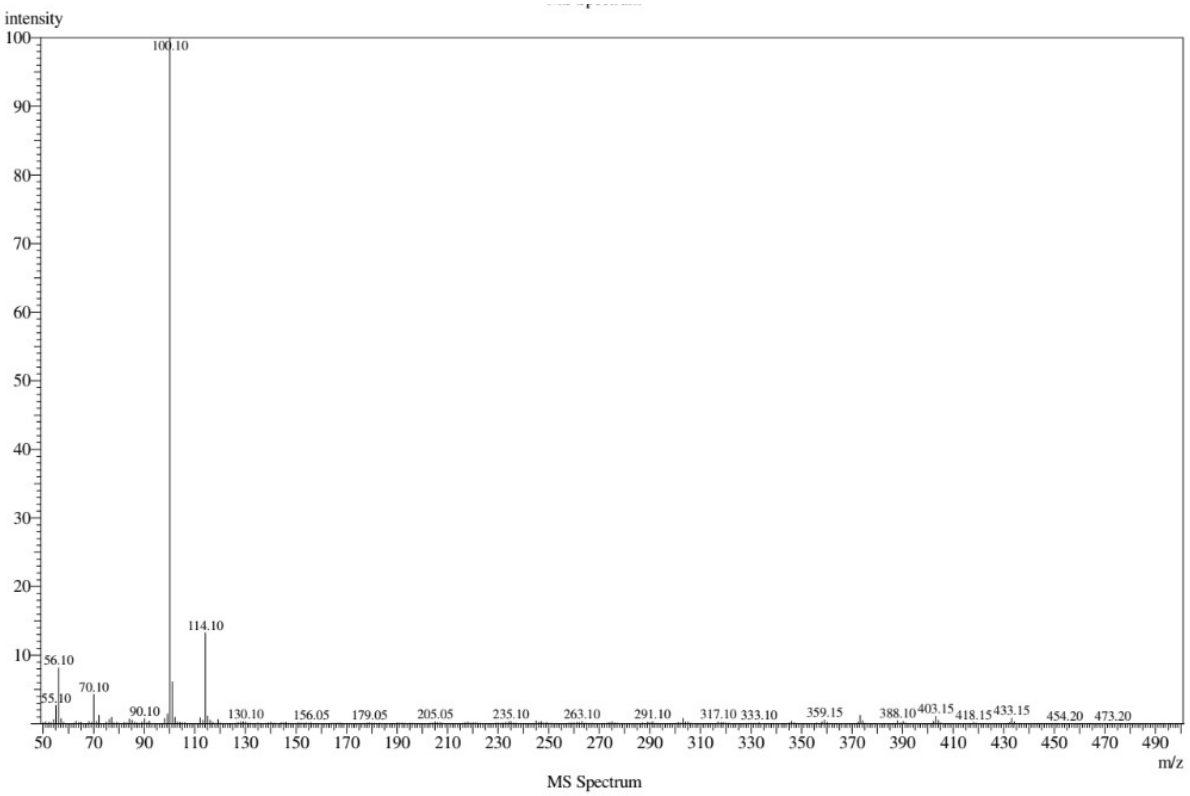

Figure 70: EI-MS of 6a: m/z $[M]^+$ for $C_{25}H_{27}N_3O_4^+$ calculated: 433.20; observed: 433.15.

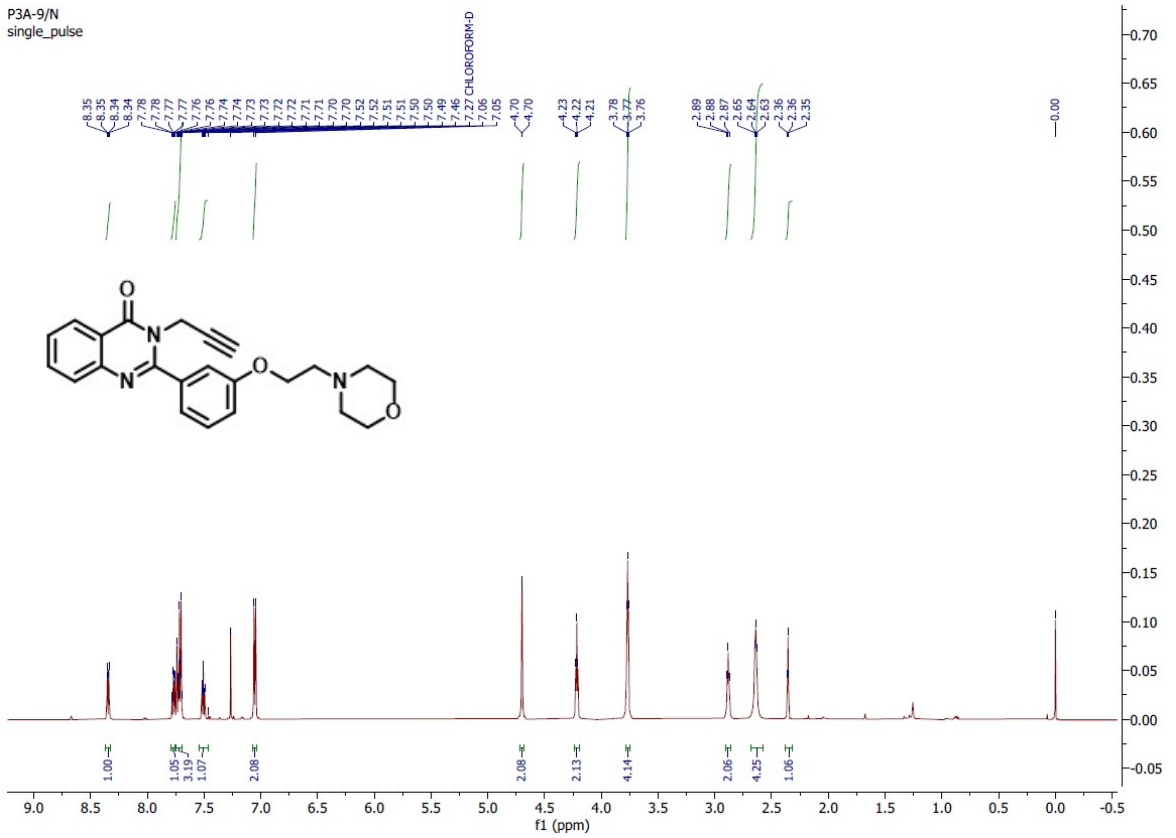

Figure 71: [1]H NMR spectra of 6b

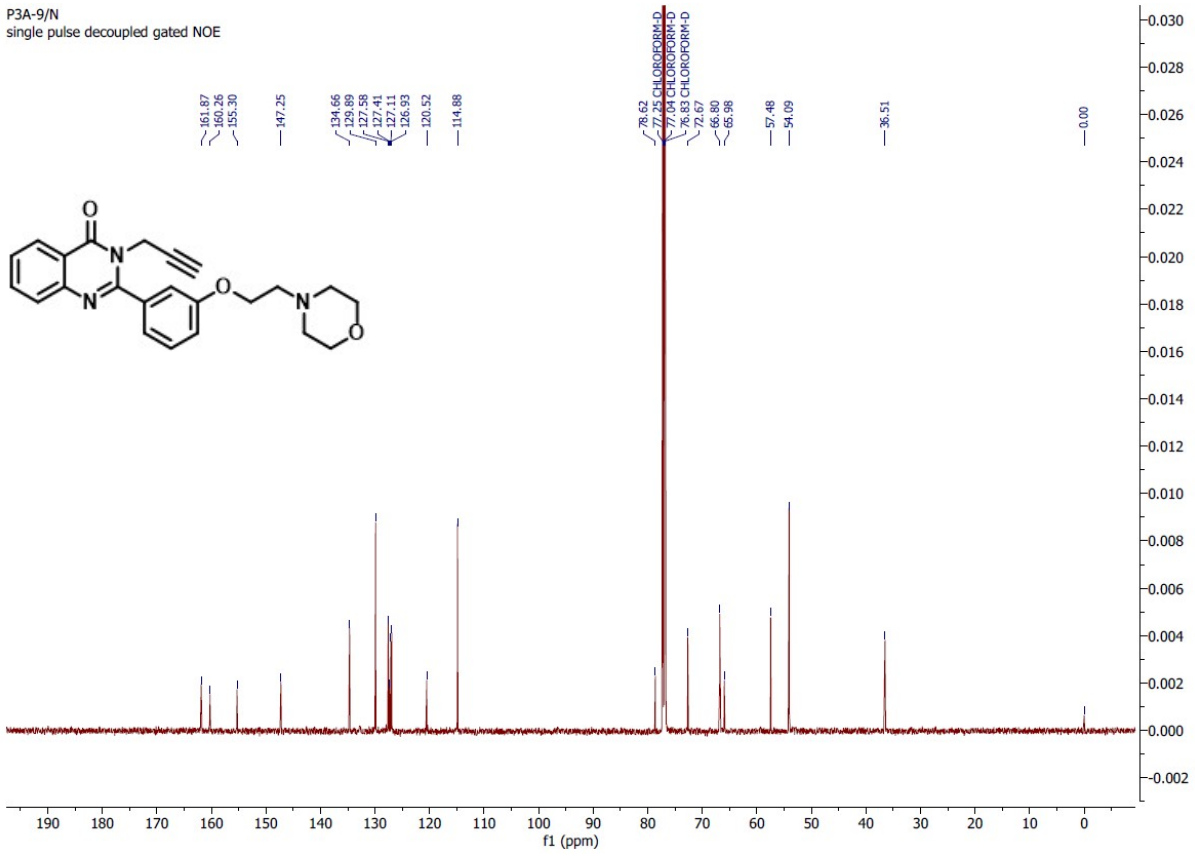

Figure 72: [13]C NMR spectra of 6b

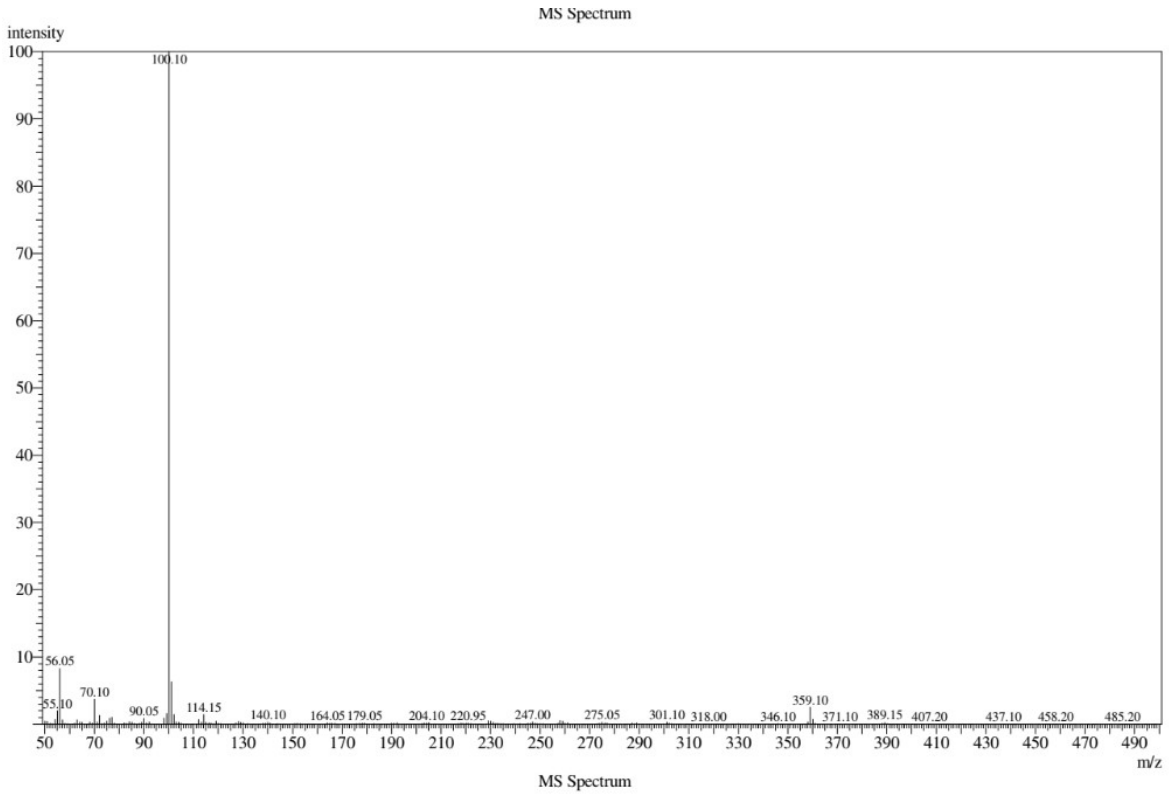

Figure 73: EI-MS of 6b: m/z [M]$^+$ for $C_{23}H_{23}N_3O_3^+$ calculated: 389.17; observed: 389.10.

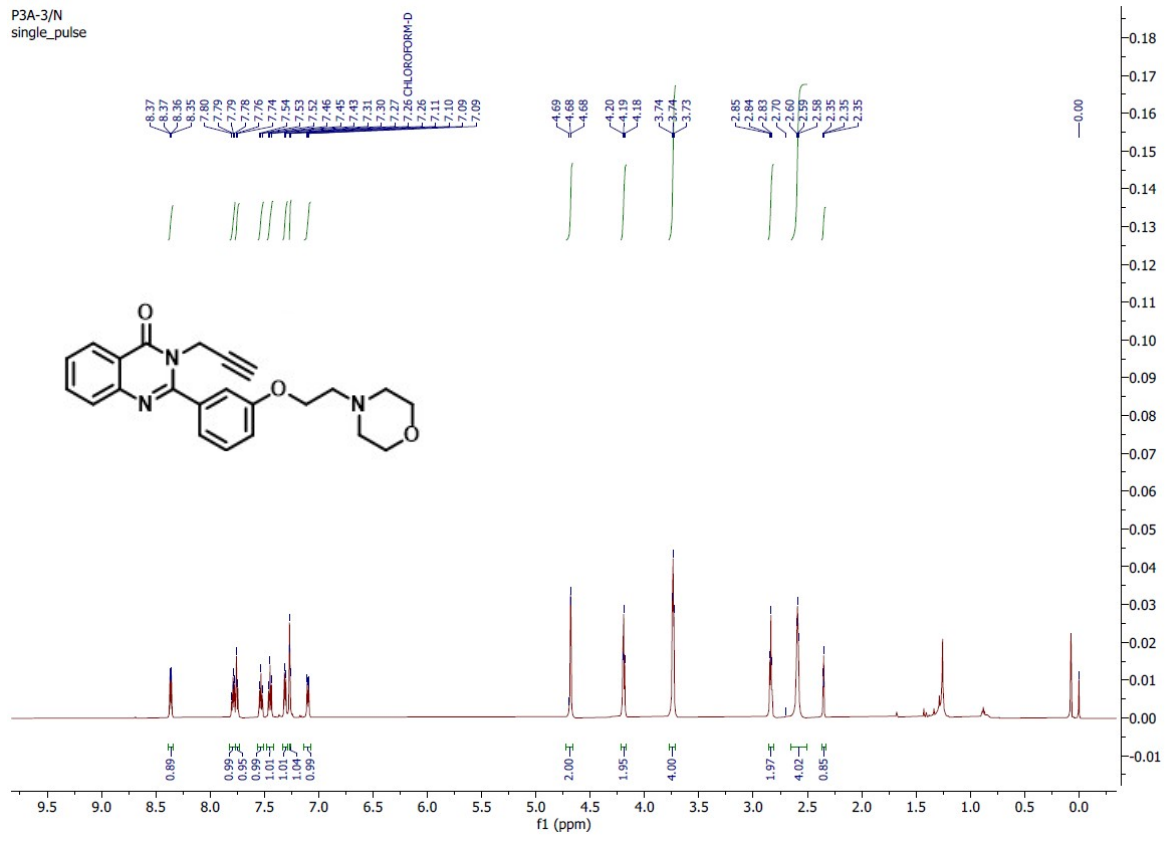

Figure 74: [1]H NMR spectra of 6c

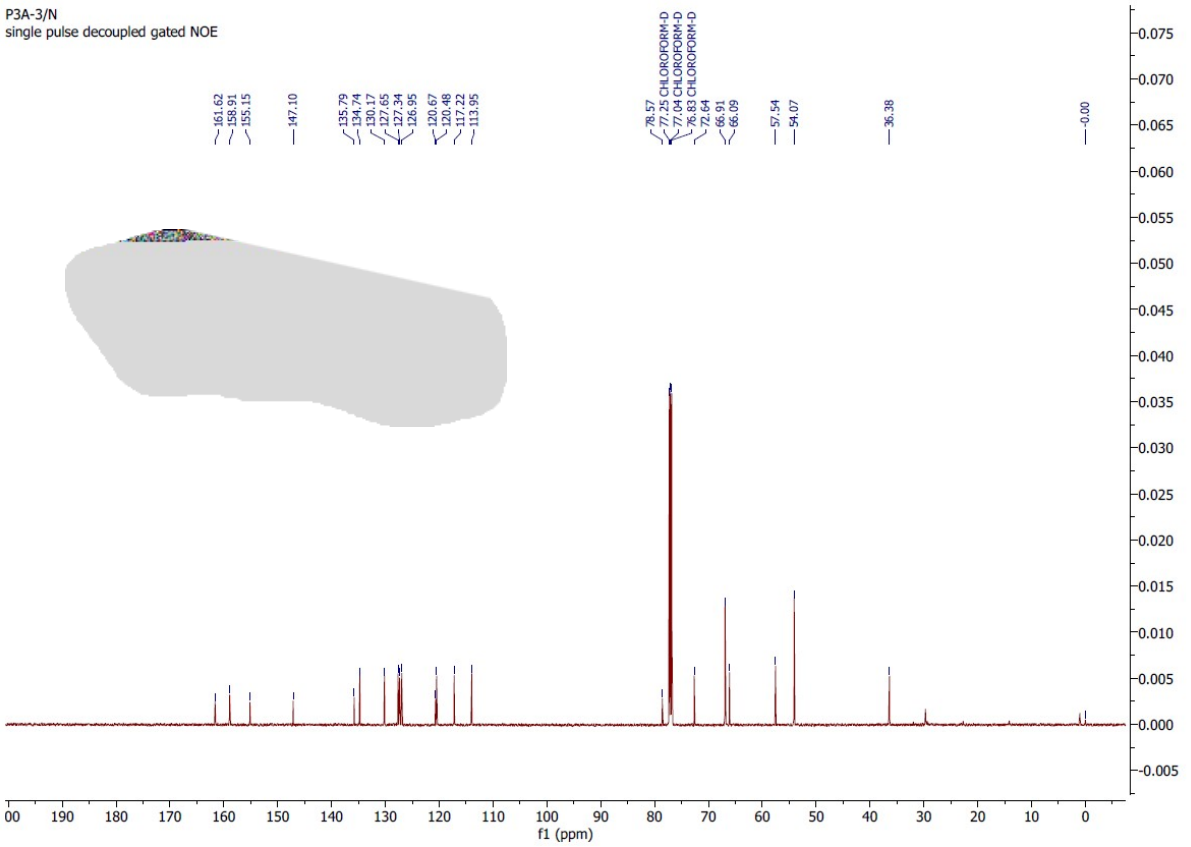

Figure 75: ^{13}C NMR spectra of 6c

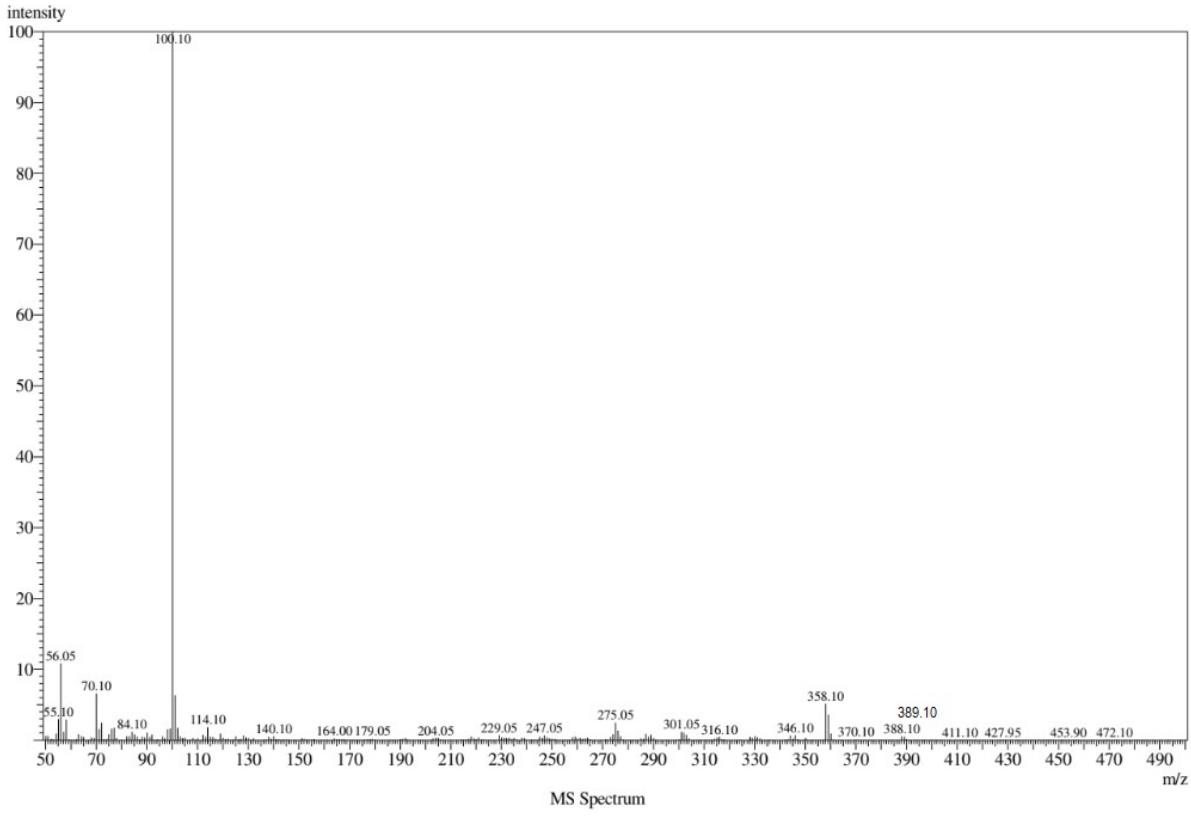

Figure 76: EI-MS of 6c: m/z $[M]^+$ for $C_{23}H_{23}N_3O_3^+$ calculated: 389.17; observed: 389.10.